

UCSF

UC San Francisco Electronic Theses and Dissertations

Title

Synthesis and structure-reactivity studies of 2'-substituted nicotinamide nucleoside analogs of NAD⁺

Permalink

<https://escholarship.org/uc/item/2251c4r4>

Author

Handlon, Anthony L.

Publication Date

1991

Peer reviewed|Thesis/dissertation

**Synthesis and Structure-reactivity Studies of 2'-Substituted
Nicotinamide Nucleoside Analogs of NAD⁺**

by

Anthony L. Handlon

DISSERTATION

Submitted in partial satisfaction of the requirements for the degree of

DOCTOR OF PHILOSOPHY

in

Pharmaceutical Chemistry

in the

GRADUATE DIVISION

of the

UNIVERSITY OF CALIFORNIA

San Francisco



To my parents

Acknowledgments

First and foremost I wish to thank Professor Norman J. Oppenheimer for his advice and encouragement during my time in his laboratory. His office door was always open and he was always willing to lend undivided attention to my questions. I would also like to thank Drs. George L. Kenyon and Paul Ortiz de Montellano for their suggestions and prompt reading of this manuscript.

I am lucky to have shared the HSE-1181 laboratory with so many interesting and talented people. I particularly want to thank Tom Marschner and Randy Johnson for helping me get started in the lab. I appreciate Larry Wainschel for pulling my nose off the grindstone and reminding me to wake up and smell the hops. I thank Neil Buckley for stimulating and animated discussions about science and politics. I am obliged to Tom Xu for his synthetic prowess without which my project would be incomplete.

My deepest appreciation goes to Dr. Ronda Ott for her love, encouragement, and understanding.

I acknowledge all past and present roommates (including Kasha) at 1849 Oak St. where I lived for my entire 5 1/2 year graduate school tenure. Thanks for being there. I'll always remember you.

Finally, I am indebted to the department of Pharmaceutical Chemistry and the National Institutes of Health. Without their financial support, none of this would have been possible.

Anthony L. Handlon

San Francisco, California

January, 1991.

**Synthesis and Structure-reactivity Studies of 2'-Substituted Nicotinamide
Nucleoside Analogs of NAD⁺**

Abstract

Anthony L. Handlon

The chemical mechanism of hydrolytic cleavage of the glycosyl bond has been investigated for a series of 2'-substituted nicotinamide nucleosides in which the 2'-hydroxyl has been replaced by -H, -F, -NH₂, -NH₃⁽⁺⁾, -N₃, or -NHAc in either the ribose or arabinose configuration. The syntheses of these nicotinamide 2'-substituted β-D-ribo- and arabinofuranosides are described. The rates of hydrolysis have been measured over a range of pH and temperature and the activation parameters, ΔH[‡] and ΔS[‡], are discussed. With noted exceptions, the reactivity of the analogs correlates linearly with the electronic character of the 2'-substituent (Taft ρ_I = -7.1) consistent with a dissociative mechanism *via* a cationic intermediate. The reactivity of the 2'-NH₃⁽⁺⁾ nucleosides do not correlate with Taft sigma. The anomalous substituent effects of charged groups are discussed and a new sigma value for -NH₃⁽⁺⁾ is calculated based on the ¹H NMR chemical shift of the 2'-proton. The 2'-substituted nicotinamide nucleosides are presented as a good model for the study of substituent effects on the chemical stability of glycosides and nucleosides. The biochemistry and mechanism of enzymes that catalyze the cleavage of the nicotinamide-glycosyl bond of NAD⁺ are reviewed. The potential function of the 2'-substituent in the mechanisms of base-catalyzed and enzyme-catalyzed hydrolysis of NAD⁺ is discussed.

The rates and equilibrium constants for the reversible formation of 1,4-dihydro cyanide adducts with the nicotinamide 2'-substituted β-D-ribo- and arabinofuranosides have been measured to model the steric, polar, and stereochemical influence of the 2'-substituent to the oxidation-reduction properties of NAD⁺. The cyanide affinities of the nucleosides correlate

linearly with the Taft sigma constant for the 2'-substituents. The 2'-NHCOR analogs show unexpectedly high affinity for cyanide that is independent of the polarity of R. The larger reduction potential of NAD⁺ over ara-NAD⁺ is shown to derive from an electronic and not a steric effect. The implications for the mechanism of NAD⁺-dependent dehydrogenases and the design of NAD⁺ analogs are discussed.

Table of Contents

Abstract	v	
List of Tables	x	
List of Figures	xi	
List of Schemes	xiii	
Chapter 1	Introduction	1
	The mechanism of NAD ⁺ hydrolysis	2
	2'-Substituted nicotinamide nucleosides as mechanistic probes	5
	References	6
Chapter 2	Enzymes that Cleave the Glycosyl Bond of NAD⁺: ADP- Ribosyltransferases and NAD⁺ Glycohydrolases	8
	ADP-ribosyltransferases: MonoADP-ribosylation	10
	Cholera toxin.....	11
	Pertussis toxin.....	12
	Diphtheria toxin.....	13
	Botulinum toxins.....	14
	Other ADP-ribosyltransferase activities.....	15
	ADP-ribosyltransferases: Poly(ADP-ribosylation)	16
	NAD⁺ Glycohydrolases	18
	Coenzyme analogs and inhibitors.....	19
	Mechanistic overview.....	21
	References	25
Chapter 3	The Synthesis of the 2'-substituted Nicotinamide Nucleosides	29
	Introduction	30
	Results and Discussion	31
	The synthesis of nicotinamide 2'-deoxy ribofuranoside	31
	The synthesis of nicotinamide 2'-fluoro-2'-deoxy-β-D- ribofuranoside	33

	The synthesis of nicotinamide 2'-N ₃ -and 2'-NH ₂ -2'- deoxy-ribofuranoside and nicotinamide 2'-N ₃ -, 2'-NH ₂ -, and 2'-F-2'-deoxy-arabinofuranoside.....	35
	Anomeric ratios.....	37
	Azide reduction.....	38
	The 2'-N-acylated derivatives.....	40
	The 2'-OH nucleosides.....	40
	NMR and mass spectral analysis.....	40
	Experimental	44
	References	58
Chapter 4	Structure-Reactivity In the 2'-substituted Nicotinamide Nucleosides: Probing the Mechanism of Glycosyl Bond Cleavage	60
	Introduction	61
	Results	64
	Discussion	73
	Mechanism of nicotinamide nucleoside hydrolysis.....	73
	Activation energies.....	74
	Mechanism of NAD ⁺ hydrolysis.....	77
	Anchimeric assistance.....	79
	Substituent effects in glycosyl bond cleavage.....	81
	Mechanism of enzymatic glycosyl bond cleavage.....	82
	Experimental	84
	References	85
Chapter 5	The Hydrolysis of the 2'-NH₃⁺ Nicotinamide Nucleosides	89
	Introduction	90
	Results and Discussion	90
	pH dependence.....	90
	NMR titrations.....	92
	Temperature dependence.....	95
	The -NH ₃ ⁺ sigma constant.....	97
	Reevaluating the sigma constant for -NH ₃ ⁺	100
	Experimental	104
	References	105

Chapter 6	Cyanide Addition to the 2'-substituted Nicotinamide	
	Nucleosides: Modelling the Influence of the	
	Carbohydrate Moiety on the NAD⁺/NADH Couple.....	107
	Introduction.....	108
	Results.....	110
	Discussion.....	122
	Studies on cyanide addition of N-substituted	
	nicotinamide derivatives.....	122
	Substituent effects on the kinetics of cyanide addition.....	123
	Effect of configuration.....	124
	Substituent effects in cyanide addition versus glycosyl	
	hydrolysis.....	125
	Cyanide addition to the 2'-N-acyl arabinofuranosides.....	126
	Enzymatic oxidation/reduction of NAD⁺.....	127
	Experimental.....	128
	References.....	128

List of Tables

Table 2.1.	Acceptor preferences for the ADP-ribosyltransferases	11
Table 2.2.	Rates of hydrolysis and NAD ⁺ glycohydrolase inhibition constants of NAD ⁺ analogs	20
Table 2.3.	Activation parameters for NAD ⁺ hydrolysis at 25 °C.....	24
Table 3.1.	¹ H NMR chemical shifts of the nicotinamide and furanose ring protons for the 2'-substituted nicotinamide β-D-ribo- and arabinofuranosides in D ₂ O at 20 °C and molecular ion masses from liquid secondary ion mass spectrometry	41
Table 3.2.	¹ H NMR coupling constants (Hertz) of the furanose ring protons for the 2'-substituted nicotinamide β-D-ribo- and arabinofuranosides in D ₂ O.....	42
Table 4.1.	Hydrolysis rate constants for the 2'-substituted nicotinamide nucleosides at 37 °C.....	67
Table 4.2.	Entropies and enthalpies of activation for the hydrolysis of the 2'-substituted nicotinamide nucleosides	69
Table 5.1.	First order rate constants for the hydrolysis of the 2'-amino-nicotinamide nucleosides	92
Table 5.2.	Summary of the pK _a values of the 2'-amino nicotinamide nucleosides	94
Table 5.3.	Summary of the activation energies for the hydrolysis of the 2'-amino nicotinamide nucleosides.....	96
Table 5.4.	¹ H NMR chemical shift of the 2'-proton (ppm) and hydrolysis rate constants at 37 °C for the 2'-substituted nicotinamide nucleosides	101
Table 6.1	Cyanide addition rate and equilibrium constants for the nicotinamide 2'- substituted β-D-arabinofuranosides at 25 °C.....	113
Table 6.2.	Cyanide addition rate and equilibrium constants for the nicotinamide 2'- substituted β-ribofuranosides and β-NAD ⁺ at 25 °C.....	114
Table 6.3.	Cyanide addition rate and equilibrium constants for the nicotinamide β-D- 2'-N-acyl arabinofuranosides at 25 °C.....	117
Table 6.4.	Equilibrium constants for cyanide addition to the 2'-substituted β-ara- NAD ⁺ analogs and β-NAD ⁺	119
Table 6.5.	Cyanide addition rate and equilibrium constants for the 3-substituted pyridine adenine dinucleotide analogs.....	120
Table 6.6.	Summary of the ρ ₁ values for cyanide addition	123
Table 6.7.	Cyanide addition equilibria and Gibbs free energy differences between the arabinosides and ribosides	124

List of Figures

Figure 1.1.	The nicotinamide adenine dinucleotide (NAD ⁺) coenzyme showing the numbering scheme on the ribose and nicotinamide rings	2
Figure 1.2.	The pH/rate profile for the hydrolysis of NAD ⁺ at 37 °C	4
Figure 1.3.	The alcoholysis of 1,2-anhydro-3,4,6-tri-O-acetyl-glucose (Brigl's anhydride) gives both the α and β glucosides	5
Figure 2.1.	Generalized cleavage of the nicotinamide-ribosyl bond with formation of a linkage to a new nucleophile.....	9
Figure 2.2.	α-ADP-ribosylarginine.....	12
Figure 2.3.	Diphthamide.....	13
Figure 2.4.	Structure of the ADP-ribosyl linkage to the γ-carboxylate of glutamate that attaches the poly(ADP-ribose) chain to a protein.....	16
Figure 2.5.	Structure of adenosine monophosphate-α-O2''-O1''-ribose-5-phosphate, the monomeric unit of poly(ADP-ribose) containing an α-glycosyl linkage to the adenine 2'-hydroxyl.....	17
Figure 2.6.	Structure of a branch point in poly(ADP-ribose) formed by attachment at the 2'-hydroxyl (formerly the nicotinamide ribose) of an ADP-ribose monomeric unit.....	17
Figure 2.7:	Ribonolactone.....	19
Figure 2.8	γ-carbaNAD ⁺	20
Figure 2.9.	2'-Fluoro-2'-deoxy-nicotinamide arabinoside adenine dinucleotide	20
Figure 3.1	The DTT reduction of AZT to 3'-aminothymidine	39
Figure 3.2.	Nicotinamide arabinofuranoside and nicotinamide ribofuranoside	40
Figure 4.1.	Brigl's anhydride	62
Figure 4.2.	pH/rate plot for the hydrolysis of the 2'-deoxy nucleoside	66
Figure 4.3.	Arrhenius plot for the hydrolysis of the nicotinamide 2'-substituted-β-D-arabinofuranosides	68
Figure 4.4.	Arrhenius plot for the hydrolysis of the nicotinamide 2'-substituted-β-D-ribofuranosides	68
Figure 4.5.	Log(k) versus sigma for the hydrolysis of the 2'-substituted nicotinamide β-D-arabinofuranosides	71
Figure 4.6.	Log(k) versus sigma for the hydrolysis of the 2'-substituted nicotinamide β-D-ribofuranosides.....	71

Figure 4.7.	ΔS^\ddagger versus $\log(k)$ for the hydrolysis of the nicotinamide 2'-substituted β -D-arabinofuranosides.....	76
Figure 4.8.	ΔH^\ddagger versus $\log(k)$ for the hydrolysis of the nicotinamide 2'-substituted β -D-arabinofuranosides.....	76
Figure 4.9.	Plot of the Gibbs free energy of activation versus sigma for the hydrolysis of the nicotinamide 2'-substituted β -D-arabinofuranosides.....	77
Figure 4.10.	$\log(k)$ versus sigma for the hydrolysis of the 2'-substituted nicotinamide nucleosides and for the pH-independent hydrolysis of NAD^+ in base.....	79
Figure 5.1.	pH/rate profiles for the hydrolysis of the 2'-amino nicotinamide nucleosides incorporating the new sigma value for $-\text{NH}_3^+$	91
Figure 5.2.	NMR titration curves for the 2'-amino nicotinamide nucleosides.....	93
Figure 5.3.	1'-2' ^1H NMR coupling constant versus pH for the 2'-amino- β -D-ribofuranoside.....	95
Figure 5.4.	Conformational change upon ionization of the 2'-amino- β -D-ribofuranoside.....	95
Figure 5.5.	Arrhenius plots for the hydrolysis of nicotinamide 2'- NH_2 - and 2'- NH_3^+ - β -D-arabino- and ribofuranoside.....	96
Figure 5.6.	The log of the rate constants for the hydrolysis of the nicotinamide 2'-substituted- β -D-ribo- and arabinofuranosides versus the Taft Sigma constant.....	98
Figure 5.7.	The log of the rate constants for the hydrolysis of the methyl 2'-substituted- β -D-glucopyranosides versus the Taft Sigma constant.....	99
Figure 5.8.	The log of the hydrolysis rate constants versus the ^1H NMR chemical shift of the 2'-proton for the 2'-substituted- β -D-ribo- and arabinofuranosides.....	102
Figure 5.9.	The chemical shift of the 2'-proton versus the Taft inductive sigma constant for the 2'-substituted- β -D-ribo- and arabinofuranosides.....	102
Figure 5.10.	$\log(k)$ versus sigma for the hydrolysis of the nicotinamide 2'-substituted- β -D-ribo- and arabinofuranosides.....	103
Figure 6.1	N-substituted nicotinamide cations (including NAD^+) react with cyanide to form 1,4-dihydro derivatives analogous to NADH.....	108
Figure 6.2.	The UV spectra of nicotinamide riboside before cyanide addition and at 10 and 16 minutes after the addition of cyanide.....	111
Figure 6.3.	Plot of the absorbance at 324 nanometers versus time for the addition of cyanide to nicotinamide 2'-azido- β -D-ribofuranoside.....	111

Figure 6.4.	Plot of the absorbance at 324 nanometers versus time for the addition of cyanide to nicotinamide 2'-N-benzoyl and 2'-amino- β -D-arabinofuranoside.....	112
Figure 6.5.	Plot of the absorbance at 324 nanometers versus time for the addition of cyanide to nicotinamide 2'-N-acetyl and 2'-deoxy- β -D-ribofuranoside	112
Figure 6.6.	Log(K_{eq}) for the addition of cyanide to the nicotinamide 2'-substituted- β -D-ribo- and arabinofuranosides versus volume of the substituent.....	114
Figure 6.7.	The log of the equilibrium constant for cyanide addition versus sigma for the 2'-substituted nicotinamide arabinosides.....	115
Figure 6.8.	The log of the equilibrium constant for cyanide addition versus sigma for the 2'-substituted nicotinamide ribofuranosides.....	115
Figure 6.9.	Second order rate constants for the addition of cyanide versus sigma for the nicotinamide 2'-substituted- β -D arabino- and ribofuranosides.....	116
Figure 6.10.	Rate constants for the dissociation of cyanide versus sigma for the nicotinamide 2'-substituted- β -D arabino- and ribofuranosides.....	116
Figure 6.11.	The log of the equilibrium constant for cyanide addition versus sigma for the nicotinamide 2'-N-acyl - β -D-arabinosides	118
Figure 6.12.	The log of the second order rate constant for cyanide addition versus sigma for the nicotinamide 2'-N-acyl- β -D-arabinosides.....	118
Figure 6.13.	The log of the rate constant for cyanide dissociation versus sigma for the nicotinamide 2'-N-acyl-arabinosides	119
Figure 6.14.	The log of the equilibrium constant for cyanide addition versus sigma for the 2'-substituted ara-NAD ⁺ analogs	120
Figure 6.15.	Resonance interaction of the 3-substituent with the lone pair on the dihydropyridine nitrogen.....	121
Figure 6.16.	Log K_{eq} versus sigma(-) for the addition of cyanide to the 3-substituted NAD ⁺ analogs.....	121
Figure 6.17.	Log k_{on} versus sigma(-) for the addition of cyanide to the 3-substituted NAD ⁺ analogs.....	121
Figure 6.18.	Potential hydrogen bonding interaction between the 2'-N-acyl substituent and the carboxamide of the nicotinamide ring.....	128

List of Schemes

Scheme 3.1.	The two general techniques for making the C-N bond between the N-1 of nicotinamide and the C-1 of a monosaccharide	32
Scheme 3.2.	The synthesis of nicotinamide 2'-deoxy- β -D-ribofuranoside	33
Scheme 3.3.	The synthesis of nicotinamide 2'-fluoro- β -D-ribofuranoside.....	34
Scheme 3.4.	The synthesis of nicotinamide 2'-fluoro-, 2'-azido-, and 2'-amino- β -D-arabinofuranoside and nicotinamide 2'-azido- and 2'-amino- β -D-ribofuranoside.....	36
Scheme 4.1.	Two mechanisms for the base-catalyzed hydrolysis of NAD ⁺	63
Scheme 4.2.	The 2'-substituted nicotinamide nucleosides	63
Scheme 4.3.	The three hydrolysis reactions of the 2'-substituted nicotinamide nucleosides.....	65
Scheme 4.4.	Anchimeric assistance by the N-acetyl group of nicotinamide 2'-N-acetyl- β -D-ribofuranoside.....	73
Scheme 4.5.	The hydrolysis of the 2'-substituted nicotinamide nucleosides by the dissociative mechanism	74
Scheme 4.6.	NAD ⁺ glycohydrolase catalyzed cleavage of the nicotinamide-glycosyl bond by the inductive stabilization mechanism	84
Scheme 6.1.	The cyanide addition reaction of a series of 2'-substituted nicotinamide β -D-ribo- and arabinofuranosides and β -NAD ⁺ analogs	109

Chapter 1
Introduction

The nicotinamide adenine dinucleotide coenzyme (NAD⁺, Figure 1.1) participates in a diversity of biochemical reactions. This coenzyme is usually associated with the oxidation-reduction chemistry catalyzed by the dehydrogenases. In this capacity the NAD⁺ molecule accepts hydride at the 4-position of the nicotinamide ring forming NADH which then acts as a repository of reducing equivalents. Less familiar is the role of NAD⁺ in enzyme-mediated group transfer. This involves fragmentation at the glycosidic bond between the N-1 of nicotinamide and the C-1' of the adjacent ribose ring generating nicotinamide and the transfer of the ADP-ribose moiety to an acceptor nucleophile. The appropriate acceptor molecule is determined by the enzyme and can include H₂O for NAD⁺ glycohydrolase, an amino acid side chain of a protein (e.g., pertussis toxin), or another ADP-ribose group (poly-ADP-ribose synthase). The proteins that catalyze the hydrolysis and group transfer reactions of NAD⁺ will be fully reviewed in chapter 2.

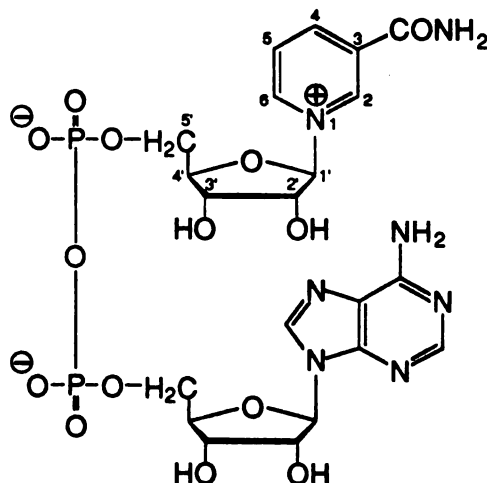


Figure 1.1. The nicotinamide adenine dinucleotide (NAD⁺) coenzyme showing the numbering scheme on the ribose and nicotinamide rings.

The mechanism of NAD⁺ hydrolysis

The nicotinamide glycosyl bond is also chemically labile and NAD⁺ is observed to hydrolyze at a measurable rate at neutral pH in the absence of enzyme. The rate of hydrolysis quickly accelerates above pH 8 becoming first order in hydroxide.¹ The mechanisms of the

enzymatic and nonenzymatic reactions have often been studied in tandem. For example, Tamus and Schuber² have synthesized a series of NAD⁺ analogs in which various 3- and 4-substituted pyridines replace the nicotinamide. They compared the rates of hydrolysis to the pK_a values of the departing pyridines in a Brønsted relationship and found β_{lg} values of -0.90 for the NAD⁺ glycohydrolase hydrolysis and -1.11 for the uncatalyzed hydrolysis at neutral pH. These values are consistent with a unimolecular dissociation of the pyridine leaving group.² Furthermore, Cordes and coworkers³ used NAD⁺ and nicotinamide mononucleotide analogs substituted with deuterium at the anomeric position to study the secondary isotope effects in the hydrolysis reaction. They found isotope effects (k_H/k_D) of 1.132 ± 0.010 for the pig brain glycohydrolase reaction, and 1.101 ± 0.005 for the pH-independent hydrolysis of NAD⁺. These isotope effects indicate substantial sp³ to sp² rehybridization in the transition state which is consistent with a dissociative mechanism involving the generation of an oxocarbenium intermediate. This group also studied the isotope effects in the hydrolysis of nicotinamide riboside.⁴ For the pH independent hydrolysis at pH 4, they found a k_H/k_D of 1.144 ± 0.008, and at pH values between 9 and 11, in which the base-catalyzed reaction dominates, they found a k_H/k_D of 1.151 ± 0.012. They point out that the most obvious explanation for the observed base catalysis would be either direct attack at the glycosyl carbon by hydroxide or an intramolecular nucleophilic displacement of nicotinamide by the ionized 2'-OH; however, the isotope effects indicate similar transition state structures and similar mechanisms between the pH-independent and base-catalyzed reactions. Thus, these results led to a puzzling question: how can a hydrolysis mechanism become first order in hydroxide (and second order overall) and still maintain its dissociative character?

To address this apparent inconsistency, Oppenheimer and coworkers⁵ reinvestigated the hydroxide-catalyzed hydrolysis of NAD⁺. They discovered that if the pH/rate profile (Figure 1.2) was extended up to pH 14, there was a levelling off in the rate of hydrolysis which is not consistent with a mechanism involving direct displacement by hydroxide. The s-shaped pH/rate profile indicated an ionization of the substrate with a pK_a of 11.7. Through a series of ¹³C NMR titration studies of NAD⁺, they determined that this pK_a corresponded to the deprotonation of the

2'-OH on the nicotinamide ribose ring. They went on to show that if the ribose diol is prevented from ionizing (by converting the diol to an isopropylidene derivative), that the base-catalyzed hydrolysis of NAD⁺ to ADP-ribose and nicotinamide is completely prevented. Furthermore, they found that if the base-catalyzed hydrolysis was conducted in methanol/water mixtures that 1) there is no selectivity by the intermediate for MeOH over H₂O as acceptor nucleophile and 2) the α and β anomers of 1-O-methyl ribose are generated in a ratio of 1:3.7. Based on these results, they favored a dissociative mechanism for NAD⁺ hydrolysis for the pH-independent as well as the base-catalyzed regions. They addressed Cordes' question by showing that the base-catalysis derives from the ionization of the 2'-hydroxyl, and proposed that the ionized diol accelerates the dissociation by electrostatically stabilizing the incipient oxocarbenium intermediate.

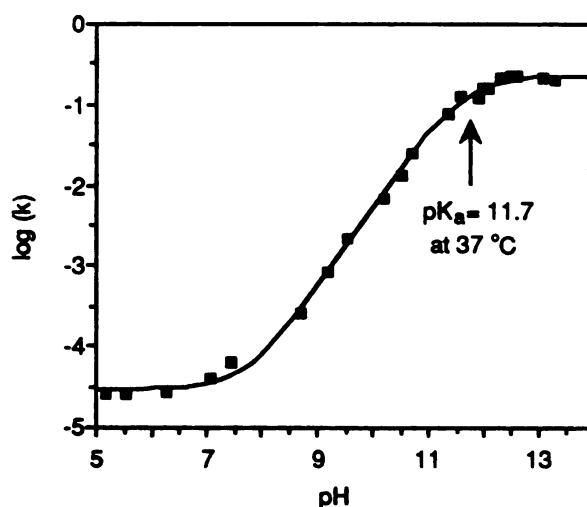


Figure 1.2. The pH/rate profile for the hydrolysis of NAD⁺ at 37 °C.⁵

The origin of the base-catalyzed hydrolysis was shown to derive from the ionization of the nicotinamide ribose diol, but the exact role of the 2'-hydroxy anion in the mechanism of the base-catalyzed hydrolysis remained a point of contention. For decades carbohydrate chemists have attributed base-catalyzed hydrolysis of glycosides to an intramolecular nucleophilic displacement by neighboring hydroxyl groups (for reviews see references 6-8). Intramolecular nucleophilic displacement has also been proposed to account for the glycosyl bond hydrolysis catalyzed by β -

galactosidase^{9,10} and lysozyme.^{11,12} In the case of NAD⁺ hydrolysis, an ionized 2'-hydroxyl could potentially act as a nucleophile displacing nicotinamide and generating a 1,2-anhydro sugar intermediate. Oppenheimer and coworkers⁵ suggested that such intermediates are probably not generated: first, an epoxide should be stable enough to discriminate between nucleophiles, yet no selectivity for methanol over water was seen in the reactions conducted in binary methanol/water mixtures. Second, they argued that if a 1,2-anhydrosugar intermediate were generated, then only β -1-O-methyl-ADP-ribose would be generated. Rather, a mixture of the α and β anomers was observed in the product ruling out an epoxide intermediate. This conclusion is suspect, however, because the most thoroughly studied 1,2-anhydrosugar, Brigl's anhydride, is known to react with alcohols in the absence of catalyst to give a mixture of anomers (Figure 1.3).¹³

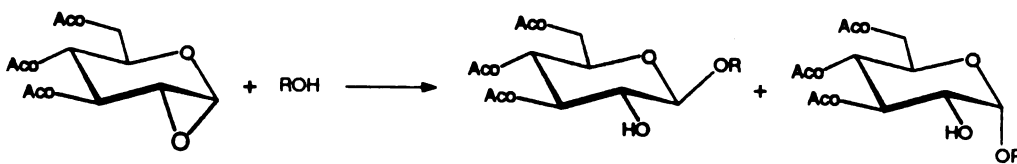


Figure 1.3. The alcoholysis of 1,2-anhydro-3,4,6-tri-O-acetyl-glucose (Brigl's anhydride) gives both the α and β glucosides.¹³

2'-Substituted nicotinamide nucleosides as mechanistic probes

The central question revolves around the specific mechanistic role of the 2'-hydroxyl in the cleavage of the nicotinamide-glycosyl bond. The present study will attempt to shed light on this question by investigating the hydrolysis kinetics of a series of 2'-substituted nicotinamide nucleosides. The substituents at the 2'-position are placed both cis and trans to the departing nicotinamide ring and have been chosen to analyze several types of substituent effects including

the electrostatic influence of charged substituents, the inductive influence of polar substituents and anchimeric assistance by nucleophilic substituents.

The 2'-substituted nicotinamide nucleosides will also be employed as substrates in the cyanide addition reaction. This reaction involves the attack of cyanide ion at the 4-position of the nicotinamide ring. The transformation between the cationic pyridinium ring and the electron-rich 1,4-dihydro adduct is analogous to the reduction NAD^+ to NADH. The cyanide addition reaction has been used as a model for studying the mechanism of NAD^+ reduction.¹⁴⁻¹⁸ Furthermore, the reactivity of pyridine nucleotides with cyanide has been found to parallel redox properties.¹⁴ The influence of the sugar moiety on the redox properties of NAD^+ has often been considered a steric effect, but the appropriate structure-reactivity study has never been conducted. Thus, the present study will be the first to model the influence of modifications in the sugar moiety to oxidation-reduction properties of the NAD^+ coenzyme.

In summary, this work will use a series of 2'-substituted nicotinamide nucleosides as models to study the effect of sugar modifications on biologically relevant reactions of the NAD^+ coenzyme. This dissertation is divided into six chapters. Chapter two will review the current knowledge of proteins that catalyze the cleavage of the nicotinamide-glycosyl bond of NAD^+ . Chapter 3 will outline the synthesis, purification and characterization of the 2'-substituted nicotinamide nucleosides. The hydrolysis kinetics will be presented in chapter 4 and implications for the mechanism of enzymatic glycosyl bond cleavage will be discussed. Chapter 5 will discuss the influence of charged substituents at the 2'-position on the hydrolysis reaction, and chapter 6 will present the cyanide addition results and will discuss the implications for the mechanism of the dehydrogenases.

References

- (1) Colowick, S.P.; Kaplan, N.O. and Ciotti, M.M. *J. Biol. Chem.* 1951, 191, 447-459.
- (2) Tamus, C. and Schuber, F. *Bioorg. Chem.* 1987, 15, 31-42.

- (3) Bull, H.G.; Ferraz, J.P.; Cordes, E.H.; Ribbi, A. and Apitz-Castro, R. *J. Biol. Chem.* **1978**, *253*, 5186-5192.
- (4) Ferraz, J.P.; Bull, H.G. and Cordes, E.H. *Arch. Biochem. Biophys.* **1978**, *191*, 431-436.
- (5) Johnson, R.W.; Marschner, T.M. and Oppenheimer, N.J. *J. Am. Chem. Soc.* **1988**, *110*, 2257-22263.
- (6) Ballou, C.E. *Adv. Carb. Chem* **1954**, *9*, 59-94.
- (7) Janson, J. and Lindberg, B. *Acta Chem. Scand.* **1959**, *13*, 138-143.
- (8) Capon, B. *Q. Rev. Chem. Soc.* **1964**, *18*, 56-106.
- (9) Wallenfels, K. and Weil, R., in "The Enzymes"; P. Boyer, Ed. Academic Press: New York, 1972; p. 575.
- (10) Jones, C.C.; Sinnott, M.L. and Souchard, I.J.L. *J. Chem. Soc. Perkin Trans II* **1977**, 1191-1198.
- (11) Piszkiwicz, D. and Bruice, T.C. *J. Am. Chem. Soc.* **1968**, *90*, 5844-5848.
- (12) Piszkiwicz, D. and Bruice, T.C. *J. Am. Chem. Soc.* **1968**, *90*, 2156-2163.
- (13) Buchanan, J.G.; Kochetkov, N.K.; Chizhov, O.S. and Bochkov, A.F., in "Carbohydrates, Organic Chemistry Series One, Volume 7"; G. O. Aspinall, Ed. Butterworths University Park Press: London, 1973; pp. 55 and 162.
- (14) Wallenfels, K. and Diekmann, H. *Justus Liebigs Ann. der Chemie* **1959**, *621*, 166-177.
- (15) Lindquist, R.N. and Cordes, E.H. *J. Am. Chem. Soc.* **1968**, *90*, 1269-1274.
- (16) Okubo, T. and Ise, N. *J. Am. Chem. Soc.* **1973**, *95*, 4031-4036.
- (17) Bunting, J.W. and Sindhuatmadja, S. *J. Org. Chem.* **1980**, *45*, 5411-5413.
- (18) Lovesey, A.C. *J. Med. Chem.* **1969**, *12*, 1018-1023.

Chapter 2

Enzymes that Cleave the Glycosyl Bond of NAD⁺: ADP-Ribosyltransferases and NAD⁺ Glycohydrolases.

The ADP-ribosyltransferases and NAD⁺ glycohydrolases represent a diverse group of enzymes that catalyze cleavage of the nicotinamide-glycosyl bond of NAD⁺ as shown in Figure 2.1. These enzymes are found throughout prokaryotic and eukaryotic life. Their function derives from the large free energy of hydrolysis of the nicotinamide-glycosyl bond that is comparable to that for the hydrolysis of the γ -phosphate of ATP. Thus NAD⁺ can be viewed as an "activated" ADP-ribose. This chapter will first provide a brief description of the enzymes involved and then discuss the chemistry and enzymology of ribosyl bond cleavage including stereochemical and mechanistic aspects (for recent reviews on biological and biochemical aspects of these enzymes see references 1 and 2).

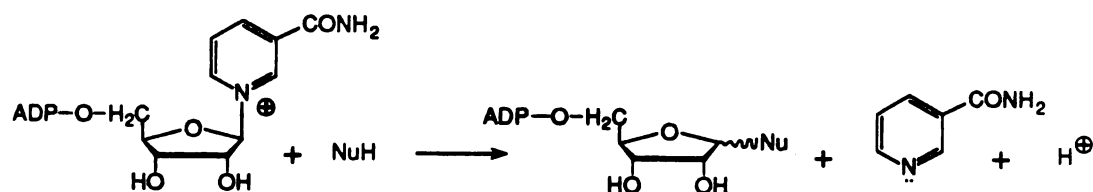


Figure 2.1. Generalized cleavage of the nicotinamide ribosyl bond with formation of a linkage to a new nucleophile.

The enzymes that catalyze cleavage of the nicotinamide ribosyl bond are divided into two major classes; ADP-ribosyltransferases and NAD-glycohydrolases. Their distinction lies in what happens after cleavage of the glycosyl bond.

ADP-ribosyltransferases catalyze the formation of an ADP-ribosyl bond to a specific amino acid residue on a target protein or other acceptor molecule. The covalent modification then alters the activity or function of the target protein. This class of proteins includes bacterial toxins, bacterial activating proteins, endogenous ADP-ribosyltransferases and the eukaryotic poly(ADP-ribose) synthase.

The NAD⁺ glycohydrolases constitute the second major class of proteins involved in nicotinamide-glycosyl bond cleavage. This activity is widely distributed in mammalian tissue as well as other prokaryotic and eukaryotic organisms although its biological function is not understood. There are two mechanistically distinct categories of NAD-glycohydrolases, strict hydrolases (nicotinamide insensitive) and those that conduct transglycosidation (nicotinamide sensitive). All NAD⁺ glycohydrolases catalyze the hydrolytic cleavage of the nicotinamide-glycosyl bond yielding ADP-ribose and nicotinamide. Those that catalyze trans-glycosidation also exchange the nicotinamide moiety of the ADP-ribose moiety with an exogenous nucleophilic acceptor or another pyridine base. These enzymes have been invaluable in the preparation of NAD⁺ analogs.³⁻⁵

ADP-ribosyltransferases: MonoADP-ribosylation.

Mono-ADP-ribosyltransferases are found in both eukaryotes and prokaryotes. The bacterial toxins are the best understood in terms of structure and function. These toxins include: cholera toxin, diphtheria toxin, pertussis toxin, botulinum D toxin and functionally related toxins. The target for ADP-ribosylation is unique for each toxin and the toxins have proven invaluable in elucidating the functioning of the targets. In all cases studied thus far the covalent attachment of the ADP-ribose group to the target proceeds with inversion at the (nicotinamide)-ribose C1 to generate α -linkages. In the absence of appropriate acceptors the mono-ADP-ribosyltransferases also catalyze a much slower hydrolysis of NAD⁺. This latter reaction occurs without detectable methanolysis, thus precluding stereochemical analysis of the hydrolytic reaction. The enzymes and acceptor preferences for these enzymes are summarized in Table 2.1.

Table 2.1. Acceptor Preferences for the ADP-ribosyltransferases.

Transferase	Acceptor
Bacterial	
Cholera Toxin	arginine ^{6, 7}
Pertussis Toxin	cysteine ^{8, 9}
Diphtheria Toxin	diphthamide ^{10, 11}
<i>Pseudomonas Aeruginosa</i> Exotoxin A	diphthamide ^{12, 13}
Botulinum C1 toxin	asparagine ¹⁴
C2 toxin	arginine ¹⁵
Eukaryotic	
NAD:Arginine ADPRTase	arginine ^{6, 16}
NAD:cysteine ADPRTase	cysteine ¹⁷
Poly(ADP-ribose) synthase	glutamic acid γ -COOH (Histone H1), adenosine ribose 2'-OH, and (nicotinamide) ribose 2'-OH ¹⁸

Cholera Toxin.

Cholera toxin catalyzes the attachment of ADP-ribose to an arginine side chain of the $G_{s\alpha}$ subunit of the guanine nucleotide binding protein in the adenylate cyclase regulatory system.^{6,19} This covalent modification disrupts the GTPase activity of the subunit leading to sustained activation of adenylate cyclase. The toxin consists of two subunits; the A subunit possesses the enzymatic activity and the B subunit is responsible for binding of the toxin to the cell surface but is otherwise non-toxic.¹⁸ In vitro, arginine and other guanidino compounds act as acceptors of ADP-ribose,¹⁹ and these compounds can inhibit the ADP-ribosylation of proteins by competing for the active site of the toxin.⁶ Cholera toxin also ADP-ribosylates arginine in transducin, a protein of retinal rod outer segments, which is homologous to G_s in both structure and function.⁷ Cholera toxin initially generates α -ADP-ribosylarginine, i.e., the reaction proceeds with inversion

of configuration at the ribose C1 as shown in Figure 2.2.²⁰ Under optimal conditions for ADP-ribosyltransferase activity of cholera toxin, the rate of ADP-ribosylation is twenty times that of NAD⁺ hydrolysis.²¹

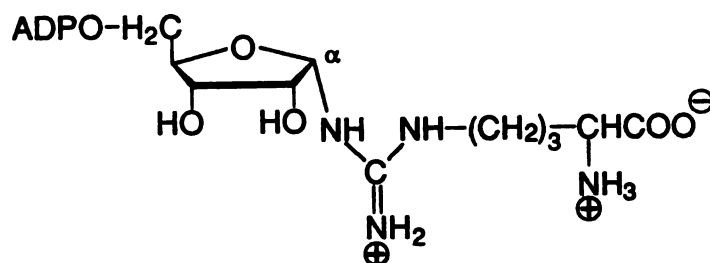


Figure 2.2. α -ADP-ribosylarginine

Pertussis Toxin.

Pertussis Toxin was first investigated as an activator of pancreatic islet cells.⁶ The toxin ADP-ribosylates G_i, the inhibitory guanine nucleotide binding protein of the adenylate cyclase regulatory system, and leads to cAMP accumulation inside the cell.⁶ Pertussis toxin reduces or abolishes G_i mediated signal transduction from a wide range of inhibitory receptors including opiate, prostaglandin E₁, alpha₂-adrenergic, muscarinic-cholinergic, dopamine and adenosine in a variety of mammalian cells.¹⁸

Pertussis toxin consists of five subunits, S1 to S5. The S1 subunit (or A protomer) is responsible for the ADP-ribosyltransferase activity and also possesses NAD⁺ glycohydrolase activity.⁹ Cysteine has been identified as the amino acid residue in transducin ADP-ribosylated by the toxin;⁸ and recently thiols, such as cysteine and dithiothreitol, have been reported to be ADP-ribosylated by pertussis toxin.⁹ No data on the stereochemistry of this linkage is available. Several groups are attempting to characterize the structure of the S1 subunit^{22, 23} and to identify the amino acid residues essential for enzymatic activity.^{24, 25} Interestingly there is a sequence identity in a portion of the active subunits of cholera and pertussis toxins, and antibodies raised to

residues 6-17 of the pertussis subunit will also bind to the A subunit of cholera toxin.²² The two toxins are clearly distinct in regards to their target specificity, yet both exhibit NAD⁺-glycohydrolase activity suggesting that the homologous regions may be responsible for binding and labilizing NAD⁺.

Diphtheria Toxin.

Diphtheria toxin disrupts cell function by ADP-ribosylating a unique, post-translationally modified histidine acceptor, diphthamide, found only in eukaryotic elongation factor-2 (Figure 2.3).¹⁰ Nuclear Overhauser enhancement experiments established that the imidazole N-1 of diphthamide is covalently linked to ADP-ribose via an α -glycosidic linkage.¹¹

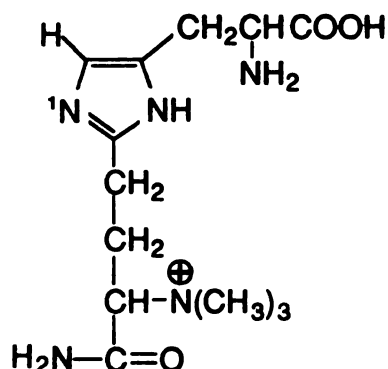


Figure 2.3. Diphthamide

Exotoxin A produced by the aerobic bacteria *Pseudomonas aeruginosa*²⁶ possesses the same catalytic activity as diphtheria toxin,¹⁸ including ADP-ribosylation of EF-2 on the same site.¹³ The reaction is reversible since ADP-ribosylated EF-2 produced by exotoxin A can be de-ribosylated (functional activity restored) by incubating with excess nicotinamide and either excess exotoxin A or subunit A of diphtheria toxin. NAD⁺ was identified as the sole product of this reverse reaction.¹³ These results also establish that the configuration and site of ADP-ribosylation catalyzed by Exotoxin A is identical to that of diphtheria toxin.

Irradiation of the NAD⁺-diphtheria toxin binary complex at 254 nm results in the photo-inactivation of the toxin and fragmentation of the NAD⁺ via attachment at the N6 position of the nicotinamide ring to the γ -methylene of Glu-148.²⁸ Glutamic acid-148 was subsequently found to be essential for catalysis (without affecting the binding of NAD⁺) using site-directed mutagenesis to substitute Glu-148 with Asp.^{28, 29} *Pseudomonas aeruginosa* exotoxin A showed an analogous photoaffinity labelling with NAD⁺; however, the nicotinamide was attached to the decarboxylated side chain of glutamic acid-553.³⁰ Site-specific substitution of Glu-553 for aspartic acid results in an 1800-fold decrease in enzymatic activity, thus confirming that the exact positioning of the carboxyl group is crucial to catalysis.³¹ Little sequence identity is noted between the two proteins using conventional comparisons, but when the active site glutamic acid residues are aligned, regions of identity in the primary structure of the active sites become apparent.³⁰

Botulinum toxins.

Strains of *Clostridium Botulinum* produce toxins with ADP-ribosylation activity. Botulinum C1 toxin ADP-ribosylates a guanine nucleotide binding protein (G_b) that is widely distributed in various mammalian tissues.³² Recent results suggest that the site of ADP-ribosylation is an asparagine residue.¹⁴ Botulinum C2 toxin ADP-ribosylates cytoplasmic actin at arginine-177, but the stereochemistry of addition has not been established.¹⁵ This result is significant since it represents the first time that an NAD-dependent toxin has been directed at a target other than a GTP binding protein and thus may signal the presence of a new range of toxin targets. Botulinum toxin type C3 has recently been purified and characterized.³³ This ADP-ribosyltransferase targets a 21-24 kDa protein in human platelets, fibroblasts and several other tissues. The substrate of ADP-ribosylation has been purified from porcine brain and has been identified as a GTP-binding protein.³⁴ The specific amino acid residue that is ADP-ribosylated has not been determined. Botulinum toxin type D ADP-ribosylates a 21 kDa protein from bovine adrenal gland which has a molecular weight similar to some recently discovered G proteins.³⁵ ADP-ribosyltransferase activity

of the type D toxin is inhibited by agmatine and L-arginine methyl ester, suggesting that the ADP-ribosyl acceptor is also the guanidino group of arginine. However, unlike cholera toxin, type D toxin does not ADP-ribosylate arginine or agmatine when incubated with NAD⁺.³⁵

Other ADP-ribosyltransferase activities.

Endogenous mono-ADP-ribosyl transferase activities have also been found in both prokaryotes and eukaryotes. In eukaryotes, these proteins represent only "activities"; their physiological purpose is not understood. Arginine-dependent ADP-ribosyltransferases have been found in a wide range of animal tissues including turkey erythrocytes, hen liver, rat liver, and porcine skeletal muscle.⁶ These enzymes, like cholera toxin, activate the nicotinamide-glycosyl bond of NAD⁺ and transfer the ADP-ribose group to arginine and other guanidines in vitro. Also like cholera toxin, the NAD:arginine ADP-ribosyltransferase from turkey erythrocytes catalyzes formation of an α -glycosidic linkage between arginine and ADP-ribose.¹⁶ A separate enzyme has been isolated from turkey erythrocytes that cleaves the arginine-ribose bond of α -ADP-ribosylarginine⁶ thus forming the basis for a possible regulatory cycle although no target metabolic pathway has been identified in eukaryotes. A hen liver nuclear enzyme that ADP-ribosylates agmatine, arginine, and histones has been purified to homogeneity.¹⁸ Its specific target protein(s) and biological function are unknown. The only such regulatory system that has all three components: a well-defined target protein, a specific ADP-ribosyltransferase, and an ADP-ribosyl hydrolase, has been identified for the prokaryotic regulation of bacterial nitrogenase activity based on reversible ADP-ribosylation at arginine.³⁶

ADP-ribosyltransferases specific for EF-2 have been isolated from rat liver³⁷ and beef liver.¹⁸ The fact that intoxication with only one molecule of diphtheria toxin A fragment is sufficient to kill a cell suggests that ADP-ribosylation of diphthamide is irreversible, i.e., there is no enzymatic activity that cleaves the α -ribosyl-diphthamide bond. Therefore the regulatory function of an endogenous protein that inactivates EF-2 is obscure. Recently, a cysteine-specific ADP-ribosyltransferase was purified from human erythrocytes that also catalyzes the ADP-ribosylation

of G_i (the target of pertussis toxin). Pretreatment of G_i with pertussis toxin and NAD^+ inhibits the human enzyme, thus suggesting that both enzymes are specific for the same acceptor residue.¹⁷ Whether the ADP-ribosylation of G_i is its physiological role remains to be determined.

ADP-ribosyltransferases: Poly(ADP-ribosylation).

Poly(ADP-ribose) synthase^{18,38} is a eukaryotic nuclear enzyme that catalyzes three reactions: i). the transfer of the ADP-ribose group of NAD^+ to other nuclear proteins (including itself), ii). the polymerization of ADP-ribose units, and iii). branching of the ADP-ribose polymers. Poly(ADP-ribose) is composed of 2 to 200 repeating adenosine diphosphate ribose units¹⁸ in which the adenosine ribose 2'-OH is linked to the next ADP-ribose group through an α -1''-2' glycosidic bond (Figure 2.4-2.6).³⁹ Pulse-chase experiments with radio-labelled NAD^+ confirm that the polymerization occurs by a mechanism in which the first ADP-ribose unit is covalently attached to the protein followed by successive additions of ADP-ribose to the adenosine 2'-OH of the previous unit.⁴⁰ Typically 2-3% of the ADP-ribose moieties in a polymer are subject to branching in which the ADP-ribose unit is linked to the 2'-OH of the (nicotinamide) ribose group instead of the adenosine ribose group.¹⁸

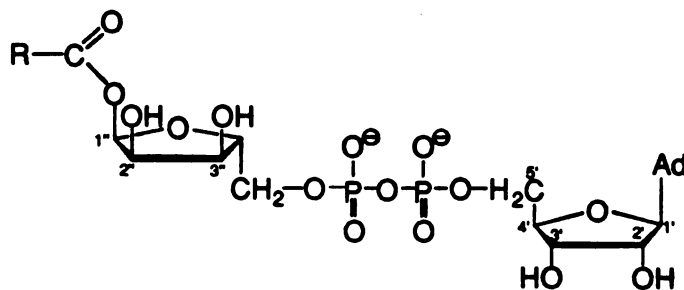


Figure 2.4: Structure of the ADP-ribosyl linkage to the γ -carboxylate of glutamate that attaches the poly(ADP-ribose) chain to a protein.

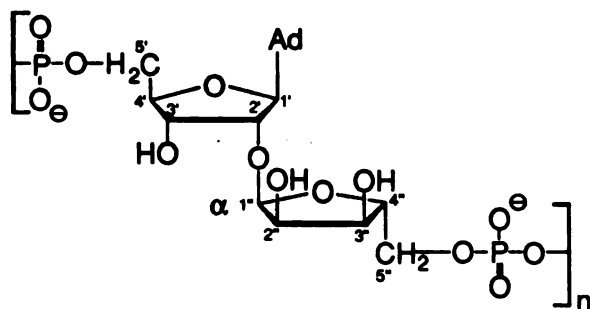


Figure 2.5. Structure of adenosine monophosphate- α -O2''-O1''-ribose-5-phosphate, the monomeric unit of poly(ADP-ribose) containing an α -glycosyl linkage to the adenine 2'-hydroxyl.

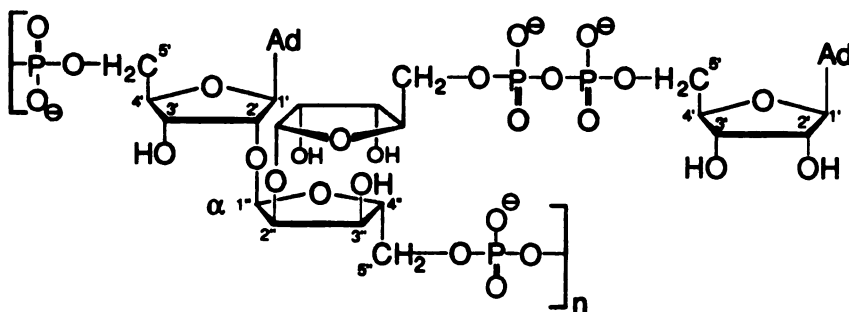


Figure 2.6. Structure of a branch point in poly(ADP-ribose) formed by attachment at the 2'-hydroxyl (formerly the nicotinamide ribose) of an ADP-ribose monomeric unit.

Stereochemically and functionally the synthase is a remarkable enzyme. All evidence points to a single protein conducting the three distinct reactions, presumably in the same active site (although the size of the protein does not rule out multiple catalytic domains). The cleavage of the nicotinamide-glycosyl bond generates an acylal linkage to a glutamate or aspartate carboxylate (stereochemistry unknown). Note that the attacking nucleophile is a carboxylate at the end of a flexible side chain. Elongation involves cleavage of the nicotinamide-glycosyl bond with formation of an α -linkage to the adenosine 2'-hydroxyl. The nucleophile is the 2'-hydroxyl, trans to the adenine ring. Finally, branching occurs through formation of an α -glycosyl linkage

with the ribose 2' hydroxyl of the polymer (the former nicotinamide ribose) cis to an adenosine moiety. The great disparity in the steric and electronic attributes of the nucleophiles engaged in the three reactions makes this either a truly unique single active site, or makes this enzyme a prime candidate for the involvement of multiple catalytic domains.

NAD⁺ Glycohydrolases.

NAD⁺ glycohydrolases (NADases) have been isolated from a diverse range of animal tissues including calf spleen,⁴¹ pig brain,⁴² bull semen,⁴³ and snake venom.⁴⁴ In contrast to the proteins already considered, very little is understood about the biological roles of the NAD⁺ glycohydrolases. The primary reaction catalyzed by these enzymes is hydrolysis of the nicotinamide-ribose bond of β -NAD⁺. The NADases have been divided into two mechanistically distinct categories, those that are nicotinamide sensitive and those that are not. The nicotinamide-sensitive NADases also catalyze alcoholysis and transglycosidation, i.e., exchange of the nicotinamide group for exogenous pyridine bases or other nucleophilic heterocycles.^{3, 5} The NAD⁺ glycohydrolase from calf spleen proceeds by a uni-bi mechanism with nicotinamide being released first followed by ADP-ribose release.⁴⁵ Catalysis of transglycosidation implies the presence of a relatively stable "high energy" ADP-ribosyl-enzyme intermediate of unknown structure.

The stereochemical outcome of the NAD⁺ glycohydrolase reaction is opposite to that of the ADP-ribosyltransferase reaction. Hydrolysis of β -NAD⁺ by calf spleen NAD-glycohydrolase in aqueous methanol solutions occurs with $\geq 99\%$ retention of configuration for the resulting 1'-O-methyl-ADP-ribose, although a small, and possibly significant, amount of inverted product is also recovered.⁴⁶ Methanolysis catalyzed by NAD⁺ glycohydrolase from pig brain also proceeds with retention of configuration.⁴⁷

Coenzyme analogs and inhibitors.

Attempts have been made to design mechanism-based inhibitors of NAD⁺-glycohydrolases based on the intermediacy of an oxocarbenium ion. Potent inhibitors of NAD⁺ glycohydrolase would be valuable in investigating the biological role of these enzymes as well as in further elucidating their enzymatic mechanism. The first such compound was ADP-ribonolactone (Figure 2.7). The K_i for ADP-ribonolactone is 115 μM, only 9 times better than ADP-ribose (K_i = 1.0 mM) despite the planar atom at C1'.^{48*} The carbocyclic analog of NAD⁺ containing a 1-N-nicotinamide-2,3-dihydroxycyclopentane adenine dinucleotide (carba-NAD⁺) is a structural analog of the substrate containing a C-N bond to the nicotinamide ring that should be resistant to hydrolysis.⁴⁹ As anticipated it is not a substrate for NAD⁺ glycohydrolase; however, it is not a particularly good inhibitor either: its inhibition constant is comparable to that for ADP-ribonolactone. Interestingly the L-carbocyclic ribose analog ψ-carbaNAD⁺ (Figure 2.8) is a better inhibitor with a K_i of 6.7 μM for the cow brain NADase.⁵⁰

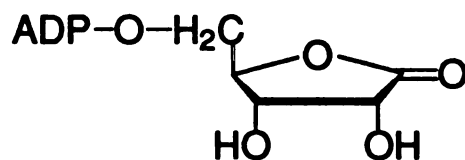


Figure 2.7: Ribonolactone

Unlike dehydrogenases, enzymes cleaving the glycosyl bond are extremely sensitive to modifications of the sugar moiety. The arabino analogs, 2'-fluoro-arabino-NAD⁺ (Figure 2.9) and arabino-NAD⁺ are both potent, slow-binding competitive inhibitors of calf spleen NADase with K_i's of 170 nM and 2 mM, respectively.⁵² The rate of enzyme-catalyzed hydrolysis of 2'-F-ara-NAD⁺ is

* A lactone has been successfully used to inhibit lysozyme, another enzyme that cleaves glycosyl-bonds and is thought to generate an oxocarbenium intermediate.⁵¹

less than 10^{-6} that for NAD^+ hydrolysis and the upper limit for the arabino- NAD^+ analog is $< 10^{-5}$ that of NAD^+ .⁵² The results are summarized in Table 2.2.

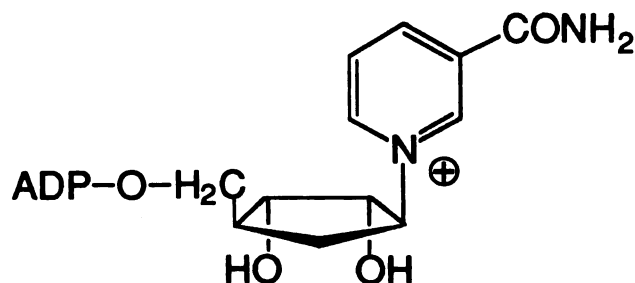


Figure 2.8 ψ -carba NAD^+

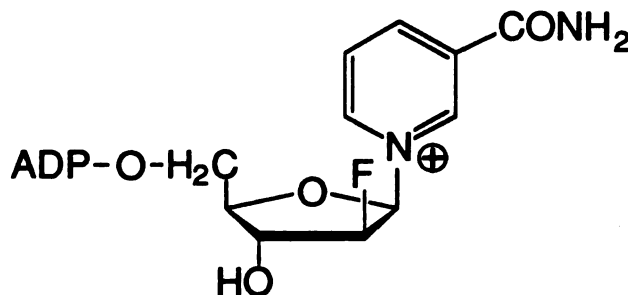


Figure 2.9: 2'-fluoro-2'-deoxy-nicotinamide arabinoside adenine dinucleotide

Table 2.2: Rates of hydrolysis and inhibitory constants for NAD analogs.

Inhibitor or (substrate)	K_i or (K_m) (μM)	dissociation rate		non-enzymatic hydrolysis
		$k_{\text{off}} \times 10^3$ (s^{-1})	$t_{1/2}$ (min)	$k_h \times 10^8$ (37 °C) (s^{-1})
ara-2'-F- NAD^+	0.17	3.45	3.35	1.6
ara- NAD^+	2.0	3.88	2.97	15.8
(NAD^+)	(15.0)	—	—	48.3

The lack of activity of the 2'-fluoro-arabino-NAD⁺ analog can be rationalized *in part* by the inductive destabilization of the putative oxocarbenium intermediate by the neighboring fluorine atom. The substituent at the 2'-position of the sugar ring exerts a powerful inductive effect on the stability of the glycosyl bond. The non-enzymatic hydrolysis of 2'-F-ara-NAD⁺ is 3% the rate of NAD⁺.⁵³ On the other hand, no such explanation can be offered for the ara-NAD⁺ analog which hydrolyzes non-enzymatically at 33% the rate of NAD⁺. Thus the intrinsic stability of the nicotinamide-glycosyl bond in the ara-NAD⁺ analogs alone does not explain why they fail to be substrates for the calf spleen NADase. Clearly alterations at the 2'-position enhance binding, yet render the coenzyme dysfunctional with respect to cleavage of the glycosyl bond. This suggests that the 2'-hydroxyl of the ribose has a key function in either catalysis or productive binding in the active site.

Mechanistic overview.

Mechanistically, the stereochemistry of the ADP-ribosyltransferases and NAD-glycohydrolases defines the relative orientations of the reactants. Thus far all the ADP-ribosyltransferases catalyze the formation of α -ribosidic linkages. These results establish that the acceptor must be bound distal to the departing nicotinamide group. Although such an arrangement would be stereochemically conducive to an in-line associative displacement reaction, the mechanism of cleavage of the nicotinamide-ribose bond and formation of the linkage to the acceptor remains to be determined. The observation of hydrolysis in the absence of acceptors suggests that ADP-ribosyltransferases labilize the nicotinamide-ribosyl bond without the need or participation of a specific acceptor nucleophile. How toxins can conduct hydrolysis but not methanolysis remains an open question, especially in view of the latter's greater nucleophilicity.^{54,55} This discrimination is neither consistent with water attacking via the site formerly occupied by the departed nicotinamide (retention), nor with water attacking in place of the acceptor moiety (inversion). Since both nicotinamide and the acceptors are considerably larger than methanol, steric exclusion of methanol seems unlikely.

The hydrolysis of β -NAD⁺ catalyzed by pig brain NADase⁴⁷ and calf spleen NADase⁴⁶ occurs with retention of configuration. These results establish that the incoming nucleophile attacks from the same side as that formerly occupied by the nicotinamide ring. Such an arrangement is fully consistent with the ping-pong kinetics and suggested enzyme-bound intermediate observed for the reaction.⁴⁵

Substantial secondary deuterium kinetic isotope effects have been observed for the hydrolysis of [1'-²H] labeled NAD⁺ and related compounds by both NADases that catalyze transglycosidation and those that are strict hydrolases. These results are consistent with appreciable sp³ to sp² rehybridization during the cleavage of the glycosyl bond,⁴² and point to an oxocarbenium ion intermediate. Linear free-energy relationships for the calf spleen NADase-catalyzed hydrolysis of NAD⁺ analogs with various substituents at either the C-3 or C-4 of the pyridine ring show that the rate of hydrolysis is inversely correlated with the pK_a of the departing pyridine.⁵⁶ A Brønsted plot of log(V_{rel}) vs. pK_a gives a slope of $\beta_{lg} = -0.9$ over 4 pK_a units. The sign and magnitude of this slope indicates the development of electron deficiency with a large degree of bond-breaking in the transition state. Interestingly, only NAD⁺ and NMN⁺ deviated from the plot and were hydrolyzed 14 and 2.8 times faster respectively than anticipated from their pK_a values. These results suggest that interactions at the carboxamide, such as increased electron withdrawal by strong hydrogen bonding to a proton donor, might be used to labilize further the glycosidic bond.

Cleavage of the glycosyl bond by calf spleen NADase differs fundamentally from the non-enzymatic reaction with respect to reactivity with exogenous nucleophiles. Non-enzymatic hydrolysis of β -NAD⁺ shows no significant discrimination on the basis of nucleophilicity of the attacking group.^{55, 57} In contrast, the calf spleen NADase discriminates strongly between acceptor nucleophiles and reacts 50 times faster with methanol than with water. This suggests that the ADP-ribosyl • enzyme intermediate generated in the reaction is equilibrated with its potential nucleophiles.⁵⁵ Given the vanishingly short life time expected for oxocarbenium ions^{58,59} the nature of stabilization in the active site is of considerable interest.

There is a mechanistic dilemma for the enzyme-catalyzed hydrolysis of NAD⁺. As discussed by Cordes and coworkers, an enzyme conducting cleavage of a nicotinamide-glycosyl bond via a dissociative mechanism has few possible means to promote catalysis.⁴² General acid catalysis is ruled out because the leaving group is already cationic. General base or nucleophilic catalysis is excluded by the large secondary kinetic isotope effects. Finally, since both the transition state and substrate possess positive charges, the importance of their differential electrostatic stabilization is greatly diminished. In the absence of viable mechanistic alternatives catalysis by distortion was invoked in order to explain how the enzyme accelerates the rate of cleavage of the glycosyl bond.

The inability of these enzymes to cleave the furanosyl bond in the arabino analogs argues against catalysis by strain. There is no obvious reason why an arabino configuration should so effectively preclude the requisite distortions, especially in view of their high affinity. The extreme sensitivity of the reaction to the sugar configuration suggests a mechanistic involvement of the 2'-hydroxyl. Recent studies of the non-enzymatic hydrolysis of NAD⁺ at high pH provides an alternative mechanism for catalysis.⁵⁷ The pH profile for the aqueous hydrolysis of NAD⁺ shows that the alkaline lability of NAD⁺ does not stem from direct attack of hydroxide. Rather, ionization of the ribose diol (pK_a = 11.9 at 37 °C) accelerates hydrolysis by over four orders of magnitude relative to hydrolysis in the neutral sugar. The rate of hydrolysis for the diol anion was attributed to electrostatic stabilization of an oxycarbocation intermediate. Direct anchimeric attack by the anion cannot be ruled out; however, the intermediacy of 1,2 anhydrosugars provides a less satisfactory explanation for most of the experimental evidence as discussed in Ref. 57.

The thermodynamic activation parameters for the chemical hydrolysis of the neutral diol and diol anion are compared in Table 2.3. Ionization of the diol results in a near complete rupture of the nicotinamide-ribosyl bond (ΔH^\ddagger decreases to 11.8 kcal/mol) that is largely compensated for by the decrease in ΔS^\ddagger to -30.8 eu, thus the overall $\Delta\Delta G^\ddagger$ is only 5.2 kcal/mol corresponding to a rate increase of approximately 10^4 . These results provide the basis for a plausible mechanism of enzyme catalysis. Electron donation directed at the 2'-hydroxyl labilizes the glycosyl linkage. If

the enzyme were to cause an increase in electron density on the diol equivalent to that of ionization, then a corresponding decrease in ΔH^\ddagger would be anticipated. If the enzyme were also to provide an entropically structured environment for the activated complex, the result would be to bring the large $-\Delta S^\ddagger$ toward zero. The overall consequence would be a rate acceleration far larger even than the four orders of magnitude increase in hydrolysis due to diol ionization observed for the solution reaction.

Table 2.3. Activation Parameters for NAD Hydrolysis at 25 °C.⁵⁷

pH	ΔH^\ddagger (kcal/mol)	ΔS^\ddagger (eu)	ΔG^\ddagger (kcal/mol)
6.2	25.2 ± 1.7	-3.3 ± 2.5	26.2 ± 2.5
13.4	11.8 ± 0.5	-30.8 ± 1.5	21.0 ± 0.9

Such a mechanism based on entropic control would circumvent the Cordes dilemma and would account for the mechanistic importance of the 2'-ribo-hydroxyl. In the absence of the properly configured 2'-hydroxyl, electrostatic interactions with basic groups in the active site would be redirected to the nicotinamide ring. Such interactions would then serve both to promote binding and to stabilize the glycosyl bond. Photoaffinity reactions of NAD⁺ combined with site-directed mutagenesis have demonstrated the presence of a carboxylate in the active sites of diphtheria toxin and pseudomonas exotoxin A.³⁰ The principles being elucidated for the NADases should be generally applicable to all glycohydrolases that operate by a dissociative mechanism and have similarly acidic functional groups at the 2' position. A classic example of an enzyme meeting these criteria is lysozyme. It has two carboxylates in the active site and a substrate with a 2'-substituent having a pK_a of approximately 12. Present theories for catalysis primarily involve "catalysis by strain or distortion" arguments (for a recent review see Reference

60) and do not satisfactorily address the chemical nature of catalysis. Therefore, lysozyme and related glycosidases are likely candidates for a mechanism similar to that outlined here.*

References

- (1) Jacobson, M. and Jacobson, E. *ADP-Ribose Transfer Reactions*; Springer-Verlag: New York, 1989.
- (2) Moss, J. and Vaughn, M. *ADP-Ribosylation and G Proteins*; American Society for Microbiology: Washington, D.C., 1990.
- (3) Woenckhaus, C. and Jeck, R., in "Pyridine Nucleotide Coenzymes"; D. Dolphin, R. Poulson and O. Avramovic, Eds. John Wiley and Sons: New York, 1987; pp. 449-568.
- (4) Anderson, B.M., in "The Pyridine Nucleotide Coenzymes"; J. Everse, B. M. Anderson and K.-S. You, Eds. Academic Press: New York, 1982; pp. 109-110.
- (5) Anderson, B.M. and Kaplan, N.O., in "Pyridine Nucleotide Coenzymes"; D. Dolphin, R. Poulson and O. Avramovic, Eds. John Wiley and Sons: New York, 1987; pp. 569-612.
- (6) Moss, J. and Vaughan, M. *Adv. Enzymol.* **1987**, *61*, 303-379.
- (7) Van Dop, C.; Tsubokawa, M.; Bourne, H.R. and Ramachandran, J. *J. Biol. Chem.* **1984**, *259*, 696-698.
- (8) West, R.E.; Moss, J.; Vaughan, M.; Liu, T. and Liu, T.Y. *J. Biol. Chem.* **1985**, *260*, 14428-14430.
- (9) Lobban, M.D. and von Heyningen, S. *FEBS Letters* **1988**, *233*, 229-232.
- (10) Van Ness, B.G.; Howard, J.B. and Bodley, J.W. *J. Biol. Chem.* **1980**, *255*, 10717-10720.

*For comparison, the parameters for the β -galactosidase-catalyzed hydrolysis of the 3-chloro-1-(β -D-galactopyranosyl)pyridinium are: $\Delta H^\ddagger = 11.6 \pm 0.8 \text{ kcal mol}^{-1}$ and $\Delta S^\ddagger = -11.8 \pm 2.7 \text{ cal mol}^{-1} \text{ }^\circ\text{K}^{-1}$.⁵⁷ However, corresponding values for the fully base-catalyzed reaction (with possible involvement of a sugar anion) are not available. Note that the activation parameters for the base-catalyzed portion of the pH profile are ambiguous. If base-catalysis is due to a sugar anion, then the large temperature-dependence of the pK_a of the ionizing group has to be taken into account. For NAD^+ this means measuring these values above the pK_a of the diol in a pH region where the reaction is pH independent.⁶¹

- (11) Oppenheimer, N.J. and Bodley, J.W. *J. Biol. Chem.* **1981**, *256*, 8579-8581.
- (12) Pastan, I. and Fitzgerald, D. *J. Biol. Chem.* **1989**, *264*, 15157-15160.
- (13) Iglewski, B.H.; Liu, P.V. and Kabat, D. *Infect. Immun.* **1977**, *15*, 138-144.
- (14) Sekine, A.; Fujiwara, M. and Narumiya, S. *J. Biol. Chem.* **1989**, *264*, 8602-8605.
- (15) Vandekerckhove, J.; Schering, B.; Barmann, M. and Aktories, K. *J. Biol. Chem.* **1988**, *263*, 696-700.
- (16) Moss, J.; Stanley, S.J. and Oppenheimer, N.J. *J. Biol. Chem.* **1979**, *254*, 8891-8894.
- (17) Tanuma, S.; Kawashima, K. and Endo, H. *J. Biol. Chem.* **1988**, *263*, 5485-5489.
- (18) Althaus, F.R. and Richter, C. *ADP-Ribosylation of Proteins*; Springer-Verlag: Berlin, 1987; pp.3-197.
- (19) Moss, J. and Vaughan, M. *Ann. Rev. Biochem.* **1979**, *48*, 581-600.
- (20) Oppenheimer, N.J. *J. Biol. Chem.* **1978**, *253*, 4907-4910.
- (21) Osborne, J.C.; Stanley, S.J. and Moss, J. *Biochemistry* **1985**, *24*, 5235-5240.
- (22) Burns, D.L.; Hausman, S.Z.; Lindner, W.; Robey, F.A. and Manclark, C.R. *J. Biol. Chem.* **1987**, *262*, 17677-17682.
- (23) Pizza, M.; Bartoloni, A.; Prugnola, A.; Silvestri, S. and Rappuoli, R. *Proc. Natl. Acad. Sci. USA* **1988**, *85*, 7521-7525.
- (24) Loch, C.; Capiou, C. and Feron, C. *Proc. Natl. Acad. Sci. USA* **1989**, *86*, 3075-3079.
- (25) Kaslow, H.R. and Lesikar, D.D. *Biochemistry* **1987**, *26*, 4397-4402.
- (26) Palleroni, N.J., in "Genetics and Biochemistry of Pseudomonads"; P. H. Clarke and M. H. Richmond, Eds. John Wiley: New York, 1975; pp. 1-36.
- (27) Thompson, M.R. and Iglewski, B.H., in "ADP-ribosylation Reactions"; O. Hayaishi and K. Ueda, Eds. Academic Press: New York, 1982; pp. 698.
- (28) Carroll, S.F. and Collier, R.J. *Proc. Natl. Acad. Sci. USA* **1984**, *81*, 3307-3311.
- (29) Tweten, R.K.; Barbieri, J.T. and Collier, R.J. *J. Biol. Chem.* **1985**, *260*, 10392-10394.
- (30) Carroll, S.F. and Collier, R.J. *J. Biol. Chem.* **1987**, *262*, 8707-8711.
- (31) Douglas, C.M. and Collier, R.J. *J. Bacteriol.* **1987**, *169*, 4967-4971.

- (32) Mori, N.; Sekine, A.; Ohashi, Y.; Nakao, K.; Imura, H.; Fujiwara, M. and Narumiya, S. *J. Biol. Chem.* **1988**, *263*, 12420-12426.
- (33) Aktories, K.; Rosener, S.; Blaschke, U. and Chhatwal, G.S. *Eur. J. Biochem.* **1988**, *172*, 445-450.
- (34) Braun, U.; Habermann, B.; Just, I.; Aktories, K. and Vandekerckhove, J. *FEBS Lett.* **1989**, *243*, 70-76.
- (35) Ohashi, Y. and Narumiya, S. *J. Biol. Chem.* **1987**, *262*, 1430-1433.
- (36) Lowery, R.G. and Luddon, P.W. *J. Biol. Chem.* **1988**, *263*, 16714-16719.
- (37) Sayhan, O.; Ozdemirli, M. and Bermek, E. *Biochem. Biophys. Res. Comm.* **1986**, *139*, 1210-1214.
- (38) Ueda, K. and Hayaishi, O. *Ann. Rev. Biochem.* **1985**, *54*, 73-100.
- (39) Ferro, A.M. and Oppenheimer, N.J. *Proc. Natl. Acad. Sci. USA* **1978**, *75*, 809-813.
- (40) Taniguchi, T. *Biochem. Biophys. Res. Comm.* **1987**, *147*, 1008-1012.
- (41) Schuber, F. and Travo, P. *Eur. J. Biochem.* **1976**, *65*, 247-255.
- (42) Bull, H.G.; Ferraz, J.P.; Cordes, E.H.; Ribbi, A. and Apitz-Castro, R. *J. Biol. Chem.* **1978**, *253*, 5186-5192.
- (43) Yuan, J.H. and Anderson, B.M. *J. Biol. Chem.* **1973**, *248*, 417-421.
- (44) Yost, D.A. and Anderson, B.M. *J. Biol. Chem.* **1983**, *258*, 3075-3080.
- (45) Schuber, F.; Travo, P. and Pascal, M. *Eur. J. Biochem.* **1976**, *69*, 593-602.
- (46) Pascal, M. and Schuber, F. *FEBS Lett.* **1976**, *66*, 107-109.
- (47) Oppenheimer, N. *FEBS Lett.* **1978**, *94*, 368-370.
- (48) Schuber, F. and Pascal, M. *FEBS Lett.* **1977**, *73*, 92-96.
- (49) Slama, J.T. and Simmons, A.M. *Biochem.* **1988**, *27*, 183-193.
- (50) Slama, J.T. and Simmons, A.M. *Biochemistry* **1989**, *28*, 7688-7694.
- (51) Secemski, I.I.; Lehrer, S.S. and Lienhard, G.E. *J. Biol. Chem.* **1972**, *247*, 4740-4748.
- (52) Schuber, F. and Muller, H.M. in press.
- (53) Handlon, A.L. and Oppenheimer, N.J. **1990**, in press.

- (54) Sinnott, M.L. and Viratelle, O.M. *Biochem. J.* **1973**, *133*, 81-87.
- (55) Tamus, C.; Muller, H.M. and Schuber, F. *Bioorg. Chem.* **1988**, *16*, 38-51.
- (56) Tamus, C. and Schuber, F. *Bioorg. Chem.* **1987**, *15*, 31-42.
- (57) Johnson, R.W.; Marschner, T.M. and Oppenheimer, N.J. *J. Am. Chem. Soc.* **1988**, *110*, 2257-22263.
- (58) Jencks, W.P. *Acc. Chem. Res.* **1980**, *13*, 161-169.
- (59) Knier, B.L. and Jencks, W.P. *J. Am. Chem. Soc.* **1980**, *102*, 6789-6798.
- (60) Sinnott, M.L., in "Enzyme Mechanisms"; M. I. Page and A. Williams, Eds. Royal Society of Chemistry, Burlington House: London, 1987; pp. 259-297.
- (61) Jones, C.C.; Sinnott, M.L. and Souchard, I.J.L. *J. Chem. Soc. Perkin Trans II* **1977**, 1191-1198.

Chapter 3
The Synthesis of the 2'-substituted
Nicotinamide Nucleosides

Introduction

Many NAD⁺ analogs have been prepared in order to investigate the structure/function relationships of this key coenzyme (for a review see reference 1). Most attention has been directed toward modifying the "working end" of NAD⁺, the nicotinamide ring. Many of these syntheses have taken advantage of the *trans*-glycosidation reaction catalyzed by NAD⁺ glycohydrolase that allows the direct substitution of the nicotinamide ring for another pyridine ring.² Relatively few efforts have been directed towards the synthesis of analogs with modifications on the nicotinamide ribose ring. The first analog of this type was prepared in 1964 by Woenckhaus and coworkers and involved the substitution of the ribofuranoside ring with a glucopyranoside ring.³ These chemists also synthesized analogs in which the nicotinamide ribose ring was substituted by a 2',3'-dideoxyribose ring and by a flexible pentamethylene chain.⁴ More subtle modifications of the ribose ring were achieved in the synthesis of ara-NAD⁺ by Kam, et al.⁵ in which the ribofuranose was replaced by an arabinofuranose ring, thus placing the 2'-hydroxyl *cis* to the nicotinamide ring. Finally, the synthesis of carba-NAD⁺ by Slama and Simmons⁶ replaced the ribose ring with a 2,3-dihydroxycyclopentane ring in order to investigate the influence of the ribose ring oxygen.

The present study requires the synthesis of a series of 2'-substituted nicotinamide nucleosides including substituents that span a wide spectrum of polar and steric properties. The substituents that have been chosen for this purpose are the 2'-H, -NH₂ (NH₃⁺), -OH, -NHCOR, -N₃ and -F. In addition, the influence of configuration of the 2'-substituent will be investigated. This requires the synthesis of the ribofuranosides as well as the arabinofuranosides in which the 2'-substituent is "up." Otherwise, it was desired to keep the 3'-OH and to retain the β-D-ribose configuration at the 1', 3', and 4' positions.

The general approach used for the syntheses of the 2'-substituted nicotinamide nucleosides involves the construction of the 2'-substituted sugar fragment followed by coupling to the nicotinamide portion. There are two general techniques that have been developed for making the C-N bond between the N-1 of nicotinamide and the C-1 of a monosaccharide (Scheme

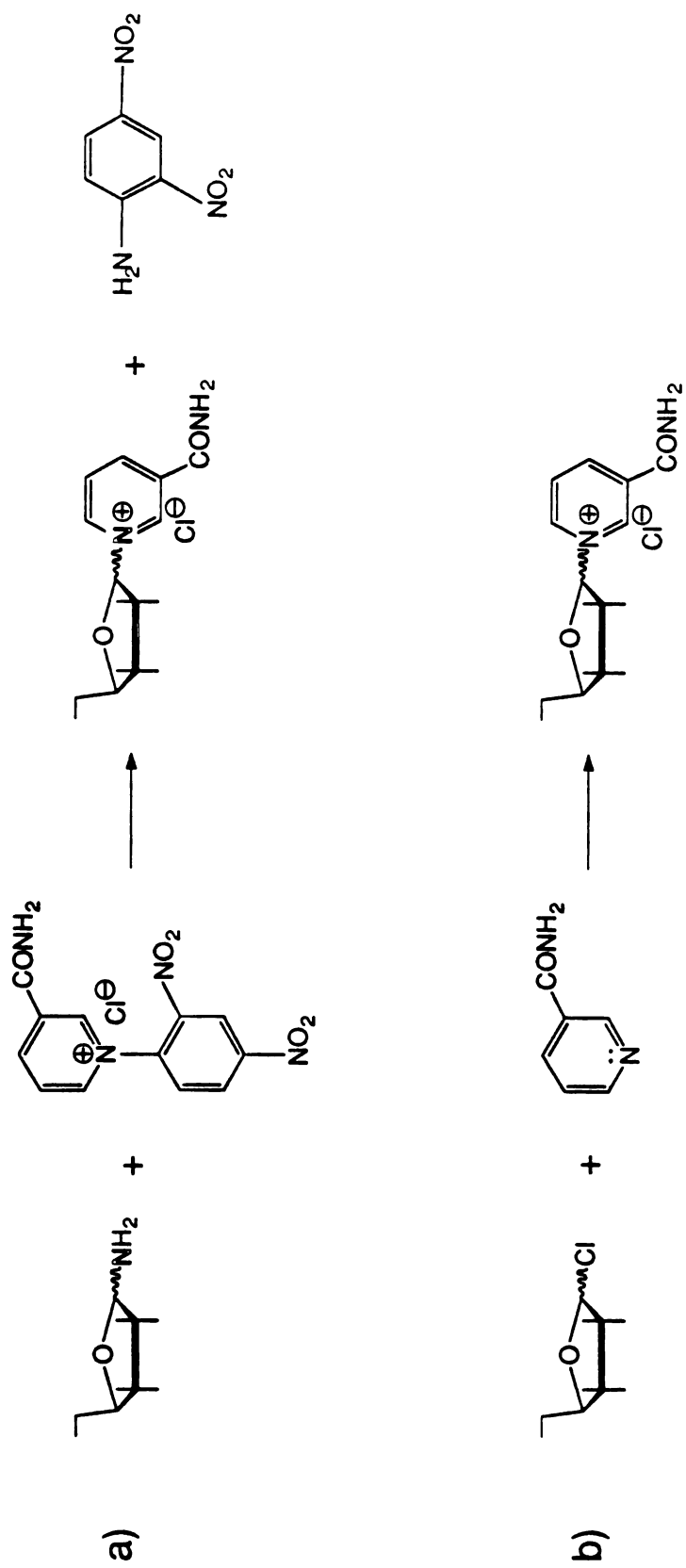
3.1), and both of these techniques have been utilized in the present study. The first (3.1.a) involves the reaction of a glycosylamine with nicotinamide dinitrobenzene (Zincke salt)⁵ to give dinitroaniline and the nicotinamide nucleoside. The second general method (3.1.b) involves a nucleophilic substitution by nicotinamide on a halosugar. The second method has been used extensively for the synthesis of 2'-substituted purines and pyrimidines. For this reason, many of the strategies that are utilized here for making the 2'-substituted nicotinamide nucleosides have been borrowed from published procedures that were designed for making purine and pyrimidine analogs. For example, the preparations of the nicotinamide 2'-amino-, 2'-azido-, and 2'-fluoro-2'-deoxy-arabinofuranosides⁷ are patterned after the syntheses of the corresponding 2'-substituted-2'-deoxyarabinofuranosyl adenine and guanine nucleosides.⁸

Results and Discussion

The synthesis of nicotinamide 2'-deoxy ribofuranoside

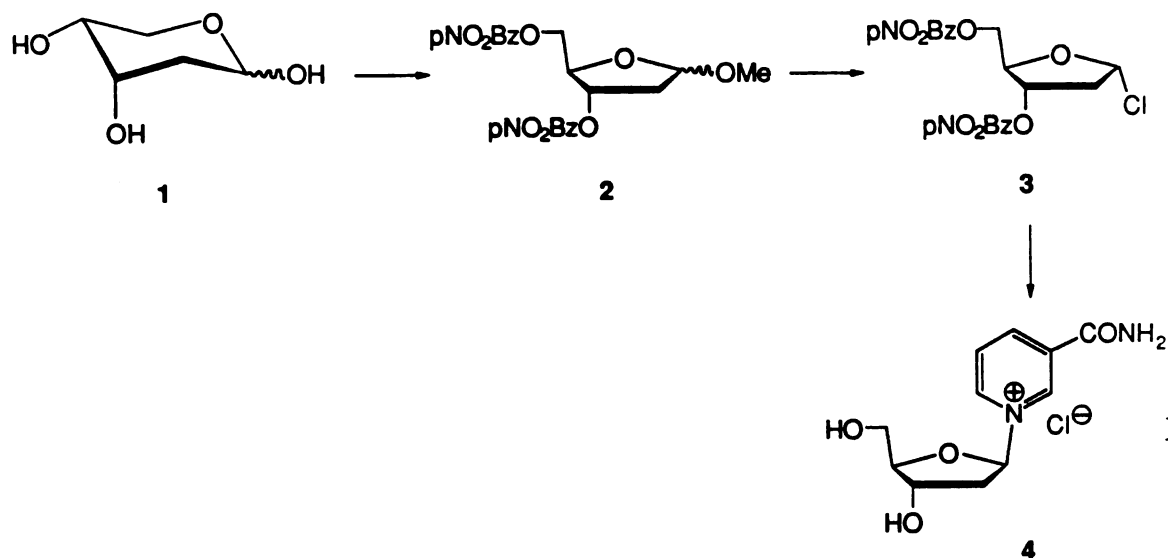
The nicotinamide 2'-deoxy- β -D-ribofuranoside (**4**) was readily prepared (Scheme 3.2) using techniques described for the synthesis of 2'-deoxyadenosine.⁹ The 2-deoxy-D-ribose (**1**) was locked into the furanose form by treatment with methanolic hydrogen chloride to give methyl 2-deoxy-D-ribose which was protected at the 3 and 5 positions by treatment with p-nitrobenzoyl chloride in pyridine to give methyl 2-deoxy-3,5-di-O-(p-nitrobenzoyl)- α,β -D-ribose (**2**) in 31% yield from 2-deoxyribose. The 1-chloro-2-deoxy-3,5-di-O-(p-nitrobenzoyl)- α -D-ribose (**3**) was prepared from **2** by treatment with hydrogen chloride in glacial acetic acid. The chloro sugar crystallized from the reaction mixture to give the pure α anomer in 81% yield. The nicotinamide nucleoside was prepared by adding nicotinamide to the chloro sugar (**3**) in acetonitrile followed by deblocking the 3- and 5-positions in methanolic ammonia. Nicotinamide 2'-deoxy- β -D-ribofuranoside (**4**) was isolated by precipitation in ether to give the pure β anomer in 63% yield. **4** was found to be stable if stored as the ether precipitate at - 20 °C. This nucleoside, however, was

Scheme 3.1



readily hydrolyzed in aqueous solution and did not withstand chromatography or rotary evaporation from aqueous solution.

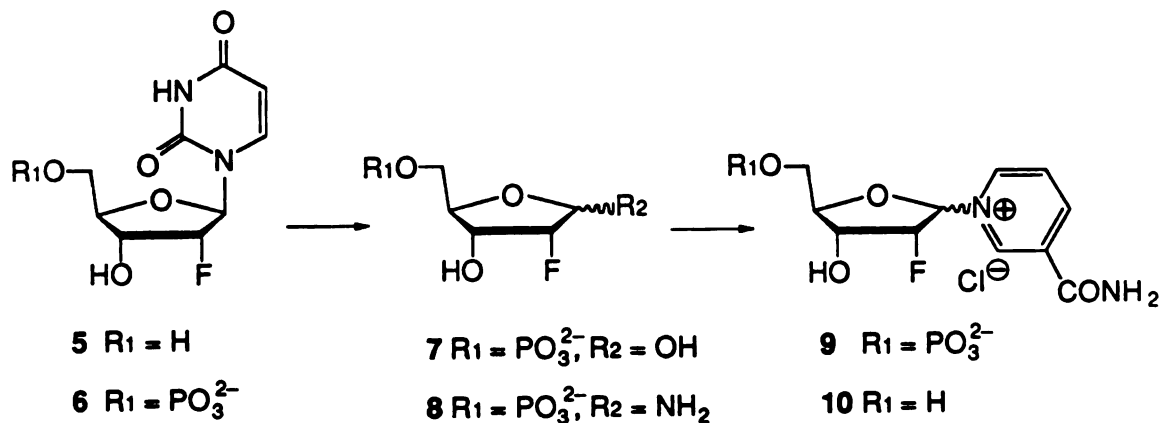
Scheme 3.2



The synthesis of nicotinamide 2'-fluoro-2'-deoxy-β-D-ribofuranoside

The nicotinamide 2'-fluoro-2'-deoxy-β-D-ribofuranoside was synthesized by Tom Cheng Xu in the Oppenheimer laboratory. The synthesis is outlined in Scheme 3.3 and will be reported in detail in subsequent publications.¹⁰ The overall strategy was developed for the synthesis of nicotinamide 2'-azido-2'-deoxy-ribofuranoside that used 2'-azido-2'-deoxy-uridine as a starting point. The uracil ring of 2'-substituted uridines is readily cleaved by hydrazine treatment¹¹ to give the corresponding 2-substituted ribose. In principle, this can be converted to the ribosylamine and reacted with Zincke salt to give the nicotinamide nucleoside using techniques described by Kam and Oppenheimer.⁵ Using this strategy, nicotinamide mononucleotide was prepared from UMP. Unfortunately, we find that the azido group at the 2' position interferes with the Zincke reaction. Nevertheless, because many 2'-substituted uridine derivatives have been described in the literature, this approach has the potential of becoming an efficient route to prepare a variety of 2'-substituted nicotinamide nucleosides.

Scheme 3.3



Based on this strategy, the synthesis of nicotinamide 2'-fluoro-2'-deoxy-ribofuranoside (10) starts with 2'-fluoro-uridine (5) which was prepared according to Knaus and coworkers.¹² The 5'-OH was phosphorylated with pyrophosphorylchloride in *m*-cresol using the procedure of Imai¹³ giving 2'-fluoro-2'-deoxy-uridine monophosphate (6). The phosphorylation serves the dual purpose of locking the geometry of the ring in the furanose form for the depyrimidination step and also serves as a site from which to build the pyrophosphate backbone of the NAD⁺ analog. The uracil ring was removed by hydrazine treatment as described by Hobbs¹¹ to give the free 2'-fluoro sugar phosphate (7). According to the procedures described by Kam⁵ and Walt,¹⁴ 7 was treated with saturated methanolic ammonia to give the 2'-fluoro-2'-deoxy-5-phosphoribosylamine (8) which was not isolated but directly treated with the Zincke reagent to make the nicotinamide 2'-fluoro-2'-deoxy-5'-phosphoriboside (9). The phosphate group was removed by the action of alkaline phosphatase according to methods outlined by Kaplan¹⁵ to afford the nicotinamide 2'-fluoro-2'-deoxy- α,β -D-ribofuranoside (10). The anomers were resolved by reverse-phase liquid chromatography. In contrast to the 2'-deoxy riboside, 10 posed no stability problems. This nucleoside was found to be very stable in aqueous solution at room temperature.

The synthesis of nicotinamide 2'-N₃- and 2'-NH₂-2'-deoxy-ribofuranoside and nicotinamide

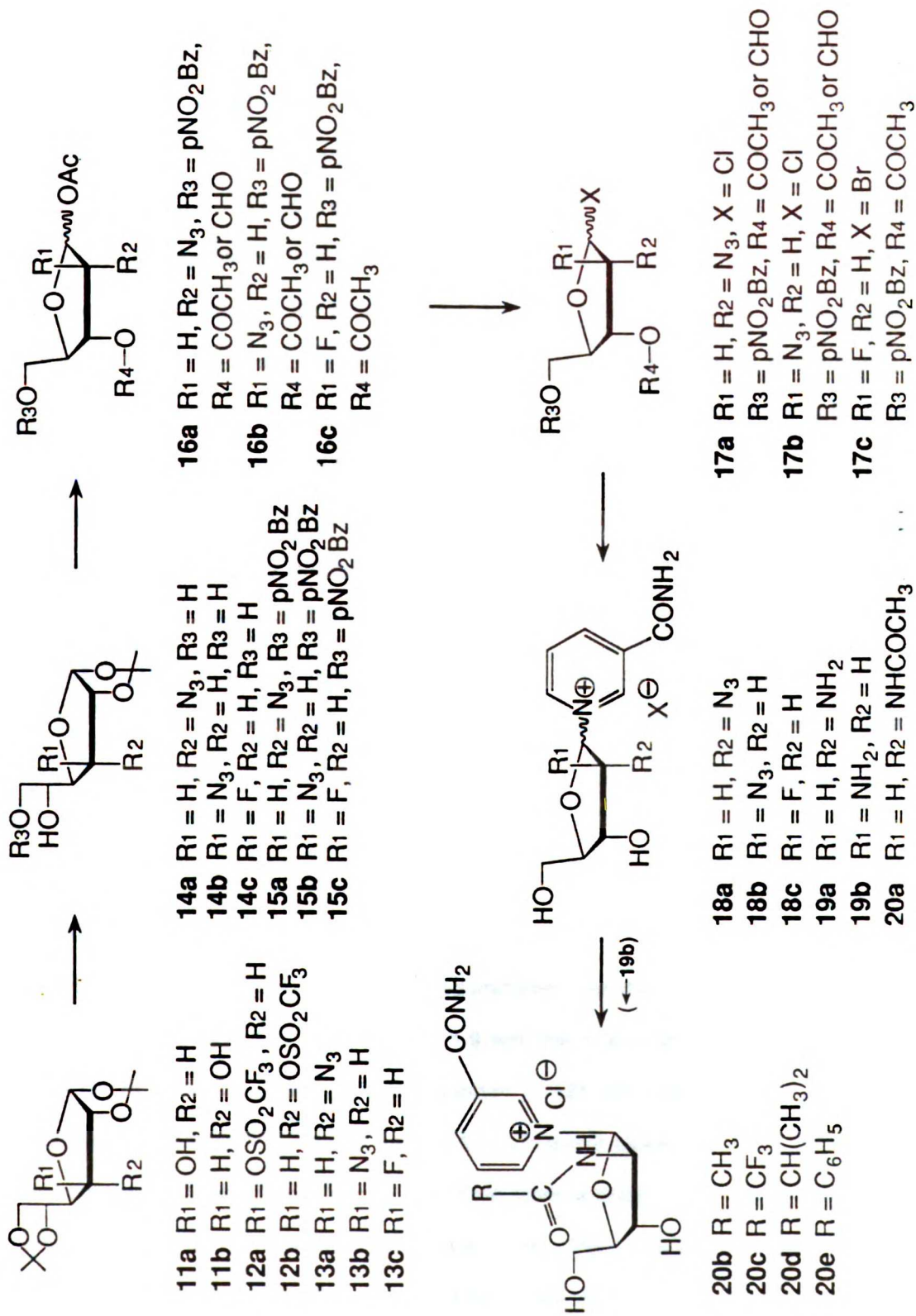
2'-N₃, 2'-NH₂, and 2'-F-2'-deoxy-arabinofuranoside

The synthesis of the nicotinamide 2'-fluoro-, 2'-azido-, and 2'-amino-2'-deoxy-arabinofuranosides as well as the 2'-azido- and 2'-amino-2'-deoxy-ribofuranosides are outlined in Scheme 3.4. This strategy represents a general method for the preparation of an array of 2'-substituted nicotinamide nucleosides from commercially available 1,2-5,6-di-isopropylidene hexofuranosides. The azido or fluoro substituent is introduced into the furanoside and converted to the nicotinamide nucleoside in several steps. In the last step the azido group is reduced to the amine which can serve as an entry point to several N-substituted derivatives.

The starting material for the riboside synthesis is 1,2-5,6-di-O-isopropylidene- α -D-glucofuranose (**11a**). The arabinoside synthesis starts with the corresponding hexose with the opposite stereochemistry at the 3-position, 1,2-5,6-di-O-isopropylidene- α -D-allofuranose (**11b**). The 3-position is activated for nucleophilic displacement by converting the 3-OH to the 3-O-triflates (**12 a,b**) with trifluoromethanesulfonic anhydride¹⁶ in CH₂Cl₂ which proceeds in over 90% yield. This is followed by displacement with lithium azide in DMF to give **13 a,b**. The azide displacement with **12b** proceeds in 93% yield, but in the case of **12a**, the 3-O-triflate is *trans* to the 4-H and reaction with azide results in appreciable elimination to the 3-4 olefin and a 51% yield of azido sugar **13a**. Similarly, the fluoro moiety is introduced into **11b** using diethylaminosulfur trifluoride (DAST)¹⁷ to generate **13c** in 53% yield. The reaction of DAST with **11a** resulted in elimination to the 3-4 olefin and prohibited this method for the synthesis of the nicotinamide 2'-fluororibofuranoside.

Once the substituent has been introduced into the 3-position, the 5,6-isopropylidene group is selectively removed with dilute acid¹⁸ to give **14a,b,c** and the 6-position is then protected with a *p*-nitrobenzoyl group to give **15a,b,c**. The latter protecting group is preferred over the more commonly used benzoyl group because pyridine nucleotides are unstable in the more vigorously basic conditions needed to remove the benzoyl group.

Scheme 3.4



The 1,2-isopropylidene group can be removed either by the procedure of Bobek⁸ or by using trifluoroacetic acid as the proton source. Oxidative cleavage of the C1-C2 bond with sodium periodate leads to spontaneous ring closure to generate the 2-substituted sugars.^{8,19} This is followed by acetylation of the free hydroxyl groups with pyridine/acetic anhydride to give **16a,b,c**. The 3-O-formyl group resulting from the periodate oxidation is only partially hydrolyzed under the reaction conditions that lead to **16a** and **16b**; it is fully hydrolyzed in the case of **16c**. The resulting mixtures of the 3-O-acetyl and the 3-O-formyl derivatives were not separated but directly converted to the 1'-halo sugars. The 1'-bromo sugar, **17c**, was prepared using 30% hydrogen bromide in acetic acid.¹⁹ This method has proven inappropriate for the synthesis of **17a,b** because alkyl azides are readily reduced by HBr. Thus, the titanium tetrachloride procedure of Bobek⁸ was used to prepare the 1-chloro sugars **17a,b**.

Coupling of the 1-halo sugars with nicotinamide was conducted in anhydrous acetonitrile²⁰ or a 2:1 acetonitrile/trifluoroethanol mixture in the case of **17a**. The 3'-acetyl and the 5'-p-nitrobenzoyl groups were removed by treating the nucleosides with methanolic ammonia at 0 °C for 2 h²⁰ (longer incubation leads to partial destruction of the nucleosides). The overall yields of the nucleosides from the di-isopropylidene furanoses were: **18a**, 12%; **18b**, 34%; and **18c**, 24%.

Anomeric ratios

With the halosugar **17c**, the α anomer predominated over the β anomer by a 9:1 ratio whereas in the final product, **18c**, the ratio was 1:9 with the β anomer predominant. Thus halogenation favors formation of the *trans* configuration of **17c** with subsequent inversion of configuration by the incoming nicotinamide, i.e., the 2'-fluoro group causes no overt influence on the stereochemistry of the reaction. In the case of the azido analogs, however, we observed unusual selectivity of attack by nicotinamide on **17a** and **17b**. The α and β -anomers of these 1-chloro sugars can be separated by flash chromatography. Regardless of the initial configuration of **17a** or **17b**, the formation of the nicotinamide nucleoside **18a** and **18b** gave predominantly

the 1'-2' *cis* isomer, i.e. with the nicotinamide moiety *cis* to the bulky 2'-azido group. When the displacement is conducted in 100% acetonitrile, the α anomer of **18a** predominated over the β anomer by 20:1. In the case of **18b**, the β anomer predominated by 6:1. The observed stereochemistry may have resulted from a combination of two factors: the selective reaction of nicotinamide *cis* to the azido group, and faster anomerization of the 1-2 *cis* chloro sugar than its displacement by nicotinamide.²¹ The origin of the differences in reaction rates remains unclear. Formation of a charge transfer complex or an electrostatic interaction between the azido group and the incoming nicotinamide moiety may be responsible for the *cis* addition.

The tendency of the azido group to direct the stereochemistry was advantageous for the synthesis of the arabinoside but was disastrous for the riboside: only a 5% yield of the desired β anomer was obtained. Numerous reaction conditions and solvent mixtures were tested to maximize the yield of the β anomer. It was found that a 30% trifluoroethanol/acetonitrile mixture with 0.7 M nicotinamide gave an α : β ratio of 4:3. The polar but non-nucleophilic trifluoroethanol allows the use of a high concentration of nicotinamide which may accelerate the displacement reaction over the anomerization of the chloro sugar. Further, it was considered that a more polar solvent such as trifluoroethanol could disrupt any intramolecular electrostatic interactions between the azido moiety and the nascent pyridinium that may be involved in the *cis*-directing effect of the azido group.

Azide reduction

The standard procedures in the literature for the reduction of azido groups to amines, e.g. catalytic hydrogenation, various forms of hydride reduction or one electron reductants,²² are all inappropriate because they would cause a concomitant reduction of the nicotinamide moiety. Indeed, the reductive lability of the nicotinamide moiety combined with the general insolubility of pyridine nucleosides in solvents other than water places severe limitations on the chemistry that can be used and precludes most standard methods of azide reduction.²³ Given the resistance of NAD⁺ to direct, chemical reduction by thiols,²⁴ these were explored as possible candidates for

the azido nucleoside reduction. Knowles and coworkers reported the reduction of aryl azides with dithiothreitol.²⁵ We explored the ability of aqueous dithiothreitol (DTT) to reduce a model alkyl azide, 3'-azido-3'-deoxythymidine (AZT, Figure 3.1) and also investigated the kinetics of AZT reduction by mercaptoethanol and glutathione.²⁶ It was found that of the three thiol reducing agents, DTT was the most rapid. DTT afforded a quantitative reduction of alkyl azide in aqueous solution at neutral pH and room temperature. In contrast, the yields using the standard catalytic hydrogenation methods for the reduction of AZT to 3'-aminothymidine are reported to range from only 57%²⁷ to 67%.²⁸

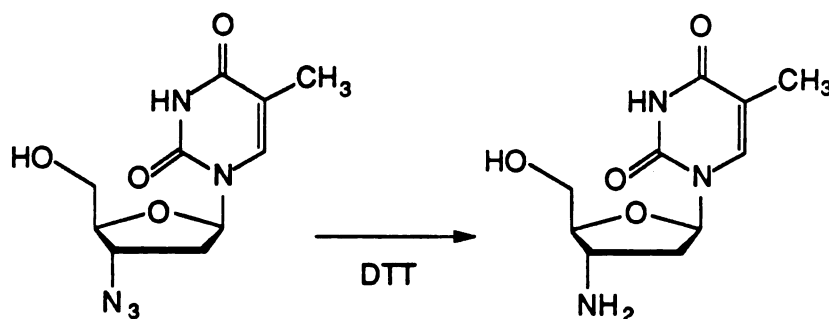


Figure 3.1 The DTT reduction of AZT to 3'-aminothymidine.

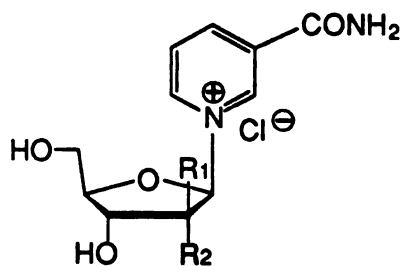
The 2'-amino nucleosides **19a,b** were prepared from the corresponding azido nucleosides **18a,b** using this new technique. The azido nucleosides were reduced without any detectable reduction of the nicotinamide moiety. This approach allowed the use of the azido group as a cryptic amine that can be unmasked at the last step, thus avoiding working with an amino group (or an amine blocking group) during the earlier phases of the synthesis. The DTT-mediated reduction of azides in aqueous solution at neutral pH should be of significant utility in the manipulation of functional groups on redox sensitive substrates.

The 2'-N-acylated derivatives

The 2'-amino nucleosides were converted to the N-acyl nucleosides (20a-20e, Scheme 3.4) by reaction with the appropriate acid anhydride. The products were recovered by precipitation in excess diethylether thus separating the unreacted acid anhydride. The acylations proceeded in high yield and the products needed no further purification.

The 2'-OH nucleosides

The nicotinamide arabinoside (21a) and nicotinamide riboside (21b, Fig. 3.2) were prepared in the Oppenheimer laboratory using published procedures. Nucleoside 21a was prepared from the reaction of 5-tritylarabinosylamine with Zincke salt.⁵ Nucleoside 21b was prepared from commercially available nicotinamide mononucleotide by the action of alkaline phosphatase.¹⁵



21a R₁ = OH

R₂ = H

21b R₁ = H

R₂ = OH

Figure 3.2 Nicotinamide arabinofuranoside and nicotinamide ribofuranoside.

NMR and mass spectral analysis

All of the 2'-substituted nicotinamide nucleosides were subject to 500 MHz ¹H NMR spectroscopy and the results are summarized in Tables 3.1 and 3.2. Assignments are based on spin decoupling experiments. The data in Table 3.1 demonstrate the sensitivity of the 2'-proton chemical shift toward the 2'-substituent. The chemical shifts of the 2'-amino nucleosides

Table 3.1. ¹H NMR chemical shifts of the nicotinamide and furanose ring protons for the 2'-substituted nicotinamide β-D-ribo- and arabinofuranosides in D₂O at 20 °C and molecular ion masses from liquid secondary ion mass spectrometry.

nucleoside	N2	N6	N4	N5	1'	2'	3'	4'	5'	5''	M+
2'-deoxy ribo 4	9.45 (s)	9.22 (d)	8.92 (d)	8.23 (t)	6.70 (d)	3.05 (m), 2.85 (d)	4.52 (d)	4.78 (t)	3.83 (dd)	3.72 (dd)	239
2'-fluoro ribo 10	9.73 (s)	9.35 (d)	8.99 (d)	8.29 (t)	6.66 (d)	5.40 (m)	4.52 (m)	4.50 (m)	4.16 (dd)	3.94 (dd)	257
2'-azido ribo 18a	9.67 (s)	9.32 (d)	9.01 (d)	8.30 (t)	6.30 (d)	4.92 (m)	4.67 (m)	4.48 (m)	4.09 (dd)	3.92 (dd)	280
2'-azido ara 18b	9.69 (s)	9.20 (d)	9.00 (d)	8.28 (t)	6.65 (d)	5.05 (d)	4.42 (t)	4.26 (m)	4.12 (dd)	3.97 (dd)	280
2'-fluoro ara 18c	9.62 (s)	9.22 (d)	8.98 (d)	8.26 (t)	6.73 (dd)	5.55 (dl)	4.56 (dl)	4.31 (m)	4.04 (dd)	3.92 (dd)	257
2'-amino ribo 19a, pH 7	9.63 (s)	9.32 (d)	9.00 (d)	8.29 (t)	6.11 (d)	3.76 (t)	4.35 (t)	4.49 (m)	4.03 (dd)	3.93 (dd)	254
2'-amino ribo 19a, pH 1	9.77 (s)	9.38 (d)	9.05 (d)	8.33 (t)	6.72 (d)	4.48 (dd)	4.80 (t)	4.54 (m)	4.10 (dd)	3.97 (dd)	-
2'-amino ara 19b, pH 7	9.73 (s)	9.22 (d)	8.97 (d)	8.28 (t)	6.48 (d)	4.05 (d)	4.18 (m)	4.11 (m)	4.13(m)	3.99 (dd)	254
2'-amino ara 19b, pH 1	9.88 (s)	9.38 (d)	9.07 (d)	8.38 (t)	6.86 (d)	4.58 (dd)	4.69 (t)	4.39 (m)	4.18 (dd)	4.00 (dd)	-
2'-N-acetyl ribo 20a	9.67 (s)	9.31 (d)	9.00 (d)	8.27 (t)	6.30 (d)	4.70 (t)	4.52 (m)	4.52 (m)	4.07 (dd)	3.96 (dd)	296
2'-N-acetyl ara 20b	9.66 (s)	9.07 (d)	9.02 (d)	8.28 (t)	6.65 (d)	4.96 (dd)	4.43 (t)	4.27 (dd)	4.17 (dd)	4.00 (dd)	296
2'-N-trifluoro- acetyl ara 20c	9.70 (s)	9.17 (d)	9.02 (d)	8.29 (t)	6.74 (d)	5.12 (t)	4.58 (t)	4.33 (d)	4.19 (d)	4.01 (d)	350
2'-N-isobutyryl ara 20d	9.57 (s)	9.13 (d)	9.02 (d)	8.30 (t)	6.69 (d)	4.92 (t)	4.52 (t)	4.29 (d)	4.17 (d)	4.00 (dd)	324
2'-N-benzoyl ara 20e	9.61 (s)	9.21 (d)	8.91 (d)	8.20 (t)	6.82 (d)	5.17 (dd)	4.66 (t)	4.38 (m)	4.22 (dd)	4.05 (dd)	358
2'-hydroxy ara 21a	9.65 (s)	9.19 (d)	9.01 (d)	8.30 (t)	6.60 (d)	4.83 (t)	4.20 (t)	4.26 (m)	4.11 (d)	3.99 (dd)	255
2'-hydroxy ribo 21b	9.61 (s)	9.27 (d)	8.98 (d)	8.28 (t)	6.25 (d)	4.52 (t)	4.36 (t)	4.48 (m)	4.05 (dd)	3.90 (dd)	255

Table 3.2. ¹H NMR coupling constants (Hertz) of the furanose ring protons for the 2'-substituted nicotinamide β-D-ribo- and arabinofuranosides in D₂O at 20 °C.

nucleoside	1'-2'	2'-3'	3'-4'	4'-5'	4'-5''	5'-5''	1'-F	2'-F	3'-F
2'-deoxy ribo 4	6.5	5.1	0	4.5	5.2	12.5			
2'-fluoro ribo 10	1.1	4.1	7.3	1.7	2.0	13.2	14.0	51.7	22.1
2'-azido ribo 18a	3.4	5.2	6.9	2.7	3.2	13.0			
2'-azido ara 18b	6.5	8.3	5.8	2.4	2.9	13.3			
2'-fluoro ara 18c	4.6	4.7	4.7	1.0	4.7	13.0	9.5	51.3	17.6
2'-amino ribo 19a, pH 7	6.4	5.8	3.0	2.8	3.4	12.6			
2'-amino ribo 19a, pH 1	4.5	6.0	5.2	2.4	2.7	13.0			
2'-amino ara 19b, pH 7	6.3	4.1	*	2.3	2.4	13.2			
2'-amino ara 19b, pH 1	5.9	7.0	6.7	2.2	1.2	13.2			
2'-N-acetyl ribo 20a	5.7	5.4	*	2.3	2.5	12.9			
2'-N-acetyl ara 20b	6.6	8.0	8.6	1.6	1.8	13.3			
2'-N-trifluoro- acetyl ara 20c	6.3	8.1	8.0	1.7	1.4	13.3			
2'-N-isobutyryl ara 20d	6.4	8.0	8.6	1.7	1.5	13.2			
2'-N-benzoyl ara 20e	6.2	8.4	8.0	2.1	2.0	13.2			
2'-hydroxy ara 21a	5.9	6.5	7.4	2.2	3.7	13.1			
2'-hydroxy ribo 21b	4.3	4.6	4.6	2.7	3.5	12.8.			

*Chemical shifts differ by less than 2 Hz.

are reported at both neutral pH and at low pH. As the amine ionizes, all of the protons in the molecule are deshielded and the chemical shifts increase. This phenomenon will be discussed more in chapter 5.

The coupling constants in Table 3.2 also vary with the 2'-substituent. For example, within the arabinoside series, bulky 2'-substituents (β 18b, and β 20b-e) led to an increase in the 2'-3' coupling constants. This is consistent with an increase in the 2'-3' dihedral angle that may result from steric interactions of the nicotinamide ring and/or the 5'-hydroxymethyl group with the bulky 2'-substituent that forces the arabinofuranose ring into a 2'-exo conformation. Interestingly, a similar increase in 2'-3' coupling constant is seen upon protonating β 19b but not β 19a in which the -NH_3^+ group and the nicotinamide are *trans*. Instead, β 19a shows a large decrease in the 1'-2' coupling which is not observed upon protonation of β 19b. These observations are fully consistent with an ionization-induced conformational change from 2'-endo to 2'-exo. Model building shows that when β 19b twists from a 2'-endo to a 2'-exo conformation (thus swinging the 2'- NH_3^+ away from the nicotinamide), there is a large increase in the 2'-3' dihedral angle but only a slight change in the 1'-2' dihedral angle. Conversely, when β 19a puckers from 2'-endo to 2'-exo, there is a decrease in the 1'-2' dihedral angle but little change in the 2'-3'-dihedral angle. Presumably the electrostatic interaction between the pyridinium ring and the ammonium tend to force these groups as far apart as possible. Why the ara and ribo analogs pucker in the same way is not clear. Perhaps this indicates a significant interaction between the 2'- NH_3^+ and the 5'-hydroxymethyl group.

The nucleosides were also analyzed by liquid secondary ion mass spectrometry. The molecular ion masses are reported in the rightmost column of Table 3.1. Most of the nucleosides also showed some fragmentation of the glycosyl bond giving peaks for the corresponding oxocarbenium and for nicotinamide.

Experimental

General Procedures. Proton nuclear magnetic resonance spectra were obtained on either a General Electric GN-500 or QE-300 instrument interfaced to a Nicolet 1280 computer. Chemical shifts (20 °C) are reported in parts per million relative to internal 3-trimethylsilylpropionate (TSP) for aqueous samples or to tetramethylsilane (TMS) for samples in organic solvents. ¹H NMR data are tabulated in the order: multiplicity (s, singlet; d, doublet; t, triplet; q, quartet, m, multiplet), number of protons, assignment, and coupling constant(s) in Hertz. Anomeric configurations were determined from nuclear Overhauser effects experiments.²⁹ Infrared spectra were obtained on a Nicolet 5DX FT IR instrument. Mass spectra were obtained on a Kratos MS50 instrument. U.V./visible spectra were obtained on a Hitachi 100-80 spectrophotometer.

AZT was generously provided by Burroughs-Wellcome. Glutathione, mercaptoethanol, and (DL)-dithiothreitol were obtained from Sigma Chemical Company. All other reagents used for synthesis were obtained from Aldrich Chemical Co., Inc. unless otherwise specified. Solvents were distilled before use as follows: acetonitrile and dichloromethane from phosphorous pentoxide; dimethylformamide from barium oxide; pyridine from calcium hydride; dioxane from sodium. Solvents were stored over 4Å molecular sieves. Flash chromatography was performed with Merck 60A silica gel and t.l.c. with Baker-flex silica gel IB2-F plates. Thin-layer chromatography (T.l.c.) plates were visualized by u.v. light, sulfuric acid charring, or with an acetone/ammonia spray. High pressure liquid chromatography (H.p.l.c.) was carried out using a Hewlett-Packard HP-1090 instrument equipped with a diode array detector.

Methyl 2-deoxy-3,5-di-O-(p-nitrobenzoyl)- α,β -D-ribofuranoside (2). To a solution of 2-deoxy-D-ribose (1, 10 g, 74.5 mmol) in 108 ml absolute methanol was added 0.50 ml methanolic HCl (1.16 N) and stirred at room temperature. After 45 minutes, 50 ml anhydrous pyridine was added to stop the reaction. The reaction mixture was rotary evaporated to a stiff gum. The gum was dissolved in 60 ml anhydrous pyridine. To the pyridine solution was added 35 g

p-nitrobenzoylchloride over ten minutes while cooling the reaction in an ice bath under nitrogen. The reaction mixture was allowed to warm to room temperature and was stirred overnight. The reaction was cooled in an ice bath; 10 ml H₂O was added and the solution stirred for 10 minutes. The reaction mixture was transferred to a separatory funnel and washed with 300 ml H₂O. The aqueous portion was extracted with 3 x 50 ml portions of CH₂Cl₂. The organic layers were combined and washed with saturated NaHCO₃, 1 N H₂SO₄, and again with NaHCO₃. The organic layer was dried with MgSO₄ and concentrated to a syrup. The product was dissolved in 30 ml hot ethyl acetate/60 ml hot absolute ethanol from which the product crystallized upon cooling to yield **2** (8.3 g, 18.6 mmol, 25 % yield). ¹H NMR. (CDCl₃): δ 8.32-8.18 (m, 8H,aromatics), 5.67 (m, 1H, H-1), 5.28 (dd, 1H, H-3),4.67 (m, 1H, H-4), 4.54-4.58 (m, 2H, H-5,5'), 2.58 (m, 1H, H-2), 2.44 (m, 1H, H-2'), 1.12 (s, 3H, methyl).

2-deoxy-3,5-di-O-(p-nitrobenzoyl)-α-D-ribofuranosyl chloride (3). To a solution of **2** (5.0 g, 11.2 mmol) in 30 ml glacial acetic acid was added 0.10 ml acetic anhydride and the solution cooled to 0 °C in an ice bath under nitrogen. HCl (g) was bubbled through this solution for 4 minutes at 0 °C. After 20 minutes, 30 ml of freshly saturated diethylether/HCl was added and HCl (g) was passed through the reaction mixture for 1 minute. Ten minutes later 30 ml pentane was added, and the chloro sugar **3** precipitated from solution. The reaction mixture was filtered and the crystals washed with ether and pentane yielding **3** (4.06 g, 9.07 mmol, 81%). ¹H NMR. (CDCl₃): δ 8.35-8.20 (m, 8H,aromatics), 6.50 (d, 1H, H-1), 5.60 (m, 1H, H-3),4.89 (m, 1H, H-4), 4.75 (dd, 1H, H-5), 4.66 (dd, 1H, H-5').

Nicotinamide 2'-deoxy-β-D-ribofuranoside (4). To a solution of **3** (1.50 g, 3.32 mmol) in 50 ml CH₃CN was added nicotinamide (1.22 g, 10 mmol). The reaction was stirred overnight at room temperature and monitored by TLC (toluene/ethyl acetate, 1:1) until no more starting material was present. The reaction mixture was added to 200 ml diethylether to precipitate the nicotinamide nucleoside. The white precipitate was dissolved in 20 ml MeOH and rotary evaporated to dryness. To this residue was added 100 ml saturated methanolic ammonia at 0 °C and the solution stirred for 90 minutes. The methanol/ammonia was rotary evaporated and the

residual ammonia coevaporated with methanol. The residue was dissolved in 15 ml MeOH and added to 200 ml diethylether which precipitated pure **4** (2.10 mmol by cyanide assay³⁰, 63%). ¹H NMR. (D₂O): δ 9.45 (s, 1H, N-2), 9.22 (d, 1H, N-6, J = 6.2 Hz), 8.92 (d, 1H, N-4, J = 8.05), 8.23 (t, 1H, N-5, J = 6.9), 6.70 (d, 1H, 1', J_{1'-2'} = 6.5 Hz), 4.78 (t, 1H, 4', J_{4'-5'} = 4.5 Hz, J_{4'-5''} = 5.2 Hz), 4.52 (d, 1H, 3', J_{2'-3'} = 5.1 Hz, J_{3'-4'} = 0 Hz), 3.83 (dd, 1H, 5', J_{5'-5''} = 12.5 Hz), 3.72 (dd, 1H, 5''), 3.05 (m, 1H, 2'), 2.85 (d, 1H, 2'', J_{2'-2''} = 15.4 Hz). Liquid secondary ion MS: 239 (M⁺), 123 (nicotinamideH⁺), 117 (M - nicotinamide).

1,2-5,6-Di-O-isopropylidene-3-trifluoromethanesulphonyl-α-D-glucofuranose (12a). 1,2-5,6-Di-O-isopropylidene-α-D-glucofuranose (**11a**, 28.11 g, 108 mmol, Pfanstiehl Labs. Inc.) was reacted with 125 mmol trifluoromethanesulfonic anhydride in 500 ml anhydrous CH₂Cl₂ following the method of Hall and Miller.¹⁶ The product was purified by flash chromatography using dichloromethane as eluant and isolated as a colorless glass (41.8 g, 106 mmol, 98%). ¹H NMR (CDCl₃): δ 5.99 (d, 1H, H-1), 5.26 (d, 1H, H-3), 5.77 (d, 1H, H-2), 4.21-4.14 (m, 3H, H-4, H-5, H-6), 3.98 (dd, 1H, H-6'') 1.43, 1.34, 1.33, 1.30, (4s, 12H, four isopropylidene methyls).

3-Azido-3-deoxy-1,2-5,6-di-O-isopropylidene-α-D-allofuranose (13a). **12a** (41.8 g, 106.5 mmol) was dissolved in dimethylformamide (500 ml) and lithium azide (15.7 g, 320 mmol, Eastman Kodak) was added and the mixture was stirred at ambient temperature for 24 h. The solvent was removed under reduced pressure and the residue was partitioned between water (200 ml) and dichloromethane (200 ml). The aqueous layer was extracted with dichloromethane (2 x 100 ml) before being dried (MgSO₄) and evaporated to give a yellow oil (14.9 g, 52.2 mmol, 49%). IR (neet) 2109 cm⁻¹ (N₃ stretch). ¹H NMR. (CDCl₃): δ 5.79 (d, 1H, H-1), 4.73 (d, 1H, H-2), 4.20-4.14 (m, 2H, H-6,6'), 4.04-3.98 (m, 2H, H-4',H-5'), 3.52 (dd, 1H, H-3), 1.58, 1.49, 1.39, 1.37, (4s, 12H, four isopropylidene methyls). Chemical Ionization MS m/z 303.2 (M + NH₄⁺), 286.2 (M + 1).

3-Azido-3-deoxy-1,2-O-isopropylidene-α-D-allofuranose (14a). **13a** (14.9 g, 52.2 mmol) was converted to **14a** (10.9 g, 44.4 mmol, 85%) following the procedure of

Bobek.⁸ ¹H NMR (CDCl₃): δ 5.82 (d, 1H, H-1), 4.77 (d, 1H, H-2), 4.14-4.09 (m, 2H, H-4, 6), 4.01 (m, 1H, H-5), 3.77 (t, 1H, H-6'), 3.61 (dd, 1H, H-3), 2.72 (d, 1H, 5-OH), 2.28 (t, 1H, 6-OH), 1.59 and 1.38 (2s, 6H, two isopropylidene methyls). Electron Impact MS m/z 230.08 (M - CH₃), 184.07 (M - C₂H₅O₂).

3-Azido-3-deoxy-6-O-p-nitrobenzoyl-1,2-O-isopropylidene-α-D-allofuranose (15a). 14a (9.1 g, 37.1 mmol) was dissolved in dichloromethane (75 ml) and pyridine (25 ml). The solution was cooled to -30 °C before p-nitrobenzoyl chloride (7.30 g, 39.3 mmol) was added slowly. The mixture was maintained at -20 °C for 12 h before the solvents were removed by rotary evaporation and the residue partitioned between toluene (100 ml) and water (100 ml). The aqueous phase was extracted with toluene (2 x 20 ml) and the combined organic layers were washed with water (3 x 20 ml) before being dried (MgSO₄) and evaporated. The residue was purified by flash chromatography (chloroform/ether 3:1, R_f product = 0.7) to give 15a (14.6 g, 37.0 mmol, 99%). ¹H NMR. (CDCl₃): δ 8.27 (A₂B₂, 4H, aromatics), 5.84 (d, 1H, H-1, J_{1,2} = 3.4 Hz), 4.82, (d, 1H, H-2, J = 11.9 Hz), 4.59-4.54 (m, 2H, H-4,6), 4.32 (m, 1H, H-5), 4.24-4.21 (m, 1H, H-6'), 3.65 (m, 1H, H-3), 2.45 (d, 1H, 5-OH), 1.58 and 1.39 (2s, 6H, two isopropylidene methyls).

1,3-DI-O-acetyl-2-azido-2-deoxy-5-O-p-nitrobenzoyl-D-ribofuranose (16a). 15a (10.5 g, 25.6 mmol) was dissolved in 200 ml of 50% trifluoroacetic acid solution (water:dioxane:trifluoroacetic acid, 1:1:2). The reaction was monitored by t.l.c. (CHCl₃/ether 2:1); after 20 h at ambient temperature all starting material had been hydrolyzed. The solvents were evaporated to give a cream-colored solid that was not purified further. The solid was dissolved in acetonitrile (70 ml) and water (70 ml), then sodium bicarbonate (2.44 g, 29 mmol) was added to buffer the solution. Sodium periodate (6.85 g, 32 mmol) was added and the mixture stirred overnight at ambient temperature. The mixture was then filtered and evaporated before being partitioned between water (80 ml) and ethyl acetate (80 ml). The aqueous layer was extracted with ethyl acetate (2 x 20 ml) and the combined organic layers were dried (MgSO₄) and the solvent removed by rotary evaporation. The residue was dissolved in 50% (v/v) pyridine/acetic anhydride

and stirred for 2 h. T.l.c. of the product (CH₂Cl₂/ethyl acetate 2:1) showed two spots (R_f 0.60 and 0.70) that were identified by ¹H NMR as **16a** and its 3-O-formyl derivative respectively (combined yield *ca.* 18.6 mmol, 73%). The product was purified by flash chromatography using the above solvent system. IR (neet) 2115 (N₃), 1771-1751 (CO), 1609 (NO₂), cm⁻¹. ¹H NMR. (CDCl₃): δ 8.31-8.21 (A₂B₂, 4H aromatics), 6.13 (s, 1H, H-1), 5.41 (dd, 1H, H-3), 4.66 (dd, 1H, H-5), 4.53 (m, 1H, H-4), 4.47 (dd, 1H, H-5'), 4.34 (d, 1H, H-2), 2.19, 2.01 (s, 6H, 2 methyls). Chemical ionization MS m/z 426 (M⁺ + NH₄⁺), 349 (M⁺ - C₂O₂H₃)

2-Azido-2-deoxy-3-O-acetyl-5-O-p-nitrobenzoyl-D-ribofuranoside chloride (17a). **16a** (2.90 g 7.1 mmol) was dissolved in dichloromethane (50 ml) at 0 °C. Titanium tetrachloride (1.32 ml, 12 mmol) was added dropwise under nitrogen. The reaction mixture was maintained at 4 °C for 4 h before being added slowly to saturated sodium bicarbonate solution (50 ml). The heterogeneous mixture was spun down in polypropylene tubes; the organic layer was separated, dried, and the solvent removed by rotary evaporation. The oil was purified by silica gel chromatography (toluene/ethyl acetate 8:1) giving **17a** (1.50 g, 3.9 mmol, 55%). Four compounds were obtained: the α- and β-anomers of **17a** and the α- and β-anomers of the 3-O-formyl derivative of **17a**. T.l.c. of the products (toluene/ethyl acetate 8:1) allowed separation of the α- and β-anomers of the two compounds with R_f's of 0.54 and 0.37 respectively. The ratio of 3-O-formyl : 3-O-acetyl compounds was 1:3 based on integration of the ¹H NMR spectrum. The ratio of α : β anomers of the two compounds was 2:3, respectively. ¹H NMR (CDCl₃) β-anomer of **17a**: δ 8.33-8.24 (m, 4H, aromatics), 6.04 (s, 1H, H-1), 5.70 (dd, 1H, H-3), 4.77-4.52 (m, 4H, H-2,4,5,5') 2.19 (s, 3H, acetyl). α-anomer of **17a**: δ 8.33-8.25 (m, 4H, aromatics), 6.36 (d, 1H, H-1), 5.40 (dd, 1H, H-3), 4.80-4.49 (m, 4H, H-2,4,5,5'), 2.21 (s, 3H, acetyl). Chemical ionization MS m/z 349 (M⁺ - Cl).

2'-Azido-2'-deoxy nicotinamide ribofuranoside chloride (18a). Nicotinamide (4.00 g, 34 mmol) was dissolved in acetonitrile/trifluoroethanol, 3:2. The solution was added to the anomeric mixture of **17a** (0.40 g, 1.04 mmol). The mixture was maintained at

room temperature 3 days and the solvent was removed under reduced pressure keeping the temperature below 35 °C.

T.l.c. of the reaction mixture (n-BuOH:H₂O:AcOH 5:3:2) showed two major spots (Rf's 0.71 and 0.54), the former corresponded to nicotinamide; the latter gave a bright fluorescent spot upon treatment with ammonia/acetone. The 3',5'-protecting groups were removed by treatment with saturated methanolic ammonia (25 ml) at 0 °C for 2 h, and the mixture was concentrated under reduced pressure. The product was co-evaporated with methanol (2 x 10 ml), then dissolved in a minimum volume of methanol and added to cold (0 °C), stirred ether (100 ml). The resulting precipitate was allowed to settle before the ether was decanted and the precipitation repeated to remove traces of nicotinamide still present in the product. The product from the second precipitation was dissolved in methanol and the solvent removed to give **18a** (0.50 mmol, cyanide addition assay, 48%). T.l.c. (n-BuOH: H₂O:AcOH, 5:3:2) showed one spot (Rf 0.45) that gave a positive acetone/ammonia test. The anomeric ratio of product was *ca.* 4:1, α : β .

The resolution of the anomers can be achieved using a reverse-phase HPLC column (Rainin Microsorb C₁₈ analytical). The anomers were eluted with a linear gradient from 0-10% acetonitrile in ammonium phosphate buffer (20 mM, pH = 2.8) over ten minutes. The retention times were 6.8 min. for α -**18a** and 7.9 min. for β -**18a** (flow rate: 1 ml/min.). ¹H NMR. β -**18a** (D₂O): δ 9.67 (s, 1H, N-2), 9.32 (d, 1H, N-6, J = 6.3 Hz), 9.00 (d, 1H, N-4, J = 8.1 Hz), 8.30 (t, 1H, N-5, J = 6.6 Hz), 6.30 (d, 1H, 1', J_{1'-2'} = 3.4 HZ), 4.92 (m, 1H, 2', J_{2'-3'} = 5.2 Hz), 4.67 (m, 1H, 3', J_{3'-4'} = 6.9 Hz), 4.48 (m, 1H, 4', J_{4'-5'} = 2.7 Hz), 4.09 (dd, 1H, 5', J_{5'-5''} = 13.3 Hz), 3.92 (dd, 1H, 5'', J_{4'-5''} = 3.2 Hz, J_{5'-5''} = 13.3 Hz). α -**18a** (D₂O): δ 9.32 (s, 1H, N-2), 9.11 (d, 1H, N-6, J = 6.3 Hz), 8.97 (d, 1H, N-4, J = 8.2 Hz), 8.23 (t, 1H, N-5, J = 6.7 Hz), 6.67 (d, 1H, 1', J = 4.6 Hz), 5.03 (t, 1H, 2'), 4.64-4.68 (m, 2H, 3', 4'), 3.92 (dd, 1H, 5', J_{4'-5'} = 3.1 Hz, J_{5'-5''} = 12.7 Hz), 3.79 (dd, 1H, 5'', J_{4'-5''} = 5.7 Hz, J_{5'-5''} = 12.7 Hz). Liquid secondary ion MS 280 (M⁺).

2'-Amino-2'-deoxy nicotinamide ribofuranoside chloride (19a). **18a** (0.090 mmol) was dissolved in water (20 ml) and the solution degassed by rotary evaporation.

Dithiothreitol (154 mg, 1.0 mmol) was added. The solution was adjusted to pH 7.1 with 0.1 M sodium hydroxide and the mixture was stirred for 4 h at ambient temperature until evolution of nitrogen had ceased. The mixture was dried down, dissolved in a minimal volume of methanol and precipitated in 100 ml ether. Cyanide addition assay gave 0.067 mmol (74 %) and NMR showed complete conversion to the amine. The anomers were separated by HPLC according to the procedure described above. ¹H NMR. α-19a (D₂O, pD 4.8): δ 9.34 (s, 1H, N-2), 9.13 (d, 1H, N-6, J = 6.1 Hz), 8.97 (d, 1H, N-4, J = 8.1 Hz), 8.24 (t, 1H, N-5, J = 7.5 Hz), 6.51 (d, 1H, 1', J_{1'-2'} = 6.1 Hz), 4.92 (t, 1H, 4', J_{3'-4'} = 4.7 Hz), 4.36 (d, 1H, 3', J_{2'-3'} = 4.8 Hz), 4.28 (t, 1H, 2', J = 5.8 Hz), 3.87 (dd, 1H, 5', J_{4'-5'} = 3.5 Hz, J_{5'-5''} = 12.5), 3.79 (dd, 1H, 5'', J_{4'-5'} = 4.7 Hz, J_{5'-5''} = 12.5). ¹H NMR. β-19a (D₂O, pD 3.7): δ 9.63 (s, 1H, N-2, J = 8 Hz), 9.32 (d, 1H, N-6, J = 6 Hz), 9.00 (d, 1H, N-4, J = 8 Hz), 8.29 (t, 1H, N-5, J = 7 Hz), 6.11 (d, 1H, 1', J_{1'-2'} = 6.4 Hz), 4.49 (m, 1H, 4', J_{3'-4'} = 3.0 Hz), 4.35 (t, 1H, 3', J_{3'-4'} = 5.8 Hz), 4.03 (dd, 1H, 5', J_{5'-5''} = 12.6 Hz, J_{4'-5'} = 2.4), 3.93 (d, 1H, 5'', J_{5'-5''} = 12.6 Hz, J_{4'-5'} = 2.7 Hz), 3.76 (t, 1H, 2', J_{1'-2'} = 6.4 Hz). Liquid secondary ion MS 254 (M⁺).

2'-N-acetyl-2'-deoxy nicotinamide β-D-ribofuranoside chloride (20a). β-19a (10 μmol) was dissolved in 400 μl methanol and 300 μl acetic anhydride added. The solution was stirred for four minutes at room temperature and the reaction mixture added to 35 ml diethylether which precipitated pure 20a (10 μmol by cyanide assay³⁰, 100 %). ¹H NMR (D₂O) δ 9.67 (s, 1H, N2), 9.31 (d, 1H, N6, J = 6.3 Hz), 9.00 (d, 1H, N4, J = 8.1 Hz), 8.27 (t, 1H, N5, J = 7.5 Hz), 6.30 (d, 1H, 1', J_{1'-2'} = 6.6 Hz), 4.70 (dd, 1H, 2', J_{2'-3'} = 8.0 Hz), 4.52 (t, 1H, 3', J_{3'-4'} = 8.6 Hz), 4.52 (dd, 1H, 4', J_{4'-5'} = 1.6 Hz), 4.07 (dd, 1H, 5', J_{5'-5''} = 13.3 Hz), 3.96 (dd, 1H, 5'', J_{4'-5'} = 1.8 Hz), 2.07 (s, 3H, methyl). LIMS 296 (M⁺), 174 (M⁺ – nicotinamide), 123 (nicotinamideH⁺).

1,2-5,6-Di-O-isopropylidene-3-trifluoromethanesulphonyl-α-D-allofuranose (12b). 1,2-5,6-Di-O-isopropylidene-α-D-allofuranose 11b (4.80 g, 18.4 mmol, Pfanstiehl Labs. Inc.) was reacted with trifluoromethanesulfonic anhydride following the method of Hall and Miller.¹⁶ The product was purified by flash chromatography using dichloromethane as eluant and isolated as a gum (6.6 g, 16.9 mmol, 92%) ¹H NMR. (CDCl₃): δ 5.83 (d, 1H, H-1), 5.04-4.63 (m, 2H, H-2, H-3), 4.30-3.75 (m, 4H, H-4,5,6,6').

3-Azido-3-deoxy-1,2-5,6-di-O-isopropylidene- α -D-glucofuranose (13b). **12b** (6.60 g, 16.9 mmol) was dissolved in dimethylformamide (25 ml) and lithium azide (2.48 g, 50.7 mmol, Eastman Kodak) was added before the mixture was stirred at 25 °C for 24 h. The workup was identical to **13a** giving a yellow oil (4.48 g, 15.7 mmol, 93%). $^1\text{H NMR}$. (CDCl_3): δ 5.85 (d, 1H, H-1), 4.62 (d, 1H, H-2), 4.19-4.00 (m, 5H, H-3,4,5,6,6'), 1.51, 1.43, 1.37, 1.32, (4s, 12H, four isopropylidene methyls).

3-Azido-3-deoxy-1,2-O-isopropylidene- α -D-glucofuranose (14b). **13b** (4.48 g, 15.7 mmol) was converted to **14b** (3.70 g, 15 mmol, 95%) following the procedure of Bobek.⁸ $^1\text{H NMR}$ (CDCl_3): δ 5.88 (d, 1H, H-1), 4.64 (d, 1H, H-2), 4.20-3.70 (m, 5H, H-3,4,5,6,6'), 2.75 (s, 1H, 5-OH), 2.30 (s, 1H, 6-OH), 1.50 and 1.32 (2s, 6H, two isopropylidene methyls).

3-Azido-3-deoxy-6-O-p-nitrobenzoyl-1,2-O-isopropylidene- α -D-glucofuranose (15b). **14b** (3.70 g, 15 mmol) was dissolved in dichloromethane (25 ml) and pyridine (7 ml). The solution was cooled to -30 °C and p-nitrobenzoyl chloride (2.92 g, 15.7 mmol) was added slowly. The mixture was maintained at -20 °C for 12 h and the workup proceeded as for **15a**. The product was purified by flash chromatography (chloroform/ether 3:1, R_f product = 0.7) to give **15b** (5.30 g, 13.4 mmol, 89%). $^1\text{H NMR}$. (CDCl_3): δ 8.27 (A_2B_2 , 4H, aromatics), 5.91 (d, 1H, H-1, $J_{1,2} = 3.4$ Hz), 4.76 (d, 1H, H-6, $J_{6,6'} = 11.9$ Hz), 4.68 (d, 1H, H-2, $J_{2,1} = 3.4$ Hz), 4.50 (dd, 1H, H-6', $J_{6',6} = 11.9$ Hz), 4.24-4.21 (m, 3H, H-3,-4,-5), 2.59 (s, 1H, 5-OH), 1.50 and 1.34 (2s, 6H, two isopropylidene methyls).

1,3-Di-O-acetyl-2-azido-2-deoxy-5-O-p-nitrobenzoyl-D-arabinofuranoside (16b). **15b** (5.30 g, 13.4 mmol) was dissolved in 200 ml of 50% trifluoroacetic acid solution (water:dioxane:trifluoroacetic acid, 1:1:2) and treated according to the procedure outlined for **16a**. T.l.c. of the product (CHCl_3 /ethyl acetate 2:1) showed two spots (R_f 0.40 and 0.50) that were identified by $^1\text{H NMR}$ as **16b** and its 3-O-formyl derivative respectively (combined yield ca. 10.2 mmol, 76%). The mixture was used without further purification although the compounds were separable by flash chromatography using the above solvent system. $^1\text{H NMR}$. (CDCl_3) β -**16b** δ 8.2-8.3 (m, 4H, aromatics), 6.39 (d, 1H, H-1), 5.46 (t, 1H, H-3), 4.37 (m, 1H, H-4), 4.14 (m,

1H, H-2), 2.11 (s, 3H, acetyl); α -16b δ 8.2-8.3 (m, 4H, aromatics), 6.19 (s, 1H, H-1), 5.13 (m, 1H, H-3), 4.55 (m, 1H, H-4), , 4.22 (m, 1H, H-2), 2.13 (s, 3H, acetyl).

2-Azido-2-deoxy-3-O-acetyl-5-O-p-nitrobenzoyl-D-arabinofuranoside chloride (17b). 16b and its 3-O-formyl derivative from the preceding step were dissolved in dichloromethane (60 ml) at 0 °C. Titanium tetrachloride (1.75 ml, 16 mmol) was added dropwise under nitrogen. The reaction mixture was maintained at 4 °C for 4 h before being added slowly to saturated sodium bicarbonate solution (100 ml). The workup procedure for 17a was followed giving 17b (3.20 g, 8.3 mmol, 78%). Four compounds were obtained: the α - and β -anomers of 17b and the α - and β -anomers of the 3-O-formyl derivative of 17b. T.l.c. of the products (toluene/ethyl acetate 8:1) allowed separation of the α - and β -anomers of the two compounds with Rf's of 0.54 and 0.37 respectively. The ratio of 3-O-formyl : 3-O-acetyl compounds was 1:3 based on integration of the ¹H NMR spectrum. The ratio of α : β anomers of the two compounds was 1:6, respectively. ¹H NMR. (CDCl₃) β -anomer of 17b: δ 8.33-8.24 (m, 4H, aromatics), 6.26 (d, 1H, H-1), 5.58 (t, 1H, H-2), 4.87-4.34 (m, 4H, H-3,4,5,5') 2.17 (s, 3H, acetyl). α -anomer of 17b: δ 8.33-8.25 (m, 4H, aromatics), 6.12 (s, 1H, H-1), 5.06 (d, 1H, H-2), 4.80-4.47 (m, 4H, H-3,4,5,5'), 2.18 (s, 3H, acetyl). β -anomer of 3-O-formyl derivative of 17b: δ 8.33-8.24 (m, 4H, aromatics), 8.16 (s, 1H, formyl), 6.28 (d, 1H, H-1), 5.70 (t, 1H, H-2), 4.87-4.34 (m, 4H, H-3,4,5,5'). α -anomer of 3-O-formyl derivative of 17b: δ 8.33-8.25 (m, 4H, aromatics), 8.15 (s, 1H, formyl), 6.15 (d, 1H, H-1), 5.18 (t, 1H, H-2), 4.80-4.47 (m, 4H, H-3,4,5,5').

2'-Azido-2'-deoxy nicotinamide arabinofuranoside chloride (18b). Nicotinamide (2.00 g, 16.4 mmol) was dissolved in acetonitrile (80 ml) by refluxing under nitrogen. The solution was allowed to cool to room temperature before being added to the anomeric mixture of 17b (3.20 g, 8.3 mmol). The mixture was maintained at room temperature overnight and the solvent was removed under reduced pressure keeping the temperature below 35 °C.

T.l.c. of the reaction mixture (n-BuOH:H₂O:AcOH 5:3:2) showed two major spots (Rf's 0.68 and 0.57), the former corresponded to nicotinamide; the latter gave a bright fluorescent spot upon treatment with ammonia/acetone. The 3',5'-protecting groups were removed

according to procedures outlined for **18a**. The product from the second precipitation was dissolved in methanol and the solvent removed to give **18b** (1.96 g, 6.2 mmol, 75%). T.l.c. (n-BuOH: H₂O:AcOH, 5:3:2) showed one spot (R_f 0.45) that gave a positive acetone/ammonia test. The anomeric ratio of product was *ca.* 1:6 α : β .

The resolution of the α and β anomers of **18b** can be achieved using a reverse-phase HPLC column (Rainin Microsorb C₁₈ analytical). The anomers were eluted with a linear gradient from 0-10% acetonitrile in ammonium phosphate buffer (20 mM, pH = 2.8) over ten minutes. The retention times were 6.3 min. for α -**18b** and 7.6 min. for β -**18b** (flow rate: 1 ml/min.). ¹H NMR. β -**18b** (D₂O): δ 9.69 (s, 1H, N-2), 9.20 (d, 1H, N-6, J = 6.3 Hz), 9.00 (d, 1H, N-4, J = 8.1 Hz), 8.28 (t, 1H, N-5, J = 6.6 Hz), 6.65 (d, 1H, 1', J = 6.5 Hz), 5.05 (t, 1H, 2', J = 8.3 Hz), 4.42 (t, 1H, 3', J = 8.3 Hz), 4.26 (dt, 1H, 4', J_{3'-4'} = 8.4 Hz, J_{4'-5'} = 2.5 Hz), 4.12 (dd, 1H, 5', J_{4'-5'} = 2.5 Hz, J_{5'-5''} = 13.5 Hz), 3.97 (dd, 1H, 5'', J_{4'-5'} = 2.4 Hz, J_{5'-5''} = 13.3 Hz). α -**18b** (D₂O, pD = 2.59): δ 9.46 (s, 1H, N-2), 9.23 (d, 1H, N-6, J = 6.3 Hz), 9.01 (d, 1H, N-4, J = 8.2 Hz), 8.30 (t, 1H, N-5, J = 6.7 Hz), 6.34 (d, 1H, 1', J = 4.6 Hz), 4.71 (t, 1H, 2'), 4.55 (t, 1H, 3'), 3.98 (dd, 1H, 5', J_{4'-5'} = 3.1 Hz, J_{5'-5''} = 12.7 Hz), 3.87 (dd, 1H, 5'', J_{4'-5'} = 5.7 Hz, J_{5'-5''} = 12.7 Hz). LSIMS 280 (M⁺)

2'-Amino-2'-deoxy nicotinamide arabinofuranoside chloride (19b). **18b** (152 mg, 0.48 mmol) was dissolved in water (30 ml) and dithiothreitol (215 mg, 2.40 mmol) was added. The solution was adjusted to pH 7.1 with 0.1 M sodium hydroxide and the mixture was stirred for 4 h at 25 °C, until evolution of nitrogen had ceased. The mixture was then diluted to 200 ml with water, degassed, and applied to a Bio-Rex 70 (200-400 mesh, 10 ml resin) column generated in the pyridinium form. The amino nucleosides were eluted with a 0-1M pyridinium acetate gradient at pH 6.0 with a flow rate of 0.9 ml/min. The eluant was collected in 8 ml fractions. Each fraction was assayed for the pyridinium moiety by monitoring the absorbance at 326 nm following addition of cyanide. The β -anomer eluted in fractions 58-70 and the α -anomer in fractions 88-98. Hydrochloric acid (2 equivalents with respect to the nucleoside) was added to the combined fractions for each anomer, and the water and pyridinium acetate were removed by rotary evaporation. The residue was coevaporated with methanol to remove traces of water and volatile

salts. Yield α -anomer of **19b** = 17 mg, 0.06 mmol, 12.5%, β -anomer of **19b** = 84 mg, 0.29 mmol, 60.4%. $^1\text{H NMR}$. α -**19b** (D_2O , pD 4.8): δ 9.49 (s, 1H, N-2), 9.27 (d, 1H, N-6), 9.02 (d, 1H, N-4), 8.32 (dd, 1H, N-5), 6.72 (d, 1H, 1'), 4.92 (q, 1H, 4'), 4.58 (t, 1H, 3') 4.25 (t, 1H, 2'), 4.04 (dd, 1H, 5'), 3.89 (dd, 1H, 5''). $^1\text{H NMR}$. β -**19b** (D_2O , pD 3.7): δ 9.88 (s, 1H, N-2, J = 8 Hz), 9.38 (d, 1H, N-6, J = 6 Hz), 9.07 (d, 1H, N-4, J = 8 Hz), 8.38 (t, 1H, N-5, J = 7 Hz), 6.71 (d, 1H, 1', J = 6 Hz), 4.46 (t, 1H, 3', J = 7 Hz), 4.37 (t, 1H, 2', J = 6 Hz), 4.31 (d, 1H, 4', J = 8 Hz), 4.16 (d, 1H, 5', J = 13.5 Hz), 3.99 (d, 1H, 5'', J = 13.5 Hz). Liquid secondary ion MS 254 (M^+).

2'-N-acetyl-2'-deoxy nicotinamide β -D-arabinofuranoside chloride (20b). **β 19b** (45 μmol) was dissolved in 10 ml 30% H_2O / acetic anhydride and stirred for 2 h at room temperature after which the solvent was removed by rotary evaporation yielding **20b** (42 μmol by cyanide assay³⁰, 93 %). The product was purified by reverse-phase HPLC (Rainin Microsorb C₁₈ analytical) and eluted with 2.5% acetonitrile in 10 mM ammonium phosphate buffer (pH 5.5). $^1\text{H NMR}$ (D_2O) δ 9.66 (s, 1H, N2), 9.07 (d, 1H, N6, J = 6.3 Hz) 9.02 (d, 1H, N4, J = 8.1 Hz), 8.28 (t, 1H, N5, J = 7.5 Hz), 6.65 (d, 1H, 1', J_{1'-2'} = 6.6 Hz), 4.96 (dd, 1H, 2', J_{2'-3'} = 8.0 Hz), 4.43 (t, 1H, 3', J_{3'-4'} = 8.6 Hz), 4.27 (dd, 1H, 4', J_{4'-5'} = 1.6 Hz), 4.17 (dd, 1H, 5', J_{5'-5''} = 13.3 Hz), 4.00 (dd, 1H, 5'', J_{4'-5''} = 1.8 Hz), 1.82 (s, 3H, methyl). LIMS 296 (M^+), 174 (M^+ – nicotinamide), 123 (nicotinamideH⁺).

2'-N-trifluoroacetyl-2'-deoxy nicotinamide β -D-arabinofuranoside chloride (20c). **β 19b** (46 μmol) was dissolved in 3 ml trifluoroacetic anhydride and stirred for 1 h after which 4 ml of H_2O was added and the solvents removed by rotary evaporation. The residue was coevaporated with toluene and H_2O to remove traces of trifluoroacetic acid giving pure **20c** (45 μmol by cyanide assay³⁰, 99 %). $^1\text{H NMR}$ (D_2O) δ 9.70 (s, 1H, N2), 9.17 (d, 1H, N6, J = 6.1 Hz), 9.02 (d, 1H, N4, J = 7.7 Hz), 8.29 (t, 1H, N5, J = 7.5 Hz), 6.74 (d, 1H, 1', J_{1'-2'} = 6.3 Hz), 5.12 (t, 1H, 2', J_{2'-3'} = 8.1 Hz), 4.58 (t, 1H, 3', J_{3'-4'} = 8.0 Hz), 4.33 (d, 1H, 4', J_{4'-5'} = 1.7 Hz), 4.17 (d, 1H, 5', J_{5'-5''} = 13.3 Hz), 4.00 (d, 1H, 5'', J_{4'-5''} = 1.4 Hz). LSIMS 350 (M^+).

2'-N-isobutyryl-2'-deoxy nicotinamide β -D-arabinofuranoside chloride (20d). **β 19b** (25 μmol) was dissolved in 1.5 ml dimethylformamide and 0.5 ml isobutyric

anhydride was added and the solution stored overnight. The reaction mixture was added to 75 ml stirred, cold diethylether precipitating pure **20d**. The white precipitate was taken up in methanol and an aliquot taken for cyanide assay³⁰ and the product reprecipitated in ether. Yield: 21 μ mol (84%). ¹H NMR (D₂O) δ 9.57 (s, 1H, N2), 9.13 (d, 1H, N6, J = 6.1 Hz), 9.02 (d, 1H, N4, J = 7.7 Hz), 8.30 (t, 1H, N5, J = 7.5 Hz), 6.69 (d, 1H, 1', J_{1'-2'} = 6.4 Hz), 4.92 (t, 1H, 2', J_{2'-3'} = 8.0 Hz), 4.52 (t, 1H, 3', J_{3'-4'} = 8.6 Hz), 4.29 (d, 1H, 4', J_{4'-5'} = 1.7 Hz), 4.17 (d, 1H, 5', J_{5'-5''} = 13.2 Hz), 4.00 (d, 1H, 5'', J_{4'-5''} = 1.5 Hz), 2.28 (m, 1H, methine), 0.95 (d, 3H, methyl, J = 6.7), 0.81 (d, 3H, methyl, J = 6.8). LSIMS 324 (M⁺) 202 (M⁺ - nicotinamide) 123 (nicotinamideH⁺).

2'-N-benzoyl-2'-deoxy nicotinamide β -D-arabinofuranoside chloride (20e). **β 19b** (80 μ mol) was dissolved in 4 ml dimethylformamide and benzoic anhydride (226 mg 1 mmol) was added and the solution stored overnight. The reaction mixture was added to 125 ml stirred, cold diethylether precipitating pure **20e**. The white precipitate was taken up in methanol and an aliquot taken for cyanide assay³⁰ and the product reprecipitated in ether. Yield: 45 μ mol (57%). ¹H NMR (D₂O) δ 9.61 (s, 1H, N2), 9.21 (d, 1H, N6, J = 6.1 Hz), 9.02 (d, 1H, N4, J = 8.0 Hz), 8.29 (t, 1H, N5, J = 7.3 Hz), 7.62-7.44 (m, 5H, aromatics), 6.82 (d, 1H, 1', J_{1'-2'} = 6.2 Hz), 5.17 (t, 1H, 2', J_{2'-3'} = 8.4 Hz), 4.66 (t, 1H, 3', J_{3'-4'} = 8.0 Hz), 4.38 (d, 1H, 4', J_{4'-5'} = 2.1 Hz), 4.22 (d, 1H, 5', J_{5'-5''} = 13.2 Hz), 4.05 (d, 1H, 5'', J_{4'-5''} = 2.0 Hz). LSIMS 358 (M⁺).

3-Fluoro-3-deoxy-1,2-5,6-di-O-isopropylidene- α -D-glucofuranose(13c). Diethylaminosulfur trifluoride (DAST) was reacted with 1,2-5,6-di-O-isopropylidene- α -D-allofuranose **11b** (10.41 g, 40.0 mmol, Pfanstiehl Labs. Inc.) following the method of Tewson and Welch.¹⁷ The solvents were evaporated and the residue was partitioned between water (10 ml) and dichloromethane (10 ml) and the organic layer was separated, dried (MgSO₄) and evaporated down to give **13c** (5.70 g, 21.4 mmol, 53%). ¹H NMR. (CDCl₃): δ 5.95 (d, 1H, H-1, J_{1,2} = 4.5 Hz), 4.70 (dd, 1H, H-2, J₂₋₁ = 3.7 Hz, J_{2-F} = 10.6 Hz), 5.02 (dd, 1H, H-3, J₃₋₂ = 2.2 Hz, J_{3-F} = 49.8 Hz), 4.29 (m, 1H, H-5), 4.16-4.02 (m, 3H, H-4,6,6'), 1.51, 1.48, 1.44, 1.42, (4s, 12H, isopropylidene methyls).

3-Fluoro-3-deoxy-1,2-O-isopropylidene- α -D-glucofuranose (14c). **13c** (5.70 g, 21.4 mmol) was dissolved in p-dioxane-ethanol-5 M sulfuric acid (60:30:10 ml), kept at room temperature and monitored by t.l.c. (benzene-ether 9:1 according to Foster et al.³¹) until the starting material disappeared completely (*ca.* 4h). The mixture was neutralized with saturated sodium bicarbonate solution, concentrated by rotary evaporation, and extracted with dichloromethane (6 x 20 ml). The combined organic extracts were dried (MgSO₄) and the solvent removed by rotary evaporation to give **14c** (4.75 g, 21 mmol, 98%). ¹H NMR. (CD₂Cl₂): δ 5.95 (d, 1H, H-1, J₁₋₂ = 3.8 Hz), 5.07 (dd, 1H, H-3, J₃₋₄ = 2.2 Hz, J_{3-F} = 49.9 Hz), 4.70 (dd, 1H, H-2, J₂₋₁ = 3.8 Hz, J_{2-F} = 10.9 Hz), 4.14 (dq, 1H, H-4, J_{4-F} = 29.7 Hz, J₄₋₃ = 2.2 Hz, J₄₋₅ = 8.7 Hz), 3.92 (m, 1H, H-5), 3.83 (dd, 1H, H-6, J_{6-6'} = 11.4 Hz, J₆₋₅ = 3.2 Hz), 3.72 (dd, 1H, H-6, J_{6'-6} = 11.4 Hz, J_{6'-5} = 5.2 Hz), 1.47, 1.32 (2s, 6H, two isopropylidene methyls).

3-Fluoro-3-deoxy-6-O-p-nitrobenzoyl-1,2-O-isopropylidene- α -D-glucofuranose (15c). **14c** (4.75 g, 21.0 mmol) was dissolved in pyridine (10 ml) and dichloromethane (25 ml) and the mixture was cooled to -30 °C. p-Nitrobenzoyl chloride (4.29g, 23.1 mmol) was added slowly with vigorous stirring, then the mixture was stored overnight at -20 °C. The solvent was removed by rotary evaporation and the residue partitioned between water (100 ml) and dichloromethane (100 ml). The organic layer was washed with water (2 x 50 ml), dried (MgSO₄) and then removed by rotary evaporation to give crude **15c**. The product was purified by flash chromatography, eluting first with dichloromethane and then with methanol to give pure **15c** (6.31 g, 16.8 mmol, 80%). ¹H NMR. (CDCl₃): δ 8.25 (A₂B₂, 4H, aromatics), 5.99 (d, 1H, H-1), 5.14 (dd, 1H, H-3), 4.78-4.20 (m, 5H, H-2,4,5,6,6'), 1.49 and 1.34 (2s, 6H, isopropylidene methyls).

1,3-Di-O-acetyl-2-fluoro-2-deoxy-5-O-p-nitrobenzoyl- α,β -D-arabinofuranoside (16c). **15c** (6.31 g, 16.8 mmol) was dissolved in dioxane (100 ml) and water (100 ml) at 80 °C before Dowex-50 (H⁺) resin (25 ml) was added. The mixture was stirred at 80 °C for *ca.* 20 h; t.l.c. indicated hydrolysis of the isopropylidene function was complete (R_f product = 0.55, benzene-ethanol 7:1). The solvents were removed under reduced pressure and the residue coevaporated with methanol (2 x 50 ml) and dissolved in acetonitrile (75 ml) and water

(125 ml) containing sodium bicarbonate (2.00 g). Sodium periodate (1.1 equivalents, 18.5 mmol, 3.95 g) was added slowly with stirring at room temperature. The mixture was allowed to stand overnight before the acetonitrile was removed and the residue was extracted with chloroform (5 x 30 ml). The extracts were dried and the solvent rotary evaporated. The residue was dissolved in 50 ml 50% pyridine/acetic anhydride solution and allowed to stir for 2 h. The solvents were removed by rotary evaporation to give **16c** (4.98 g, 13.8 mmol, 83%). ¹H NMR. (CDCl₃): δ 8.26 (A₂B₂, 4, aromatics), 6.32 (d, 1H, H-1), 5.14 (d, 1H, H-2), 4.83 (dd, 1H, H-3), 4.65-4.50 (m, 3H, H-4,5,5'), 2.22 (s, 3H, acetyl), 2.08 (s, 3H, acetyl).

2-Fluoro-2-deoxy-3-O-acetyl-5-O-p-nitrobenzoyl-D-arabinofuranoside bromide (17c). **16c** (4.98 g, 13.8 mmol) was dissolved in dichloromethane (50 ml) and 30% hydrogen bromide in acetic acid (5 ml) was added. The mixture was maintained at room temperature overnight before the solvents were removed under reduced pressure; the residue was co-evaporated with toluene (2 x 50 ml) to give **17c** (5.48 g, 13.5 mmol, 98%). Product >95% α-anomer. ¹H NMR. (CDCl₃): δ 8.27 (A₂B₂, 4H, aromatics), 6.55 (d, 1H, H-1, J_{1-F} = 12.3 Hz), 5.47 (d, 1H, H-2, J_{2-F} = 50.1 Hz), 5.24 (dd, 1H, H-3, J_{3-F} = 23.0 Hz, J₃₋₄ = 4.2 Hz), 4.84 (dd, 1H, H-5, J_{5-5'} = 12.2 Hz, J₅₋₄ = 2.1 Hz), 4.69 (dd, 1H, H-5', J_{5'-5} = 12.2 Hz, J_{5'-4} = 4.0 Hz), 4.65 (m, 1H, H-4) and 2.22 (s, 3H, acetyl).

2'-Fluoro-2'-deoxy nicotinamide arabinofuranoside bromide (18c). **17c** (5.48 g, 13.5 mmol) was treated following the procedure described for **17b** to yield **18c** (3.28 g, 9.7 mmol, 72%). T.l.c. (n-BuOH: H₂O :AcOH/ 5:3:2) showed one spot (R_f = 0.51) which gave a positive acetone/ammonia test. ¹H NMR. β-**18c** (CD₃OD): δ 9.80 (s, 1H, N-2), 9.47 (d, 1H, N-6, J = 6 Hz), 9.07 (d, 1H, N-4, J = 8 Hz), 8.32 (dd, 1H, N-5, J = 7 Hz), 6.72 (dd, 1H, 1', J_{1'-2'} = 4.6 Hz, J_{1'-F} = 9.5 Hz), 5.51 (dt, 1H, 2', J_{2'-3'} = 4.7 Hz, J_{2'-F} = 51.3 Hz), 4.53 (dt, 1H, 3', J_{3'-4'} = 5 Hz, J_{3'-F} = 17.6 Hz), 4.24 (m, 1H, 4', J_{3'-4'} = 5 Hz, J_{4'-5'} = 2.6 Hz, J_{4'-5''} = 3.7 Hz), 4.03 (dd, 1H, 5', J_{4'-5'} = 2.6 Hz, J_{5'-5''} = 12.5 Hz), 3.90 (dd, 1H, 5'', J_{4'-5''} = 3.7 Hz, J_{5'-5''} = 12.5 Hz). LSIMS: 257 (M⁺).

References

- (1) Woenckhaus, C. and Jeck, R., in "Pyridine Nucleotide Coenzymes"; D. Dolphin, R. Poulson and O. Avramovic, Eds. John Wiley and Sons: New York, 1987; pp. 450-555.
- (2) Anderson, B.M. and Kaplan, N.O., in "Pyridine Nucleotide Coenzymes"; D. Dolphin, R. Poulson and O. Avramovic, Eds. John Wiley and Sons: New York, 1987; p. 581.
- (3) Woenckhaus, C.; Volz, M. and Pfeleiderer, G.Z. *Z. Naturforsch.* **1964**, *19b*, 467-470.
- (4) Woenckhaus, C. and Jeck, R., in "Pyridine Nucleotide Coenzymes"; D. Dolphin, R. Poulson and O. Avramovic, Eds. John Wiley and Sons: New York, 1987; pp. 523-525.
- (5) Kam, B.L.; Malver, O.; Marschner, T.M. and Oppenheimer, N.J. *Biochemistry* **1987**, *26*, 3453-3461.
- (6) Slama, J.T. and Simmons, A.M. *Biochem.* **1988**, *27*, 183-193.
- (7) Sleath, P.R.; Handlon, A.L. and Oppenheimer, N.J. *submitted for publication*.
- (8) Bobek, M. *Carbohydr. Res.* **1979**, *70*, 263-273.
- (9) Ness, R.K., in "Synthetic Procedures in Nucleic Acid Chemistry"; W. W. Zorbach and R. S. Tipson, Eds. Wiley Interscience: New York, 1968; pp. 183-87.
- (10) Xu, T.C. and Oppenheimer, N.J. *manuscript in preparation*.
- (11) Hobbs, J.B. and Eckstein, F. *J. Org. Chem.* **1977**, *42*, 714-719.
- (12) Abrams, D.N.; Mercer, J.R.; Knaus, E.E. and Wiebe, L.L. *Int. J. Appl. Radiat. Isot.* **1985**, *36*, 233-238.
- (13) Imai, K.; Fujii, S.; Takanoashi, Y.; Furukawa, T.M. and Honjo, M. *J. Org. Chem.* **1969**, *34*, 1547-1550.
- (14) Walt, D.R.; Findeis, M.A.; Rios-Mercadillo, V.M.; Auge, J. and Whitesides, G.M. *J. Am. Chem. Soc.* **1984**, *106*, 234-239.
- (15) Kaplan, N.O. and Stolzenbach, F.E. *Methods Enzymol* **1957**, *3*, 899-905.
- (16) Hall, L.D. and Miller, D.C. *Carb. Res.* **1976**, *47*, 299-305.
- (17) Tewson, T.J. and Welch, M.J. *J. Org. Chem.* **1978**, *43*, 1090-1096.

- (18) Collins, P.M. *Tetrahedron* **1965**, *21*, 1809-1904.
- (19) Reichman, U. and Watanabe, K.A. *Carb. Res.* **1975**, *42*, 233-239.
- (20) Jarman, M. and Ross, W.C.J. *J. Chem. Soc. (C)* **1969**, 199-206.
- (21) Ueda, T., in "The Chemistry of Nucleosides and Nucleotides"; L. B. Townsend, Eds. Plenum Press: New York, 1988; p. 5.
- (22) Scriven, E.F. and Turnbull, K. *Chem. Rev.* **1988**, *88*, 297-328.
- (23) Saegusa, T.; Ito, Y. and Shimizu, T. *J. Org. Chem.* **1970**, *35*, 2979-2986.
- (24) You, K.S. *Crit. Rev. Biochem.* **1985**, *17*, 313-332.
- (25) Staros, J.V.; Bayley, H.; Standing, D.N. and Knowles, J.R. *Biochem. Biophys. Res. Comm.* **1978**, *80*, 568-572.
- (26) Handlon, A.L. and Oppenheimer, N.J. *Pharm. Res.* **1988**, *5*, 297-299.
- (27) Horwitz, J.P.; Chua, J. and Noel, M. *J. Org. Chem.* **1964**, *29*, 2076-2078.
- (28) Lin, T.S. and Prusoff, W.H. *J. Med. Chem.* **1978**, *21*, 109-112.
- (29) Sanders, J.K.M. and Hunter, B.K. *Modern NMR Spectroscopy*, Oxford: New York, 1988; ch. 6.
- (30) Colowick, S.P.; Kaplan, N.O. and Ciotti, M.M. *J. Biol. Chem.* **1951**, *191*, 447-59.
- (31) Foster, A.B.; Hems, R. and Webber, J.M. *Carb. Res.* **1967**, *5*, 4387-4393.

Chapter 4

**Structure-Reactivity in the 2'-substituted nicotinamide nucleosides:
Probing the Mechanism of Glycosyl Bond Cleavage.**

Introduction

The NAD⁺ coenzyme participates directly in an array of biochemical reactions that are central to the maintenance of mammalian health and some that are responsible for the initiation of mammalian disease. These include the non-redox roles for NAD⁺ that involve the cleavage of the nicotinamide-glycosyl bond. The enzymes and toxins that catalyze ADP-ribosylation and NAD⁺ hydrolysis were discussed in Chapter 2. The NAD⁺ molecule also undergoes base-catalyzed chemical hydrolysis. The mechanism of the chemical hydrolysis has provided insight into the enzymatic mechanism and also the nature of glycosyl bond cleavage in general.

Because of their ease of synthesis, many NAD⁺ analogs have been synthesized with substituents at the 3-position of the pyridine ring.¹ Tarnus and Schuber² have used such analogs to study the mechanism of NAD⁺ hydrolysis including the NAD⁺ glycohydrolase catalyzed reaction. They measured the rate of cleavage of the glycosyl bond and related this to the pK_a of the departing pyridine. Brønsted plots gave slopes (β) of -1.11 and -0.90 for the non-enzymatic and enzymatic reactions, respectively, which are consistent with a dissociative mechanism.* Few studies have been conducted, however, that analyze the influence of the sugar moiety. This is a significant omission because specific mechanistic roles have been proposed for the nicotinamide ribose diol in glycosyl bond cleavage. For example, Johnson et al.³ demonstrated that ionization of the ribose diol of NAD⁺ (pK_a = 11.7) results in a 10⁴ increase in the rate of hydrolysis, and proposed that this acceleration results from an electrostatic stabilization of the oxocarbenium intermediate by the diol anion. Furthermore, a replacement of the nicotinamide ribose 2'-OH with -OH or -F in the arabinose ("up") configuration results in a tight-binding competitive inhibitor of NAD⁺ glycohydrolase which is hydrolyzed at <10⁻⁵ the rate of NAD⁺ itself.⁴

The 2'-substituent has been implicated in a number of different mechanistic roles in glycosyl bond cleavage. Sinnott and coworkers⁵ have observed base-catalyzed hydrolysis of

* The term "dissociative" is meant to encompass unimolecular mechanisms A₁ and S_N1 without implying anything about the degree of bond-breakage in the transition state; it is intended to imply a substitution mechanism involving an electron-deficient intermediate.

pyridinium glucoside and have proposed that the 2'-hydroxyl ionizes and directly displaces the pyridinium giving an 1,2-anhydro sugar intermediate. Such an intramolecular nucleophilic participation, often referred to as anchimeric assistance, has precedent in the carbohydrate literature. After Brigl synthesized 3,4,6-tri-O-acetyl-1,2-anhydro-glucopyranose⁶ (Brigl's anhydride, Figure 4.1) in 1922, anhydrosugar intermediates have often been proposed for base-catalyzed hydrolyses in which the aglycon is trans to a free hydroxyl. Although anchimeric assistance has often been invoked for base-catalyzed glycosyl bond cleavage,^{7, 8} the intermediate anhydrosugars have not been characterized.

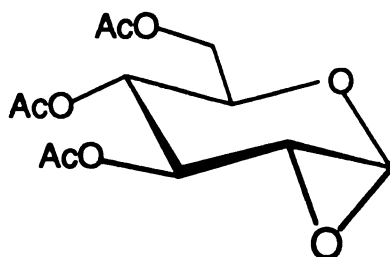
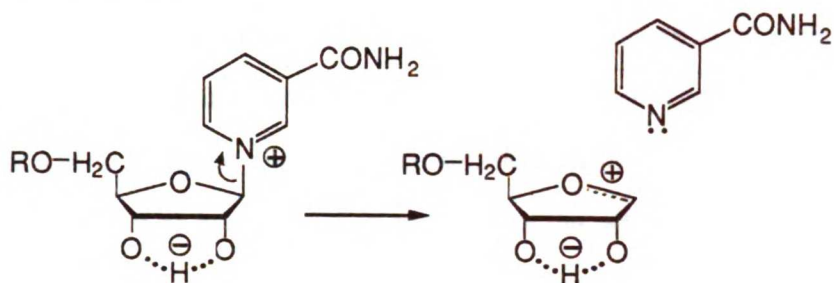


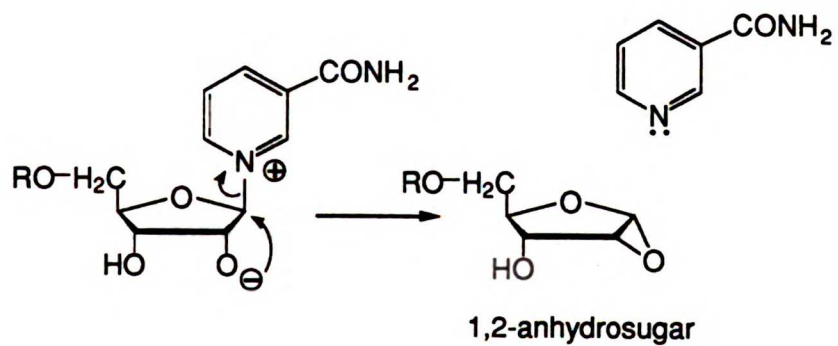
Figure 4.1. Brigl's Anhydride

There seems to be a consensus that the 2'-substituent is important in glycosyl bond cleavage, but the specific mechanistic role remains a point of contention. On one extreme, the 2'-hydroxyl is implicated as an intramolecular nucleophile, and at the other extreme, the influence of the 2'-hydroxyl is thought to derive from its ability to electrostatically stabilize an oxocarbenium intermediate (Scheme 4.1).³ In order to explore the role of the 2'-substituent in the glycosyl bond cleavage of NAD⁺, the hydrolysis reaction of a series of 2'-substituted nicotinamide nucleoside analogs (Scheme 4.2) were investigated. The 2' substituents were selected to span a range of electronic properties and are oriented either cis or trans to the departing nicotinamide ring. This chapter will present the kinetic results and will discuss the mechanism of nicotinamide nucleoside and NAD⁺ hydrolysis. The results of this investigation also have important implications for the mechanism of enzymatic glycoyl bond cleavage.

Scheme 4.1.

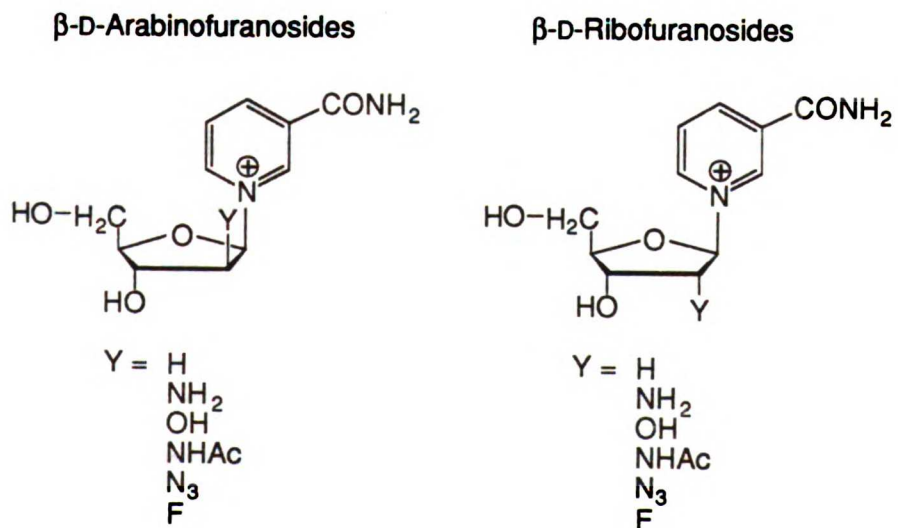


Diol anion stabilized dissociation of nicotinamide.



Direct displacement of nicotinamide by
the 2'-hydroxy anion.

Scheme 4.2.



The 2'-substituted nicotinamide nucleosides also represent an excellent model system to study substituent effects in glycoside and purine nucleoside hydrolysis. Because of the cationic pyridinium aglycone, a nicotinamide nucleoside is analogous in structure to the conjugate acid of a glycoside or purine nucleoside. Thus, the hydrolysis of a nicotinamide nucleoside is pH independent over a wide pH range. Any observed substituent effects in the hydrolyses of these nucleosides will result from its direct inductive influence on the activated complex. In contrast, studies of substituent effects of acid-catalyzed glycoside or purine nucleoside hydrolysis are intrinsically ambiguous because the substituents can perturb both the pK_a of the leaving group as well as influence the stability of the activated complex or putative intermediates.

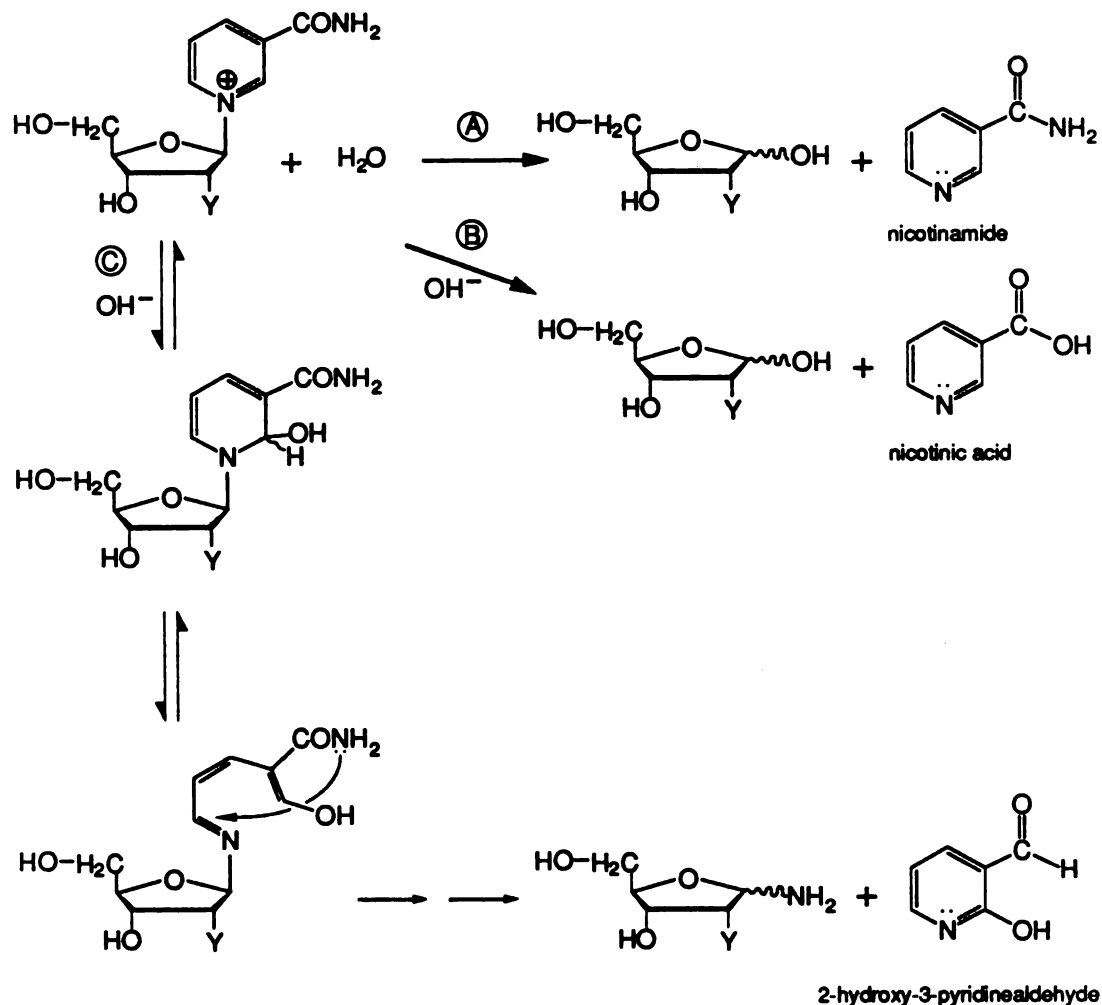
Results

The 2'-substituted nicotinamide nucleosides were synthesized according to procedures outlined in chapter 3. All nucleosides were purified to over 98% anomeric purity by reverse-phase HPLC and analyzed by liquid secondary ion mass spectrometry which reported appropriate molecular ion m/z values. Initially the hydrolysis experiments were conducted at 37 °C with the exception of the 2'-fluoro-nucleoside, in which the hydrolysis kinetics were conducted at four temperatures over the range from 65-97 °C and the values of the rate constants extrapolated back to 37 °C. The hydrolysis of the 2'-substituted nucleoside (Scheme 4.3) was monitored by UV absorbance at the appropriate λ_{max} using a discontinuous cyanide addition assay⁹ which is specific for N-substituted nicotinamide cations. First order rate constants were derived from a least squares fit of $\log[\text{nucleoside}]$ vs. time which were linear for over four half-lives.

The hydrolysis kinetics were determined for each of the nucleosides over a wide range of pH (usually 2-12). For example, Figure 4.2 shows the pH/rate profile for the 2'-deoxy nucleoside. The acceleration in rate of hydrolysis at high pH was seen for each of the 2'-substituted nucleosides. Nevertheless, each nucleoside displayed a region of pH independent hydrolysis which extended at least up to pH 7 and represented nicotinamide release only (Scheme 4.3A).

Scheme 4.3. The three hydrolysis reactions of the nicotinamide nucleosides.

Pathways B and C occur only in the pH-dependent region (above pH 8).



The pH independent rates are summarized in Table 4.1. The 2'-amino nucleosides displayed a break in the pH/rate curve that corresponded to the protonation of the amine; this behavior will be explored more fully in chapter 5.

Product analysis of the reaction mixtures from each hydrolysis experiment was conducted by reverse-phase HPLC as described in the experimental section. In the pH independent region only nicotinamide release was observed. At high pH the products were no longer exclusively nicotinamide (Scheme 4.3B). Above pH 8 nicotinic acid was detected which results from the

hydrolysis of the carboxamide moiety of nicotinamide. Above pH 11, 2-hydroxy-pyridinealdehyde was detected which results from the attack of hydroxide on the pyridinium moiety (Scheme 4.3C).³

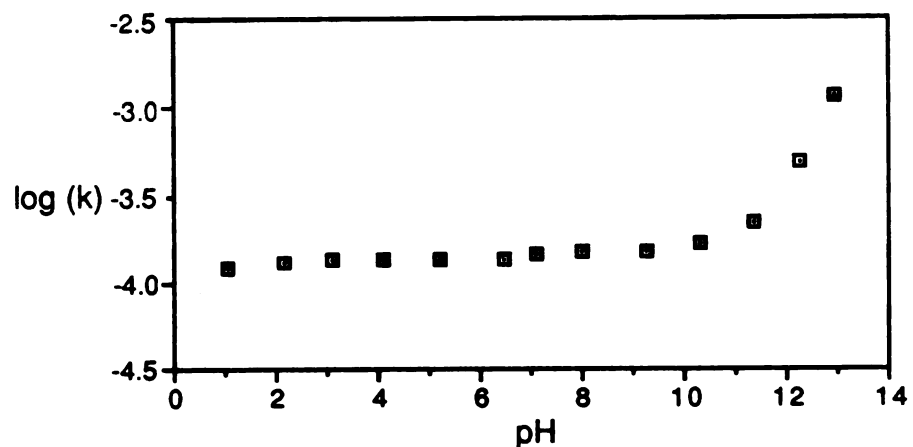
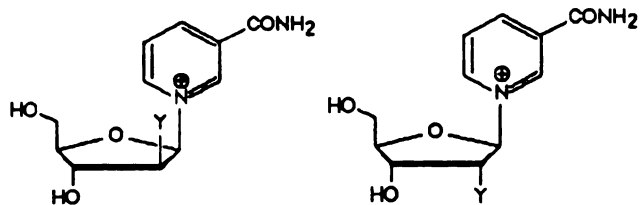


Figure 4.2. pH/rate plot for the hydrolysis of the 2'-deoxy nucleoside.

After the pH-dependence for the hydrolysis was established at 37 °C, the temperature dependence was explored by performing the hydrolysis of each nucleoside at three more temperatures within the pH independent region. The products were analyzed by HPLC to confirm that only nicotinamide release was occurring. The Arrhenius plots for the temperature-dependent hydrolysis of the 2'-substituted nicotinamide nucleosides are presented in Figures 4.3 and 4.4. The slopes and y-intercepts from these plots were used to calculate the energies of activation according to Carpenter.¹⁰ The ΔH^\ddagger and ΔS^\ddagger values are summarized in Table 4.2.

Table 4.1. Hydrolysis Rate Constants ($s^{-1} \times 10^8$) at 37 °C



2'-substituent	β -Arabinosides	β -Ribosides
H	14,454	14,454
NH ₂	1,071	1,778
NHAc	99.3	54,998
OH	97.1	169
N ₃	20.0	28.2
F	4.17	3.00

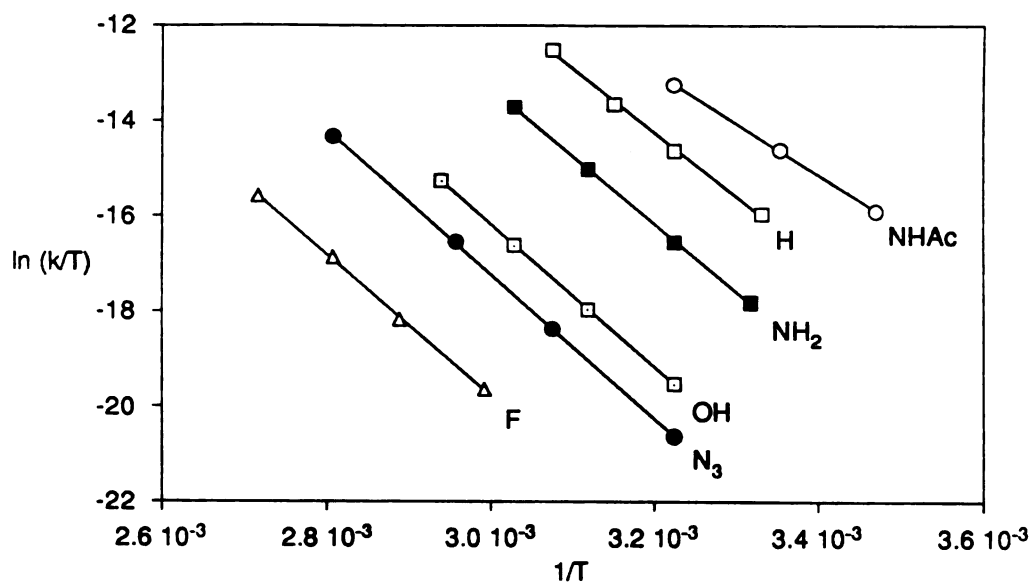


Figure 4.3. Arrhenius plot for the hydrolysis of the nicotinamide 2'-substituted- β -D-arabinofuranosides.

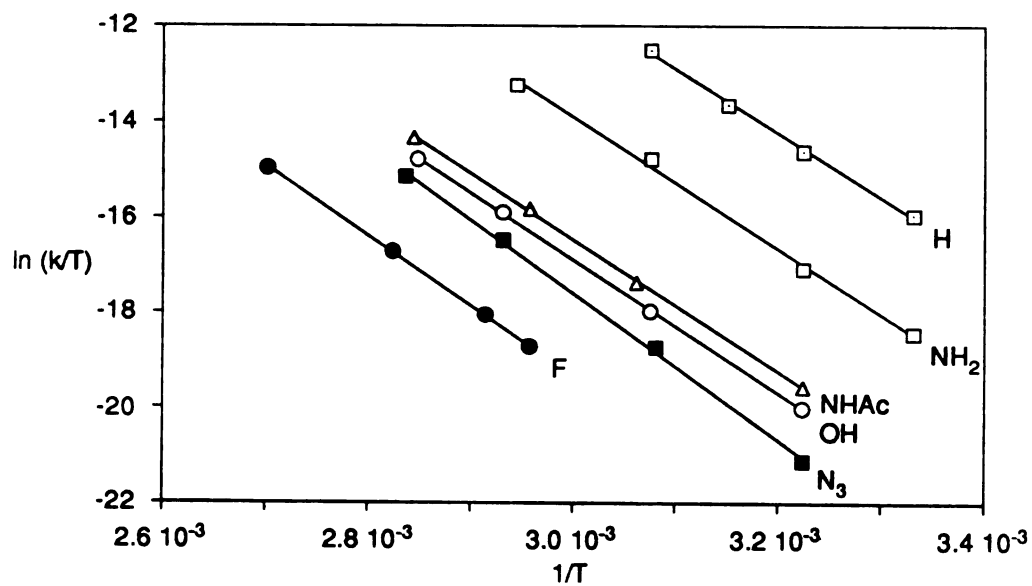


Figure 4.4. Arrhenius plot for the hydrolysis of the nicotinamide 2'-substituted- β -D-ribofuranosides.

Table 4.2. Entropies and Enthalpies of Activation for the Hydrolysis of the 2'-Substituted Nicotinamide Nucleosides

Arabinofuranosides

<u>2'-Substituent</u>	<u>ΔH^\ddagger (Kcal/mol)</u>	<u>ΔS^\ddagger (cal/mol deg)</u>
H	26.6 \pm 0.8	9.5 \pm 2.5
NH ₂	27.2 \pm 0.9	6.7 \pm 2.8
NHAc	27.4 \pm 0.4	2.2 \pm 1.2
OH	27.7 \pm 0.3	2.3 \pm 0.8
N ₃	30.5 \pm 0.7	9.3 \pm 2.3
F	29.1 \pm 0.2	1.6 \pm 0.7

Ribofuranosides

<u>Substituent</u>	<u>ΔH^\ddagger (Kcal/mol)</u>	<u>ΔS^\ddagger (cal/mol deg)</u>
NHAc	21.4 \pm 0.3	-4.5 \pm 1.1
H	26.6 \pm 0.8	9.5 \pm 2.5
NH ₂	28.9 \pm 0.5	13.2 \pm 2.2
OH	29.7 \pm 0.5	9.8 \pm 1.8
N ₃	30.4 \pm 0.6	9.7 \pm 2.1
F	29.3 \pm 0.7	1.6 \pm 0.6

The first order rate constants from Table 4.1 show that the reactivity of the nucleosides is very sensitive to the 2'-substituent. In the ribofuranoside series, for example, there is a 4800 fold increase in the rate of hydrolysis in going from 2'-F to 2'-H. The rates are independent of the steric bulk of the substituent. If a charge is developing in the transition state, then the rates would be expected to vary with the polarity of the 2'-substituent. The most commonly used parameter that reflects polarity is the inductive sigma constant, σ_I .¹¹ Sets of sigma constants were originally compiled by Charton¹² based on the seminal work by Taft and coworkers.¹³⁻¹⁵ As shown in Figure 4.5 the first order rate constants for the arabinoside hydrolyses correlate linearly with the inductive sigma constant according to the equation $\log(k) = \rho_I \cdot \sigma_I + \log(k_0)$ giving a slope, ρ_I of -6.8 (R = 0.99). The log of the rate constants of hydrolysis also correlate linearly with another set of sigma values, σ_I^Q ,¹⁶ (plot not shown), giving a value of ρ_I^Q of -1.4 (R = 0.99). The log k versus σ_I plot for the ribofuranosides is shown in Figure 4.6. In this series the 2'-substituent is trans to the nicotinamide. Nevertheless, the slope is similar to that obtained in the arabinoside series in which the substituents are cis. With the exception of the 2'-N-acetyl, the correlation between the rates and the inductive substituent constant is good (R = 0.99).

The nicotinamide 2'-N-acetyl- β -D-ribofuranoside hydrolyzed at a rate about 300 times greater than expected on the basis of its σ_I value and about 550-fold greater than the corresponding arabinofuranoside. The rate constant for the pH independent hydrolysis of 2'-N-acetyl- α -D-ribofuranoside (in which the N-acetyl is cis to the nicotinamide) was found to be 4.47×10^{-7} . There is ample precedent for the N-acetyl group to participate as an intramolecular nucleophile to catalyze the cleavage of glycosyl bonds (Scheme 4.4).¹⁷⁻²⁰

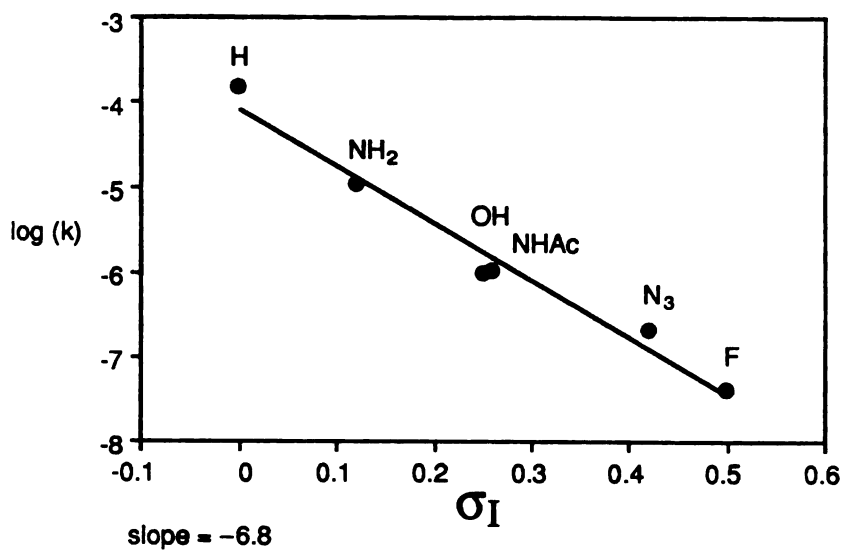


Figure 4.5. Log(k) versus sigma for the hydrolysis of the 2'-substituted nicotinamide β -D-arabinofuranosides.

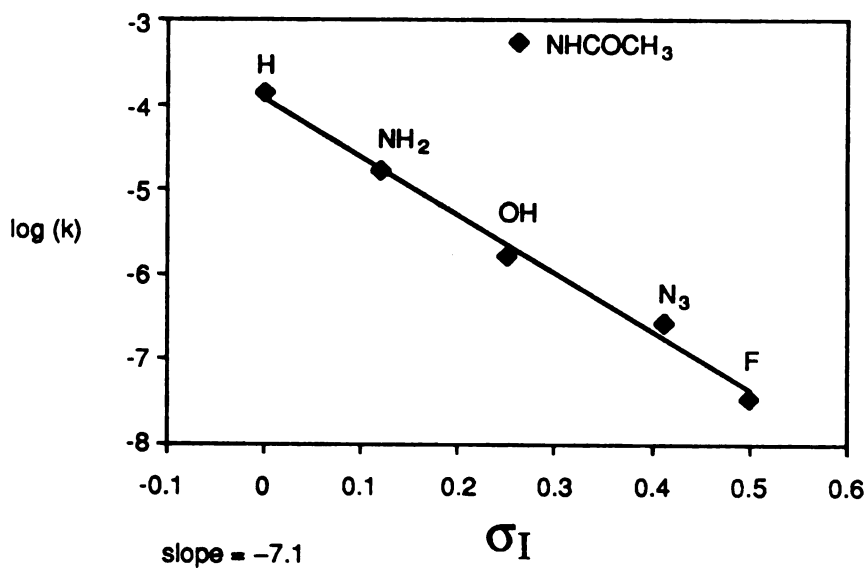
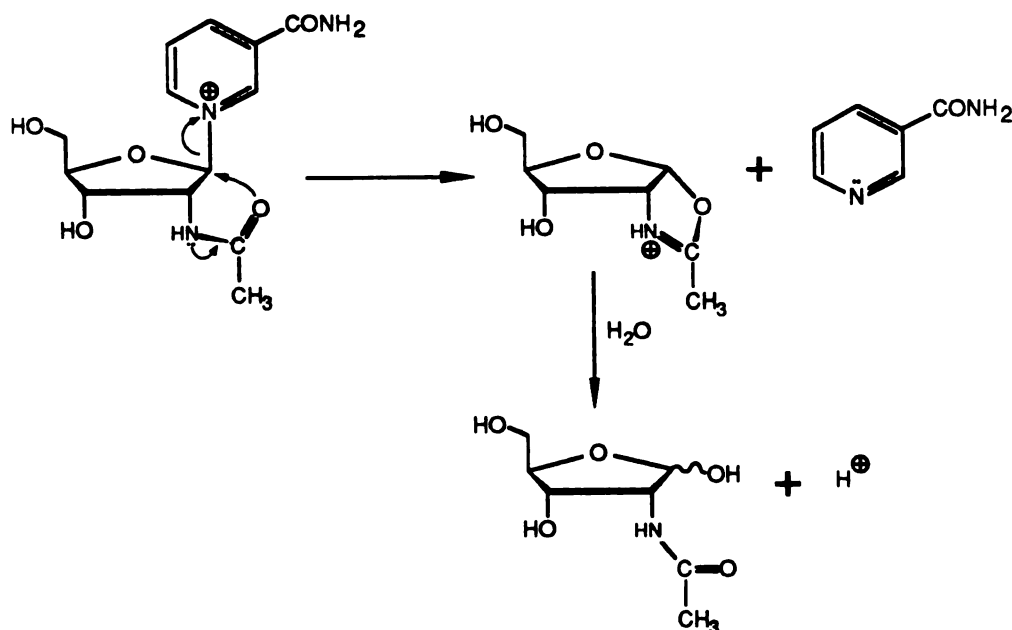


Figure 4.6. Log(k) versus sigma for the hydrolysis of the 2'-substituted nicotinamide β -D-ribofuranosides.

Initial attempts to synthesize the nicotinamide 2'-N-acetyl- β -D-ribofuranoside according to procedures that had been used for the arabinosides resulted in failure; only nicotinamide was isolated. It was not realized that the 2'-N-acetyl- β -D-ribofuranoside was unstable until the N-acetylation of the 2'-amino- β -D-ribofuranoside was followed by ^1H NMR and the resulting acetamide was found to hydrolyze quickly with a half-life of 24 minutes at 37 °C and pH 3.3. The temperature dependence was determined by repeating the hydrolysis experiments at 15 °C and 25 °C (at pH 3.3) and the activation parameters are summarized in Table 4.2. The pH dependence was determined by buffering the samples with 500 mM phosphate at pH 6.1, 8.0, and 10.3 and following the reactions by ^1H NMR at 25 °C. The hydrolysis was pH independent throughout this range and only nicotinamide release was observed.

Ballardie et al.²⁰ investigated the neighboring group participation of acetamido groups in the hydrolysis of glucopyranosyl fluoride and used ^1H to identify the oxazoline intermediate that resulted from the intramolecular attack of the acetamide on the anomeric carbon. They followed the disappearance of the glucopyranosyl fluoride in MeOH- d_4 and saw a new doublet grow in at 6.03 ppm which was assigned to the anomeric proton of the intermediate. This peak reached a maximum after 100 minutes and disappeared after 18 hours to give the methyl glucopyranoside. Based on their findings, the hydrolysis of the 2'-N-acetyl- β -D-ribofuranoside was followed over time at pH 10.3. The anomeric proton, a doublet at 6.33 ppm, disappeared over time as a new doublet at 6.15 ppm appeared in the NMR spectrum. This resonance reached a maximum after about 95 minutes at 25 °C and disappeared after 20 hours leaving a doublet at 5.15 ppm and a singlet at 5.37 ppm which are characteristic for the α and β anomers of the free furanose.

Scheme 4.4. Anchimeric assistance by an N-acetyl group illustrated here for the hydrolysis of nicotinamide 2'-N-acetyl- β -D-ribofuranoside

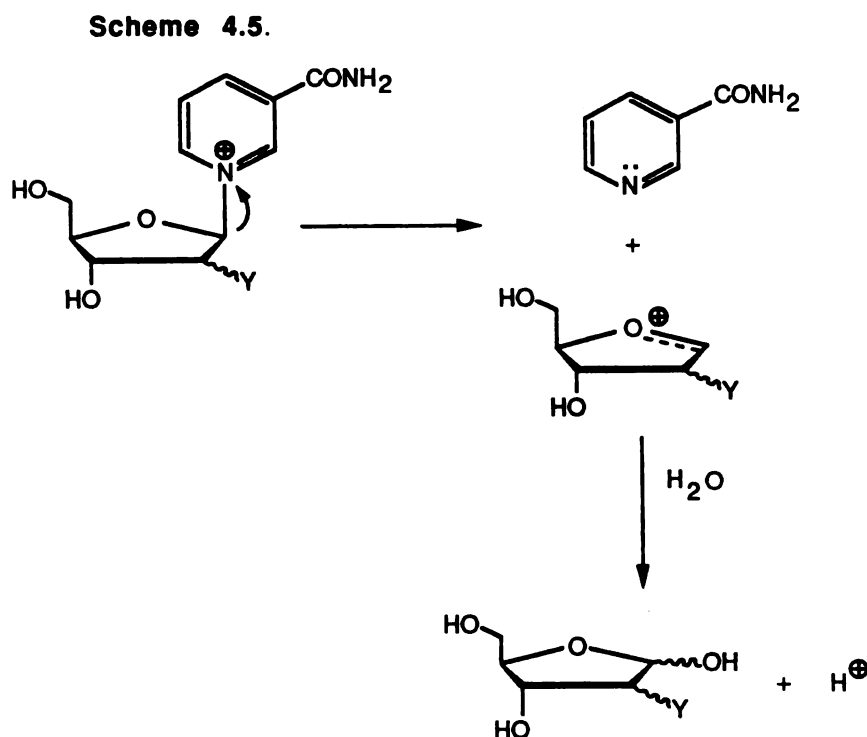


Discussion

Mechanism of nicotinamide nucleoside hydrolysis

The kinetic results in Table 4.1 demonstrate that the stability of the glycosyl bond is strongly influenced by the polarity of the 2'-substituent. The slopes (ρ_I) from Figures 4.5 and 4.6 serve as a measure of the change in electron density at the reaction center.¹⁴ The slopes measured for the nicotinamide nucleosides are similar in sign and magnitude to slopes obtained from model reactions involving highly cationic activated complexes. For example, the hydrolysis of 24 acetals and ketals gave large and negative ρ_I values consistent with the A1 mechanism for acetal hydrolysis.¹⁵ Furthermore, Grob has used the solvolysis of tertiary bridgehead tosylates as models of dissociative mechanisms involving carbocations and has found ρ_I^Q values of between -1.1 and -1.3.²¹ The hydrolysis of the nicotinamide arabinosides gave a ρ_I^Q of -1.4. In contrast, reactions that proceed by an associative mechanism, such as base-catalyzed ester hydrolysis, give positive ρ_I values consistent with an electron rich tetrahedral intermediate.²² Therefore,

these results are consistent with a unimolecular dissociative mechanism for the hydrolysis of the 2'-substituted nicotinamide nucleosides involving an intermediate with substantial oxocarbenium character as outlined in Scheme 4.5.



Activation energies

The small and positive entropies of activation in Table 4.2 support a dissociative mechanism. Studies of model dissociative reactions such as acetal and glycoside hydrolysis give ΔS^\ddagger values in the range of 2-16 e.u.²³⁻²⁵ This is reasonable because dissociative mechanisms involve an increase in disorder in going to the transition state. In contrast, negative entropies of activation (-10 to -30 e.u.) usually indicate associative (A-2 or S_N2) mechanisms such as the base-catalyzed hydrolysis of esters, epoxides, and aziridines.²³

As demonstrated in Figure 4.5, the rate of hydrolysis of the arabinofuranosides decreases as the electron density at the reaction center is drawn away by the 2'-substituent. The plots in Figures 4.7 and 4.8 indicate that both the entropy and the enthalpy components

contribute to the substituent effects observed. As the 2'-substituent becomes more electron withdrawing, there is an increase in order to the transition state. A similar drop in ΔS^\ddagger has been observed in the hydrolysis of methyl 2-chloro- β -D-glucopyranoside by Buncl and Bradley.²⁶ They found that in going from 2-OH to 2-Cl there was a 35-fold decrease in rate of acid-catalyzed hydrolysis and a drop in ΔS^\ddagger of 6.1 e.u.* Their interpretation was that as the 2'-substituent becomes less able to provide inductive stabilization of the oxocarbenium intermediate, there is a concomitant increase in ordering of the solvent shell around the reaction center in order to provide more solvent stabilization. Along with the changes in entropy, there is a concomitant increase in the glycosyl bond energy (as reflected by ΔH^\ddagger , Figure 4.8) with increasing electron withdrawal of the 2'-substituent. The enthalpy of activation of the 2'-N₃ arabinofuranoside is much greater than would be expected from its rate of hydrolysis. At the same time, the entropy of activation is correspondingly elevated and compensates for the enthalpic term resulting in an overall ΔG^\ddagger that correlates with sigma (Figure 4.9). This type of anomalous behavior for the azido substituent has been observed in the energies of activation for the methanolysis of 4-substituted chloro-benzenes.²⁷

The activation parameters for the hydrolysis of the 2'-N-acetyl β -D-ribofuranoside (Table 4.2) are anomalous and are consistent with a change in mechanism. Typically, when anchimeric assistance is invoked for *bimolecular* reactions, there is an increase in the entropy to the transition state.^{28,29} Dissociative reactions, on the other hand, show increasing order to the transition state if a neighboring group acts as an intramolecular nucleophile. This was demonstrated by Piszkiwicz and Bruce¹⁸ for the hydrolysis of a series of *o*-carboxyphenyl β -D-glucopyranosides.

* It should be pointed out that one of the intrinsic problems with studying substituent effects in acid-catalyzed reactions is the ambiguity regarding the chemical step being perturbed. It has always been *assumed* that the ΔS^\ddagger represents the bond cleavage step. The observed changes in ΔS^\ddagger may reflect the pre-equilibrium protonation step, however. The nicotinamide nucleosides represent a much "cleaner" system because they are not subject to acid-catalyzed hydrolysis.

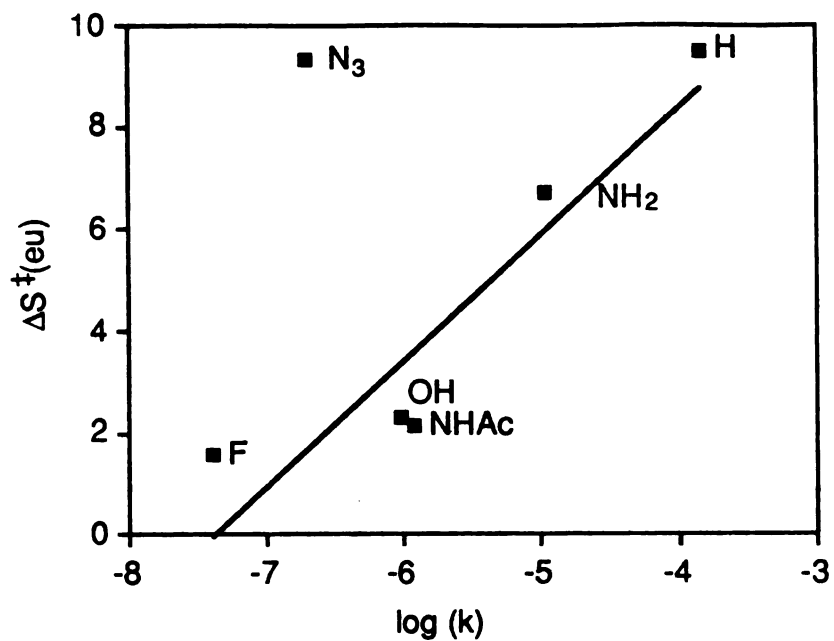


Figure 4.7. ΔS^\ddagger versus $\log(k)$ for the hydrolysis of the nicotinamide 2'-substituted β -D-arabinofuranosides

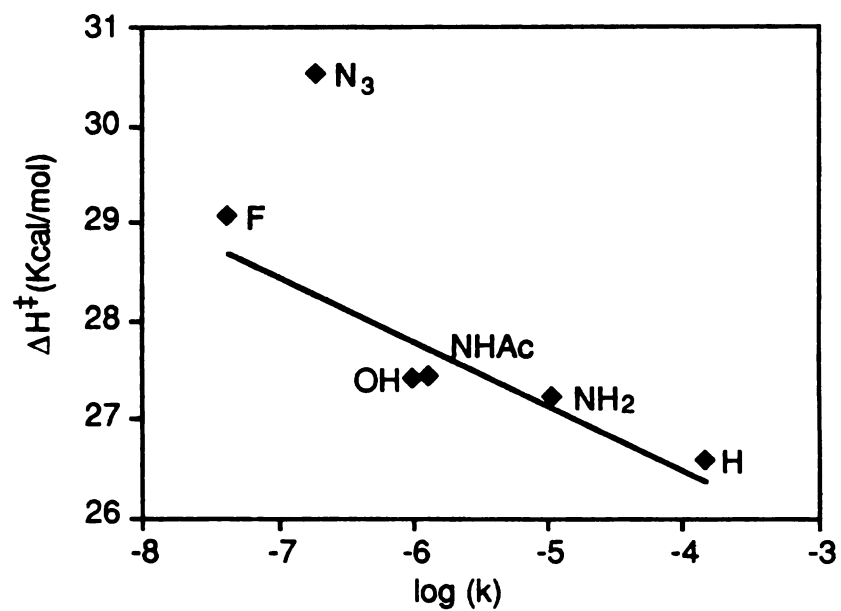


Figure 4.8. ΔH^\ddagger versus $\log(k)$ for the hydrolysis of the nicotinamide 2'-substituted β -D-arabinofuranosides

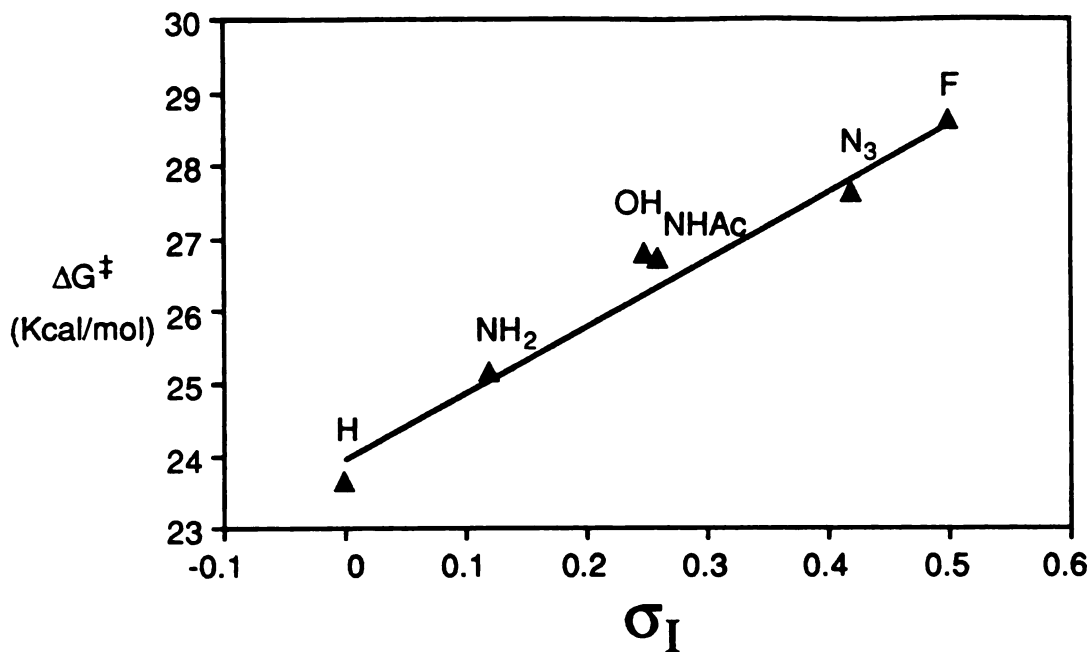


Figure 4.9. Plot of the Gibb's free energy of activation versus sigma for the hydrolysis of the nicotinamide 2'-substituted β -D-arabinofuranosides

They found that when the 2'-hydroxyl is replaced by a 2'-N-acetyl, the anchimeric assistance accounts for a 16-fold rate acceleration and that the entropy of activation decreases by 6.4 e.u. Table 4.2 shows that in going from the ara to the ribo 2'-N-acetyl, the entropy of activation decreases by 6.7 e.u. and that when the trans 2'-OH is replaced by the 2'-N-acetyl there is a 14.3 e.u. decrease (despite the near equivalence of the sigma values of these substituents). Therefore, the activation parameters suggest an anchimeric assistance mechanism for the 2'-N-acetyl ribofuranoside but not for other substituents such as the 2'-NH₂.

Mechanism of NAD⁺ hydrolysis

The nicotinamide nucleosides in these studies were designed as models of NAD⁺ to probe transition state structure and the role of the 2'-substituent. The observed substituent effects suggest a dissociative mechanism for NAD⁺ hydrolysis. Previous structure-activity relationships also have pointed to a dissociative mechanism for NAD⁺ hydrolysis. For example,

the rate of hydrolysis of NAD⁺ analogs containing modified pyridinium bases was shown to be dependent on the pK_a of the departing pyridine; a Brønsted plot gave a large negative slope indicating an electron deficient activated complex.² Cordes and coworkers investigated the secondary deuterium isotope effects for the hydrolysis of NAD⁺,³⁰ nicotinamide mononucleotide³⁰ and nicotinamide riboside³¹ containing deuterium at the anomeric position. They reported isotope effects of 10, 13, and 14 percent, respectively, values consistent with a dissociative mechanism.

The substituent effects reported here also have important implications for the mechanism of the base-catalyzed hydrolysis of NAD⁺. In base, the ribose diol of NAD⁺ is ionized and this leads to a 10⁴ acceleration in rate of hydrolysis. Johnson, et al.³ propose that this acceleration results from an electrostatic interaction between the 2'-hydroxy anion and the oxocarbenium ion intermediate. Figure 4.10 shows the sigma plots of the arabinosides and the ribosides plus a point representing the pH independent hydrolysis of NAD⁺ in base from the Johnson study.³ Appropriately, the sigma value for this point represents O(-).³² This plot indicates that inductive effects have a profound influence on the lability of the nicotinamide-glycosyl bond and suggests that the rate acceleration that Johnson et al. observed can be accounted for by the *electronic* influence of the 2'-hydroxy anion. Thus, it is not necessary to invoke anchimeric assistance for the diol anion: the electron donating effect of the anion is sufficient to inductively stabilize the oxocarbenium ion intermediate.

Table 2.3 summarizes the activation energies for the hydrolysis of NAD⁺ and shows that in base the ΔH^\ddagger is lowered to 11.8 kcal/mol and the ΔS^\ddagger plummets to -30.8 eu. While the lowering in ΔH^\ddagger with faster hydrolysis is consistent with the nicotinamide nucleoside observations, the lowering of the ΔS^\ddagger is not. In fact, the nicotinamide nucleosides show a continuous *increase* in the ΔS^\ddagger as the 2'-substituent becomes more electron donating. The drastic lowering of the ΔS^\ddagger

seen with the diol anion may indicate an ordering of the solvent shell around the reaction center* or a total change in mechanism.

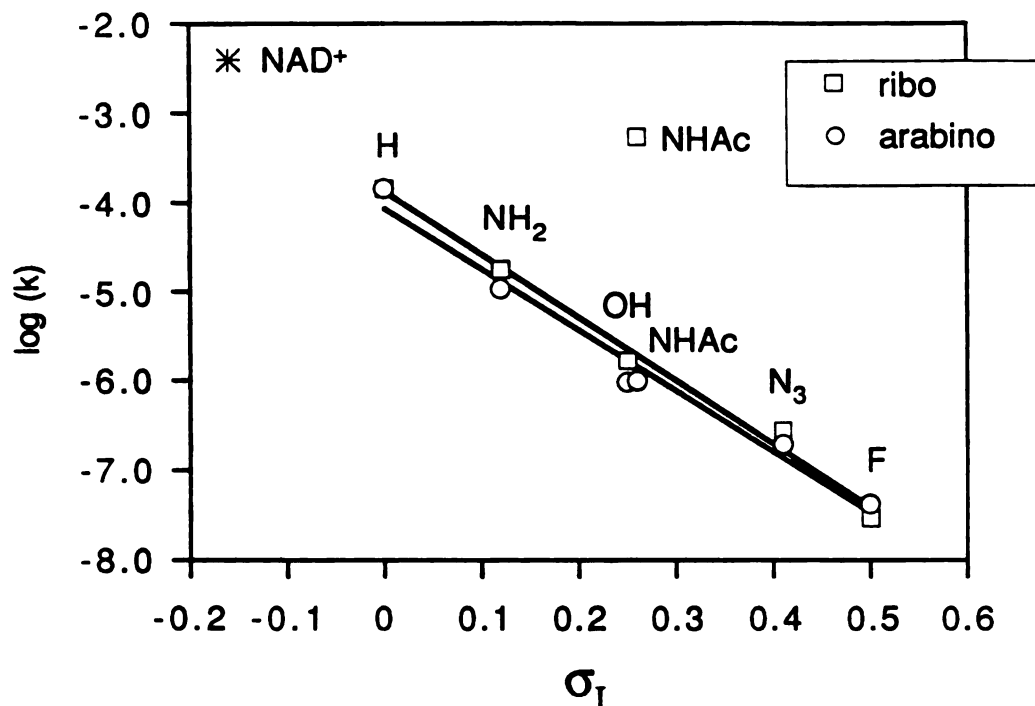


Figure 4.10. Log(k) versus sigma for the hydrolysis of the 2'-substituted nicotinamide nucleosides and for the pH-independent hydrolysis of NAD⁺ in base.

Anchimeric assistance

The 2'-substituents in the present study were selected to span a range of electronic properties and also to include substituents that are good nucleophiles. The amino group is considered to be an extremely powerful intramolecular nucleophile.^{33, 34} This characteristic is responsible for the reactivity and toxicity of the nitrogen mustards.³⁵ The amino group in the β -

* The additional charge in the transition state may lead to an increase in the ordering of the hydration shell and a lower ΔS^\ddagger ; however, by electrostriction arguments (for a discussion see ref 66), bringing together opposite charges in the transition state should lead to an increase in ΔS^\ddagger .

ribofuranoside configuration (trans to the nicotinamide) is set up for an intramolecular displacement. Nevertheless, the plot in Figure 4.10 shows that the reactivity of the 2'-amino ribofuranoside is no greater than would be expected on the basis of its inductive effect alone. The reactivity of the ribofuranosides is slightly greater than the arabinofuranosides but this is seen throughout the series regardless of the nucleophilicity of the 2'-substituent. Thus, these results are not consistent with an anchimeric assistance mechanism for the 2'-amino nucleosides.

In contrast to the 2'-amino nucleosides, the 2'-N-acetyl- β -D-ribofuranoside is about 300 times more reactive than expected on the basis of its inductive effect and about 550 times more reactive than the corresponding arabinofuranoside. Piszkiwicz and Bruice³⁶ investigated the hydrolysis of p-nitrophenyl β -D-glucopyranosides and found that the anchimeric assistance by the 2-N-acetyl group provided a 343 fold increase in rate over the corresponding 2-OH. For the comparable nicotinamide nucleosides, there is a 323 fold increase in rate in going from the 2'-OH to the 2'-N-acetyl. Piszkiwicz and Bruice also looked at the effect of anomeric configuration. They found that the 2-N-acetyl β -D-glucopyranoside hydrolyzed 1100 times faster than the corresponding α anomer (under pH independent conditions) again invoking anchimeric assistance. For the sake of comparison, the pH independent hydrolysis of nicotinamide 2'-N-acetyl- α -D-ribofuranoside was investigated and was found to hydrolyze 1230 times slower than the corresponding β anomer.

The role of anchimeric assistance in the hydrolysis of the 2'-substituted nicotinamide nucleosides was studied in order to understand the role of the 2'-hydroxy anion in the base-catalyzed hydrolysis of NAD⁺. Is a mechanism involving anchimeric assistance by a hydroxy anion in the cleavage of a pyridinium-glycosyl bond reasonable as Sinnott and coworkers³⁷ claim? These results demonstrate that anchimeric assistance by direct displacement can occur if the ring closure forms a five-membered ring (Scheme 4.4). In the case of the 2'-amine, in which a three-membered ring is formed, no anchimeric assistance is observed. Along the same lines, Piszkiwicz and Bruice³⁶ demonstrated anchimeric assistance for the 2'-N-acetyl but could find *no kinetic evidence for anchimeric participation of the 2-hydroxy anion at pH 12*. These results

suggest that nucleophilic groups (such as -NH_2 and -O^-) placed 3 bonds away from the nicotinamide ring are not sufficient to participate anchimerically and do not support the Sinnott mechanism.

Substituent effects in glycosyl bond cleavage

This investigation represents the first comprehensive study into the inductive effects of glycosyl substituents on the stability of glycosides. Substituent effects have been reported for the *acid-catalyzed* hydrolysis of glycosyl bonds.³⁸⁻⁴¹ However, as pointed out by Withers³⁸ and Moggridge and Neuberger,⁴¹ substituents influence two factors; first, the stability of the putative oxocarbenium ion intermediate generated by cleavage of the glycosyl bond, and second, the equilibrium constant for protonation (pK_a) of the aglycone which alters the concentration of the reactive protonated species in solution. In these cases, the pK_a effect obscures the inductive effect on the intermediate. Because of the cationic pyridinium ring, the nicotinamide nucleosides are not subject to acid catalysis. Thus, any substituent effects on the hydrolysis of nicotinamide nucleosides must reflect only the electronic interaction between the substituent and the activated complex.

The kinetic results indicate that electron withdrawing substituents at the 2'-position destabilize the oxocarbenium ion intermediates by about $10 \text{ Kcal}/\sigma_I$ (i.e., $7.1 \log(k)/\sigma_I \cdot 1.4 \text{ Kcal}/\log(k)$). A general understanding of structure-reactivity relationships can be useful to the fine-tuning of glycosyl bond stability in carbohydrate-containing molecules. For example, it has been found that antiviral 2'-deoxy nucleosides are chemically unstable, but that introducing a fluorine atom at the 2'-position drastically increases their stability.⁴² The introduction of a fluorine atom into naturally occurring sugars or oligosaccharides would be expected to stabilize the glycosyl bond and could serve as potent glycosidase inhibitors. Withers has proposed, for example, that 2-fluoro disaccharides could be therapeutically useful as specific glucosidase inhibitors to control glucose release from the gut.⁴³ In addition, the development of new glucosidase inhibitors has attracted interest recently in AIDS chemotherapy since trimming glucosidase inhibitors have been found to interfere with HIV-induced syncytium formation.⁴⁴

Mechanism of enzymatic glycosyl bond cleavage

Glycosidases, nucleosidases and glycosyl transferases share the unique ability to cleave glycosyl bonds. In most cases, these enzymes promote bond cleavage by a dissociative mechanism involving oxocarboxation intermediates.^{45, 46} General acid catalysis by the enzyme is a key feature in catalyzing hydrolysis of glycoside and nucleoside substrates. However, this alone does not account for the entire catalytic role of these enzymes. Sinnott has shown, for example, that galactosyl pyridiniums are good substrates for galactosidase although these molecules are not subject to acid-catalyzed chemical hydrolysis.³⁷ Furthermore, Skoog has demonstrated that nicotinamide mononucleotide is a substrate for AMP nucleosidase.⁴⁷ Thus, these authors have concluded that glycosyl bond cleaving enzymes are capable of stabilizing the oxocarboxation intermediates. Schuber has concluded that NAD glycohydrolase is able to stabilize the oxocarboxation generated in the active site.⁴⁸ While most enzymes in this class are poorly understood mechanistically, lysozyme has been the most thoroughly studied enzyme in this class and several mechanisms have been proposed to explain its ability to stabilize oxocarboxation intermediates.^{46, 49-54}

The proposed mechanisms for enzymatic stabilization of oxocarboxation intermediates have focussed traditionally on three elements 1) electrostatic stabilization; 2) covalent stabilization; and 3) conformational stabilization. The first proposes a carboxylate in the active site that stabilizes the oxocarboxation intermediate by a through-space electrostatic interaction.⁵⁵⁻⁵⁸ This idea, first proposed for lysozyme and often invoked to this day, has largely been discounted by model studies which have failed to show catalysis by ion-pair stabilization of cationic intermediates by adjacent carboxylates.^{52, 59, 60} The second element, covalent stabilization, proposes that the reactive oxocarboxation intermediate reacts with a carboxylate in the active site to form an acylal intermediate.^{37, 61} This has recently gained support from Withers and coworkers

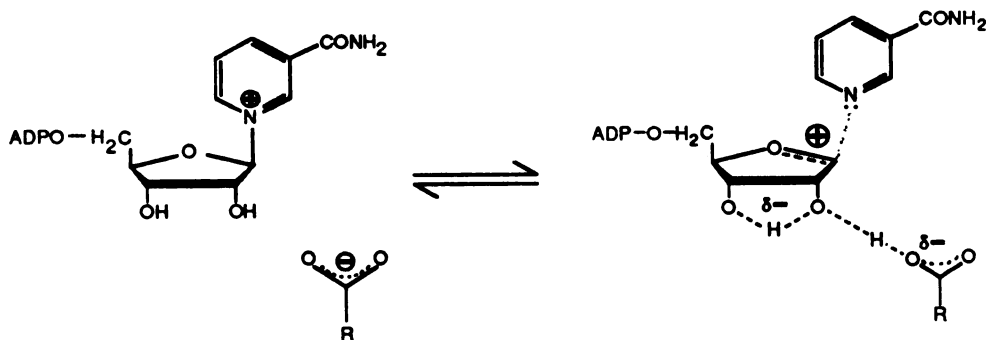
who claim to have isolated an enzyme-acylal adduct.⁶² However, this mechanism has also been criticized because the putative acylal intermediates would be too stable to account for the turnover rate of the enzyme.⁵⁵ A variant of this mechanism involves *intramolecular* covalent stabilization. Bruice and coworkers proposed that the 2-N-acetyl group of an N-acetylglucosamine residue reacts with the oxocarboation generated in the active site of lysozyme.¹⁹ The third element, also proposed for lysozyme, involves non-covalent interactions with the enzyme that induce strain in the substrate that is relieved in going to the transition state.^{49, 63} This phenomenon can also be viewed from the point of view of induced fit; i.e. the sp² hybridized intermediate binds more tightly than the substrate and that the binding energy is used to "drive" catalysis. Such a mechanism has been considered for NAD⁺ glycohydrolase also.^{2, 30}

The results of the present investigation suggest a new source of catalytic power directed to the cleavage of glycosyl bonds. The inductive effects for the 2'-substituted nicotinamide nucleosides indicate that increasing the electron density on the furanose ring greatly lowers the enthalpy of activation and labilizes the glycosyl bond. Going to the extreme case by forming the diol anion of NAD⁺ results in a 10⁴ acceleration in rate of hydrolysis.³ Glycosidases may utilize a similar strategy to cleave glycosyl bonds. As illustrated for the enzyme-catalyzed hydrolysis of NAD⁺ in Scheme 4.6, electron donation directed at the nicotinamide ribose moiety could provide a through-bond stabilization of an oxocarboation intermediate. A carboxylate residue (which was shown to exist in the active site of NAD⁺ glycohydrolase⁶⁴) could interact with the 2'-hydroxyl to relay electron density to the reaction center. This is in contrast to the through-space charge stabilization that has been invoked for enzymes such as lysozyme. The inductive stabilization mechanism could explain why NAD⁺ glycohydrolase requires that its substrate possess a 2'-hydroxyl in the *ribo* configuration. This hypothesis is also attractive because it would explain why a carboxylate does not attack the oxocarboation intermediate which would generate a covalent acylal intermediate. The enzyme-mediated inductive stabilization mechanism is worth further exploration.

Scheme 4.6



The "Lysozyme-based" Mechanism: Through-space Electrostatic Stabilization



The Proposed Mechanism: Inductive Stabilization.

Experimental

Hydrolysis.

The nicotinamide β -D-ribo- and arabinofuranosides (initial concentration ~ 0.8 mM) were incubated in 1 mL septum sealed vials containing 0.2 M buffer and 1.0 M potassium chloride and maintained at constant temperature (± 0.5 °C) in a heat block. The hydrolysis of the glycosyl-pyridinium bond was monitored by a discontinuous spectrophotometric assay based on the cyanide addition reaction.⁶⁵ First order rate constants were derived from a least squares fit of $\log[\text{nucleoside}]$ vs. time which were linear to 4 half-lives.

HPLC

The reaction mixtures were analyzed by HPLC on a Hewlett Packard HP-1090 instrument equipped with a diode array detector. Mobile Phase: 10 mM ammonium phosphate buffer (pH 5.5) with 2.5% acetonitrile. Stationary phase: Rainin Dynamax-300A 5 μ m C18 reverse-phase column (25 cm x 4.6mm). Flow rate: 1ml/min. Retention times: nicotinamide (λ_{\max} 260 nm) 7.2 min; nicotinic acid (λ_{\max} 260 nm) 3.5 min; 2-hydroxypyridinealdehyde (λ_{\max} 350 nm) 6.1 min. In all cases the product from the pH-independent reaction was nicotinamide.

NMR

Samples were present as 1-5 mM solutions in D₂O. Proton nuclear magnetic resonance spectra were obtained on a General Electric GN-500 instrument interfaced to a Nicolet 1280 computer. Chemical shifts (20 °C) are reported in parts per million relative to internal 3-trimethylsilylpropionate (TSP).

References

- (1) Anderson, B.M., in "The Pyridine Nucleotide Coenzymes"; J. Everse, B. M. Anderson and K.-S. You, Eds. Academic Press: New York, 1982; pp. 109-110.
- (2) Tarnus, C. and Schuber, F. *Bioorg. Chem.* 1987, 15, 31-42.
- (3) Johnson, R.W.; Marschner, T.M. and Oppenheimer, N.J. *J. Am. Chem. Soc.* 1988, 110, 2257-22263.
- (4) Schuber, F. and Muller, H.M. in press.
- (5) Jones, C.C.; Sinnott, M.L. and Souchard, I.J.L. *J.C.S. Perkin II* 1977, 1191-1198.
- (6) Brigl, P.Z. *Z. Physiol. Chem.* 1922, 122, 245-262.
- (7) Ballou, C.E. *Adv. Carb. Chem* 1954, 9, 59-94.
- (8) Janson, J. and Lindberg, B. *Acta Chem. Scand.* 1959, 13, 138-143.
- (9) Colowick, S.P.; Kaplan, N.O. and Ciotti, M.M. *J. Biol. Chem.* 1951, 191, 447-459.

- (10) Carpenter, B.K. *Determination of Organic Reaction Mechanisms*; Wiley-Interscience: New York, 1984; pp.124-135.
- (11) Hine, J., Wiley Interscience: New York, 1975; pp. p. 98.
- (12) Charton, M. *J. Org. Chem.* **1964**, *29*, 1222-27.
- (13) Taft, R.W. *J. Am. Chem. Soc.* **1953**, *75*, 4231-4238.
- (14) Taft, R.W. *J. Phys. Chem.* **1960**, *64*, 1805-15.
- (15) Kreevoy, M.M. and Taft, R.W. *J. Am. Chem. Soc.* **1955**, *77*, 5590-95.
- (16) Grob, C.A.; Schaub, B. and Schlageter, M.G. *Helv. Chim. Acta* **1980**, *63*, 57-62.
- (17) Salo, W.L. and Fletcher, H.G. *J. Org. Chem.* **1968**, *33*, 3585-3588.
- (18) Piszkiwicz, D. and Bruice, T.C. *J. Am. Chem. Soc.* **1968**, *90*, 2156-2163.
- (19) Piszkiwicz, D. and Bruice, T.C. *J. Am. Chem. Soc.* **1968**, *90*, 5844-5848.
- (20) Ballardie, F.W.; Capon, B.; Dearie, W.M. and Foster, R.L. *Carb. Res.* **1976**, *49*, 79-92.
- (21) Grob, C.A. *Acc. Chem. Res.* **1983**, *16*, 426-31.
- (22) Taft, R.W. *J. Am. Chem. Soc.* **1952**, *74*, 3120-3128.
- (23) Schaleger, L.L. and Long, F.A., in "Advances in Physical Organic Chemistry"; V. Gold, Eds. Academic Press: London, 1963; pp. 22-25.
- (24) Kreevoy, M.M. and Taft, R.W. *J. Am. Chem. Soc.* **1955**, *77*, 3146-3159.
- (25) De Bruyne, C.K. and Wouters-Leysen, J. *Carb. Res.* **1971**, *17*, 45-56.
- (26) Buncel, E. and Bradley, P.R. *Can. J. Chem.* **1967**, *45*, 515-519.
- (27) Biffin, M.E.C.; Miller, J. and Paul, D.B., in "The Chemistry of the Azido Group"; S. Patai, Eds. Wiley Interscience: New York, 1971; pp. 213-214.
- (28) Bruice, T.C. and Benkovic, S. *Bioorganic Mechanisms*; W.A. Benjamin: New York, 1966; pp.120-123.
- (29) March, J. *Advanced Organic Chemistry, Third Edition*; Wiley and Sons: New York, 1985; pp. 269.
- (30) Bull, H.G.; Ferraz, J.P.; Cordes, E.H.'.; Ribbi, A. and Apitz-Castro, R. *J. Biol. Chem.* **1978**, *253*, 5186-5192.

- (31) Ferraz, J.P.; Bull, H.G. and Cordes, E.H. *Arch. Biochem. Biophys.* **1978**, *191*, 431-436.
- (32) Hansch, C. and Leo, A. *Substituent Constants for Correlation Analysis in Chemistry and Biology*; Wiley and Sons: New York, 1979; p. 73.
- (33) Dermer, O.C. and Ham, G.E. *Ethylenimine and Other Aziridines*; Academic Press: New York, 1969; pp. 2-26.
- (34) Capon, B. *Q. Rev. Chem. Soc.* **1964**, *18*, 56-106.
- (35) Cohen, B.; van Artsdale, E.R. and Harris, J. *J. Am. Chem. Soc.* **1952**, *74*, 1875-1878.
- (36) Piszkiwicz, D. and Bruice, T.C. *J. Am. Chem. Soc.* **1967**, *89*, 6237-6243.
- (37) Jones, C.C.; Sinnott, M.L. and Souchard, I.J.L. *J. Chem. Soc. Perkin Trans II* **1977**, 1191-98.
- (38) Withers, S.G.; Percival, M.D. and Street, I.P. *Carbohydrate Res.* **1989**, *187*, 43-66.
- (39) York, J.L. *J. Org. Chem.* **1981**, *46*, 2171-73.
- (40) Marshall, R.D. *Nature* **1963**, *199*, 998-999.
- (41) Moggridge, R.C.G. and Neuberger, A. *J. Chem. Soc.* **1938**, 745-50.
- (42) Marquez, V.E.; Tseng, C.K.-H.; Mitsuya, H.; Aoki, S.; Kelley, J.A.; Ford, H., Jr.; Roth, J.S.; Broder, S.; Johns, D.G. and Driscoll, J.S. *J. Med. Chem.* **1990**, *33*, 978-85.
- (43) Withers, S.G.; Rupitz, K. and Street, I.P. *J. Biol. Chem.* **1988**, *263*, 7929-32.
- (44) Halazy, S.; Danzin, C.; Ehrhard, A. and Gerhart, F. *J. Am. Chem. Soc.* **1989**, *111*, 3484-85.
- (45) Sinnott, M.L., in "Enzyme Mechanisms"; M. I. Page and A. Williams, Eds. Royal Society of Chemistry, Burlington House: London, 1987; pp. 259-297.
- (46) Dahlquist, F.W.; Rand-Meir, T. and Raftery, M.A. *Biochemistry* **1969**, *8*, 4214-4221.
- (47) Skoog, M.T. *J. Biol. Chem.* **1986**, *261*, 4451-4459.
- (48) Tarnus, C.; Muller, H.M. and Schuber, F. *Bioorg. Chem.* **1988**, *16*, 38-51.
- (49) Blake, C.C.F.; Koenig, D.F.; Mair, G.A.; North, A.C.T.; Phillips, D.C. and Srma, V.R. *Nature* **1965**, *206*, 757-763.
- (50) Chipman, D.M. and Sharon, N. *Science* **1969**, *165*, 454-465.

- (51) Parsons, S.M. and Raftery, M.A. *Biochemistry* 1969, 8, 4199-4205.
- (52) Loudon, G.M.; Smith, C.K. and Zimmerman, S.E. *J. Am. Chem. Soc.* 1974, 96, 465-479.
- (53) Dahlquist, F.W.; Rand-Meir, T. and Raftery, M.A. *Proc. Natl. Acad. Sci USA* 1968, 61, 1194-1198.
- (54) Atkinson, R.F. and Bruice, T.C. *J. Am. Chem. Soc.* 1974, 96, 819-825.
- (55) Cherian, X.M.; Van Arman, S.A. and Czarnik, A.W. *J. Am. Chem. Soc.* 1990, 112, 4490-98.
- (56) Warshel, A. *Proc Natl. Acad. Sci. USA* 1978, 75, 5250-5254.
- (57) Dunn, B.M. and Bruice, T.C. *J. Am. Chem. Soc.* 1971, 93, 5725-5731.
- (58) Anderson, E. and Fife, T.H. *Chem. Comm.* 1971, 1470-471.
- (59) Dunn, B.M. and Bruice, T.C. *J. Am. Chem. Soc.* 1970, 92, 2410-2416.
- (60) Loudon, G.M. and Ryono, D.E. *J. Am. Chem. Soc.* 1976, 98, 1900-1907.
- (61) Bosker, A.D.; York, K.A. and Hogg, J.L. *J. Org. Chem.* 1986, 51, 92-96.
- (62) Withers, S.G.; Warren, R.A.J.; Street, I.P.; Rupitz, K.; Kempton, J.B. and Aebersold, R. *J. Am. Chem. Soc.* 1990, 112, 5887-5889.
- (63) Fersht, A. *Enzyme structure and mechanism*; W.H. Freeman: New York, 1985; pp. 336-338 and 435-436.
- (64) Schuber, F.; Pascal, M. and Travo, P. *Eur. J. Biochem.* 1978, 83, 205-214.
- (65) Colowick, S.P.; Kaplan, N.O. and Ciotti, M.M. *J. Biol. Chem.* 1951, 191, 447-59.
- (66) Laidler, K.J.. *Chemical Kinetics*; Harper and Row: New York, 1987; p. 195.

Chapter 5

The Hydrolysis of the 2'-NH₃⁺ Nicotinamide Nucleosides

Introduction

The preceding chapter demonstrated that substituents at the 2'-position of the sugar ring strongly influence the stability of the nicotinamide-glycosyl bond. In most cases the influence was attributed to the inductive effect of various polar but uncharged substituents. This chapter will investigate the effect of introducing charge at the 2'-position. Previous work on inductive effects have found that charged substituents are problematic: an inductive sigma constant assigned in one system is often not transferable to another system.^{1,2}

The 2'-amino-nucleosides represent an ideal system for investigating the effect of charge. In acid the amine protonates introducing a fixed positive charge. Because nicotinamide nucleoside hydrolysis is not acid-catalyzed, the suppression in rate of hydrolysis that is observed at low pH can be assigned unambiguously to the protonation of the amine. By studying both the arabino- and ribofuranosides and the α and β anomers in each series, the effect of configuration can also be investigated.

Results and Discussion

pH Dependence

The nicotinamide 2'-amino-(α,β)-ribo- and arabinofuranosides were synthesized and the anomers resolved according to procedures in chapter 3. Hydrolysis kinetics experiments were conducted at 37 °C over a wide range of pH (1-13). The cyanide addition assay was used to monitor the disappearance of nicotinamide nucleoside. First order rate constants were derived from a least squares fit of $\log[\text{nucleoside}]$ vs. time plots that were linear to nearly four half-lives. The hydrolysis products were analyzed by NMR spectroscopy of the reaction mixture or by HPLC as described in the experimental section. Only nicotinamide release was observed up to pH 12. Between pH 12 and 13 a small amount (< 15% total) of 2-hydroxypyridinealdehyde was detected which results from the direct attack of hydroxide on the pyridinium ring.³

The pH/rate profiles are shown in Figure 5.1. Regions of pH-independent hydrolysis were observed at both the low pH and high pH ends of the plot. The pH/rate data were fitted to equation 5.1 using a non-linear least-squares computer program based on an algorithm described by Cleland.⁴

$$k_{\text{obs}} = \frac{k_{\text{am}}}{1 + [\text{H}^+]/K_{\text{eq}}} + \frac{k_{\text{amH}^+}}{1 + K_{\text{eq}}/[\text{H}^+]}$$
 (5.1)

k_{obs} is the observed hydrolysis rate constant, k_{am} and k_{amH^+} are the rate constants for the high and low pH species, respectively, and K_{eq} is the apparent equilibrium constant for protonation.

The first order rate constants derived from equation 1 are summarized in Table 5.1.

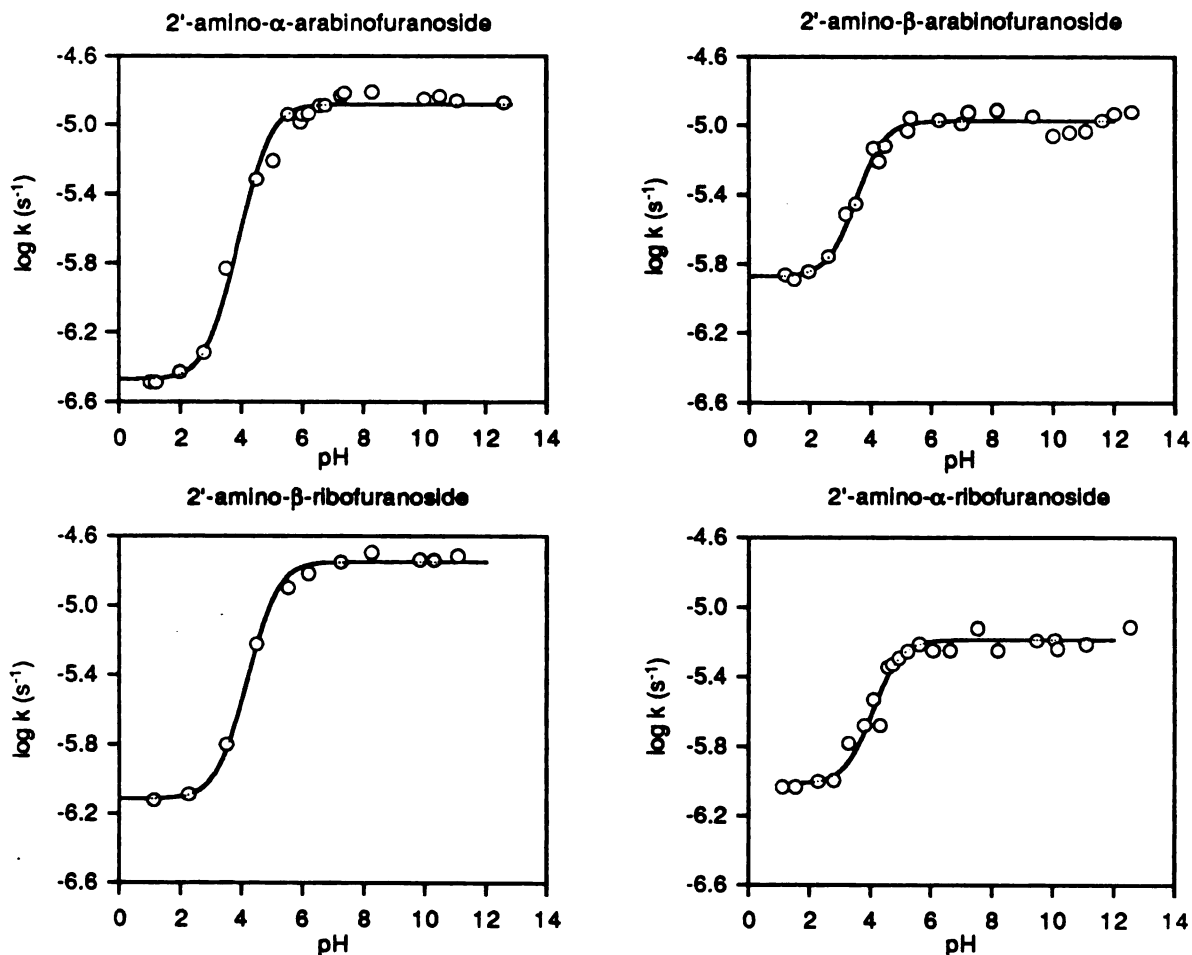


Figure 5.1. pH/rate profiles for the hydrolysis of the 2'-amino nicotinamide nucleosides.

Table 5.1. First order rate constants for the hydrolysis of the 2'-amino nicotinamide nucleosides.

Isomer	$k \text{ (S}^{-1}\text{)} \times 10^7$	
	2'-NH ₂	2'-NH ₃ ⁺
β-ribose	159	7.70
β-arabino	107	13.5
α-ribose	65.2	9.80
α-arabino	132	3.39

NMR titrations

The pK_a values were independently determined by ¹H NMR titrations at 37 °C. This technique involves following the chemical shift of the anomeric proton as a function of pH. The pH titration curves are shown in Figure 5.2. There are certain advantages of NMR titration over other methods such as potentiometric titration. The site of protonation can be localized by observing the protons that show the largest change in chemical shift. This method also insures that no decomposition of the substrate is occurring over the course of the titration.

The ¹H NMR titration data were fitted to Equation 5.2 using the same algorithm described above for the pH/rate data.

$$\delta_{obs} = \frac{\delta_{am}}{1 + H^+/K_{eq}} + \frac{\delta_{amH^+}}{1 + K_{eq}/H^+} \quad (5.2)$$

δ_{obs} is the observed chemical shift of the anomeric proton, δ_{am} is the chemical shift of the base, and δ_{amH^+} is the chemical shift of the conjugate acid.

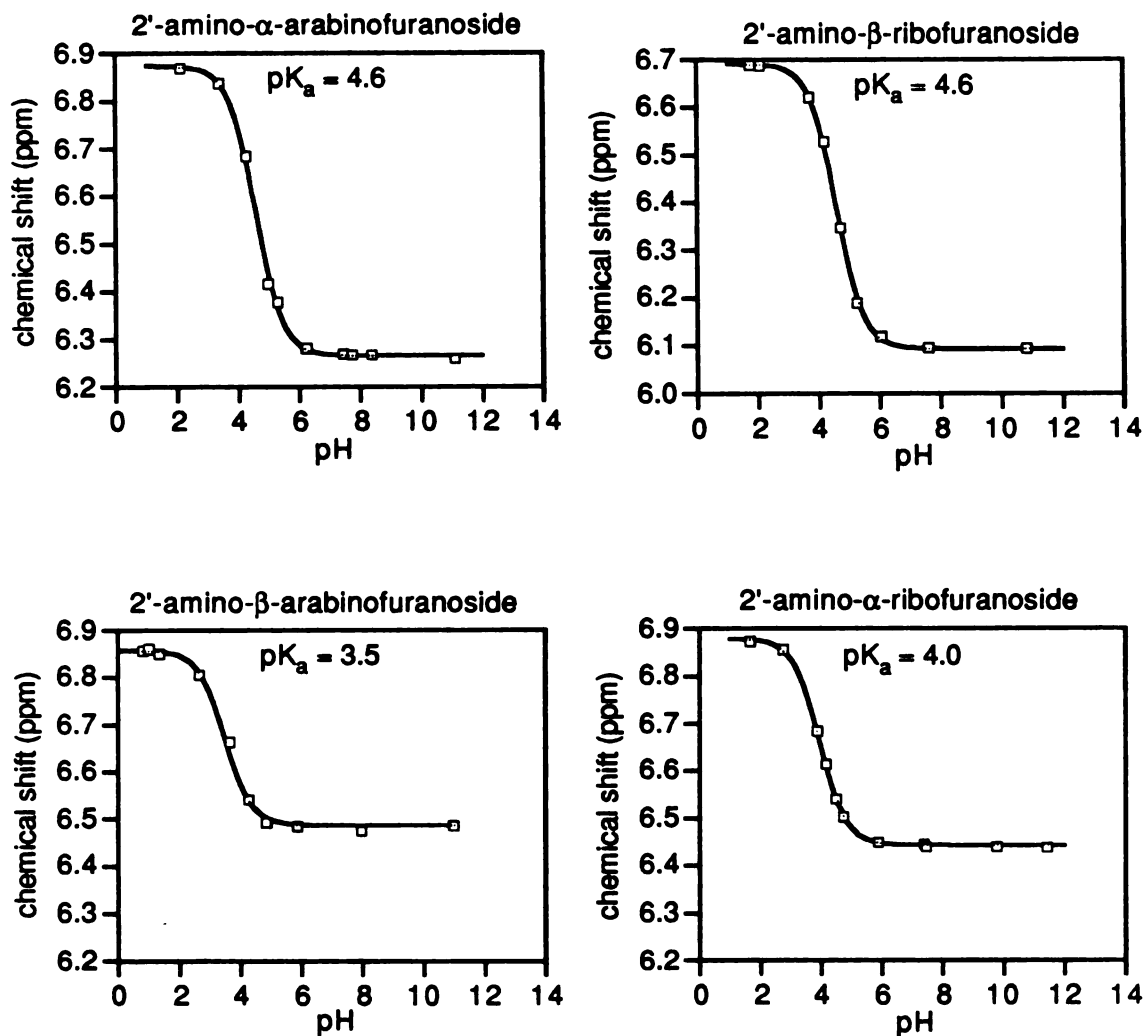
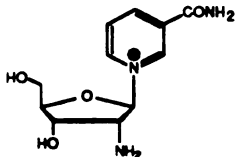
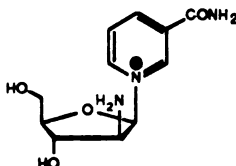
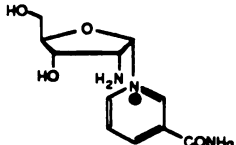
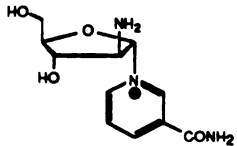


Figure 5.2. NMR titration curves for the 2'-amino nicotinamide nucleosides

The pK_{eq} values derived from the titration are summarized together with the pK_a values derived from the pH/rate curves in Table 5.2. The kinetic pK_a values agree well with the pK_a values derived from the NMR titration. Note that the pK_a values of the amino nucleosides are

quite low compared to pK_a values of normal alkyl amines (9-11). Furthermore, when the nicotinamide is cis to the 2'-amino group, the pK_a is suppressed with respect to the trans configuration by about one pK unit. This is a result of the strong electrostatic repulsion between the pyridinium ring and the 2'- NH_3^+ group. The electrostatic repulsion also leads to conformational changes in the sugar ring. Figure 5.3 shows the J coupling between the 1' and 2' protons as a function of pH. The decrease in coupling constants upon protonation of the amine is consistent with decreasing dihedral angle between the 1' and 2' protons according to the Karplus relationship⁵ (dihedral angles $< 90^\circ$ are not considered). As the 1'H-2'H dihedral angle decreases, the 2'- NH_2 group and the nicotinamide ring become more separated as illustrated in Figure 5.4.

Table 5.2. Summary of the pK_a values of the 2'-amino nicotinamide nucleosides

Isomer	pK_{eq}	$pK_{kinetic}$
β -ribose 	4.6 ± 0.1	4.8 ± 0.1
β -arabinoside 	3.5 ± 0.1	3.5 ± 0.1
α -ribose 	4.0 ± 0.1	4.0 ± 0.1
α -arabinoside 	4.6 ± 0.1	4.7 ± 0.1

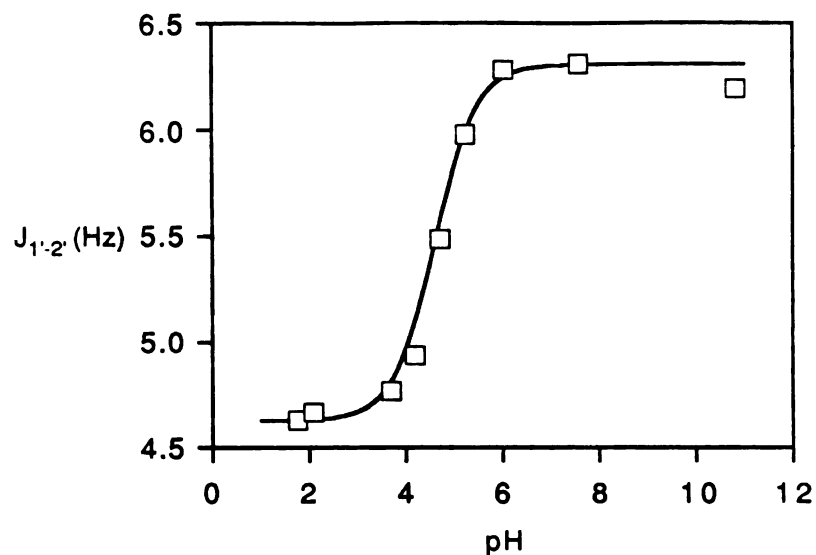


Figure 5.3. 1'-2' ^1H coupling constant versus pH for the 2'-amino- β -D-ribofuranoside

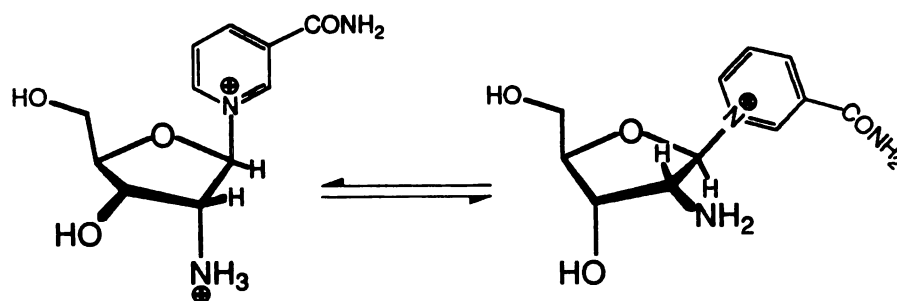


Figure 5.4. Conformational change upon ionization of the 2'-amino- β -D-ribofuranoside.

Temperature-dependence

The temperature-dependence for the hydrolysis of the β nucleosides was investigated by conducting the hydrolysis at four temperatures within each of the pH-independent regions (pH 0.9 and pH 7.2). The Arrhenius plots are shown in Figure 5.5. The ΔH^\ddagger and ΔS^\ddagger were calculated from the slopes and intercepts of the Arrhenius plots according to Carpenter⁶ and are summarized in Table 5.3.

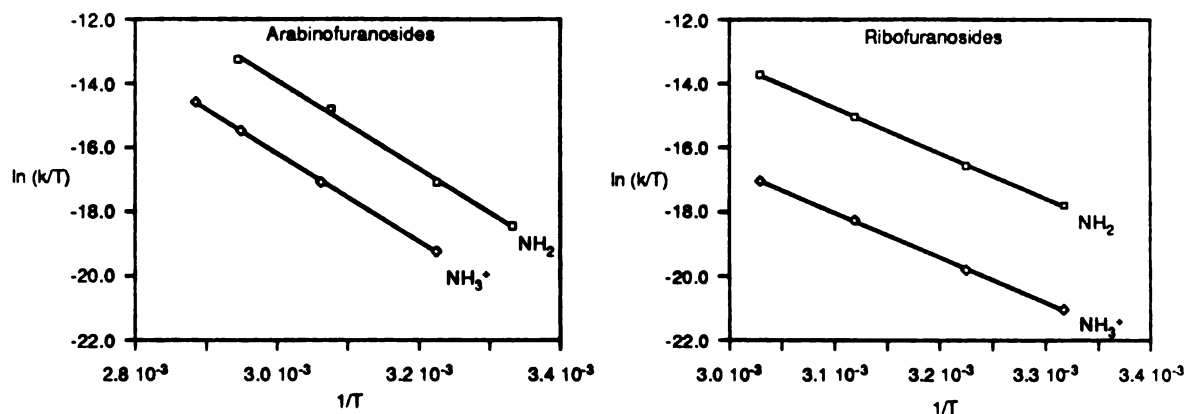


Figure 5.5. Arrhenius plots for the hydrolysis of nicotinamide 2'-NH₂- and 2'-NH₃⁺-β-D-arabino- and ribofuranoside.

Table 5.3. Summary of the activation energies for the hydrolysis of the 2'-amino-β-D-nicotinamide ribo- and arabinofuranosides.

	<u>ΔH[‡] (Kcal/mol)</u>	<u>ΔS[‡] (cal/mol deg)</u>
β-Riboside		
2'-NH ₂	28.9 ± 0.5	13.2 ± 2.2
2'-NH ₃ ⁺	27.7 ± 0.4	2.9 ± 1.6
β-Arabinoside		
2'-NH ₂	27.2 ± 0.9	6.7 ± 2.8
2'-NH ₃ ⁺	27.4 ± 0.6	2.9 ± 1.0

The -NH₃⁺ sigma constant

The rate constants in Table 5.1 demonstrate that protonation of the amine has a large effect on the rate of hydrolysis consistent with the involvement of an oxocarbenium intermediate. The effect of the ammonium at the 2' position could be relayed to the electron deficient transition state by a combination of through-bond polarizations (inductive effect) and through-space interactions (field effect). Inductive sigma constants for the -NH₃⁺ substituent have been previously established by analyzing the ΔpK_a s of substituted acetic acids and confirmed by correlation with ¹⁹F NMR of substituted fluorobenzenes that give a σ_I of 0.60.^{7,2,8} When this sigma value is plotted against the pH-independent rate of hydrolysis for 2'-NH₃⁺ nucleoside, (Figure. 5.6), a poor correlation results. The nicotinamide 2'-NH₃⁺- β -D-ribofuranoside hydrolyzes about 180 times faster than expected on the basis of its reported sigma constant and the 2'-NH₃⁺- β -D-arabinofuranoside hydrolyzes about 200 times faster. Other sets of sigma values have been compiled such as the σ_I^Q system,⁹ based on the ΔpK_a s of substituted quinuclidenes but all are found to give equally poor correlations.

Taft had warned that sigma values of charged substituents are not reliable for every system.¹ Nevertheless, the published sigma value for -NH₃⁺ is successful in many systems. For example, Marshall determined the rate constants for the acid-catalyzed hydrolysis of a series of methyl 2'-substituted glucopyranosides¹⁰ including 2'-NH₃⁺ and correlated the rates to the pK_a s of the corresponding substituted acetic acids (from which the σ_I values were subsequently derived). Figure 5.7 plots these rates versus the σ_I constants.

Why does sigma fail to correlate with the rate constants for hydrolysis of the 2'-NH₃⁺ nucleosides? The failure may result from: 1) a change in reaction mechanism, 2) only partial protonation of the amino group, or 3) a sigma value that does not reflect the "true" inductive effect of -NH₃⁺.

These points will be considered individually. First, if a change in mechanism were responsible, then it is expected that the activation energies for the hydrolysis of the 2'-NH₃⁺ nucleosides (Table 5.3) would reflect this. Rather, the activation energies are similar to the

activation energies of the other 2'-substituted nucleosides that have similar rates of hydrolysis. For example, the rate of hydrolysis of the nicotinamide 2'-NH₃⁺-β-D-arabinofuranoside is similar to both the 2'-OH and the 2'-NHAc arabinosides (Fig 5.6); likewise their ΔH[‡] and ΔS[‡] values are similar (Table 4.2). Considering the second point, the pH/rate plots tend to indicate that the amine is fully protonated at pH 1. The flatness in the curve in the low pH region suggests that further increasing hydrogen ion concentration would not change the concentration of the ammonium species in solution or further decrease the rate of hydrolysis.

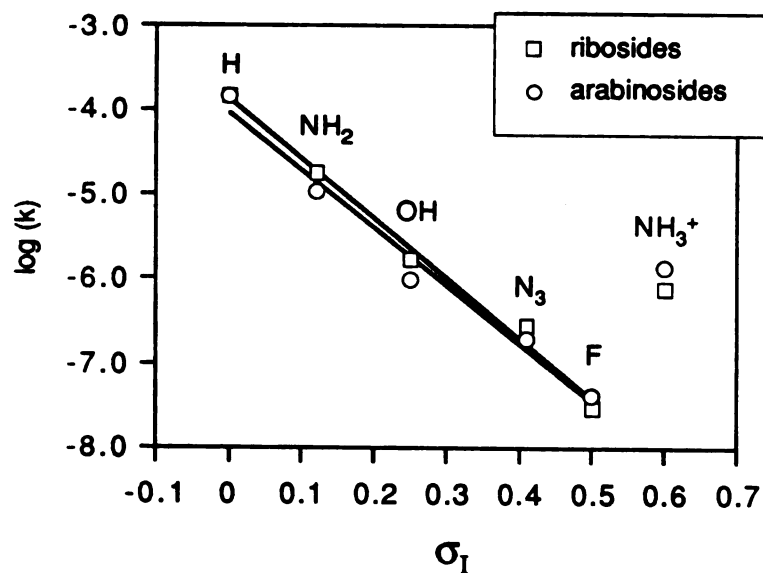


Figure 5.6. The log of the rate constants for the hydrolysis of the nicotinamide 2'-substituted-β-D-ribo- and arabinofuranosides versus the Taft Sigma constant.

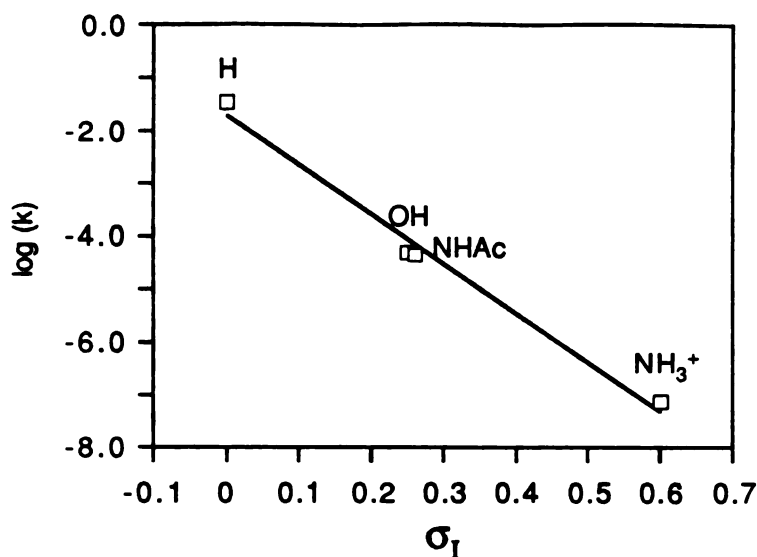


Figure 5.7. The log of the rate constants for the hydrolysis of the methyl 2'-substituted- β -D-glucopyranosides versus the Taft Sigma constant. Data from reference 10.

The failure of the sigma value for $-\text{NH}_3^+$ could derive from a complicated interplay of effects. The sigma constants were originally derived from the ΔpK_a s of substituted acetic acids.⁷ In the case of glycine, the substituent effect of the $-\text{NH}_3^+$ group on the pK_a of the carboxylate involves contributions from both the intrinsic inductive effect of the ammonium group as well as a powerful ion-pair interaction between the $-\text{NH}_3^+$ and the carboxylate. This would tend to exaggerate the apparent inductive effect and increase the σ_I constant. Likewise, reactions that proceed via protonated intermediates (e.g., A1 mechanisms) should be influenced by the corresponding overlap of effects. This may help explain why Marshall's rate for the 2'- NH_3^+ -glucopyranoside correlates with sigma. In this case the ammonium substituent has two effects: 1) it alters the extent of protonation (pK_a) of the methyl ether by a strong electrostatic repulsion and 2) destabilizes the oxocarbenium intermediate. Because nicotinamide nucleosides are not subject to acid-catalyzed hydrolysis, the influence of the ammonium will be limited to only the second effect. Thus, with the ion-pair influenced protonation step missing, the rates of hydrolysis of the nicotinamide 2'- NH_3^+ nucleosides do not correlate properly with the assigned inductive sigma constant.

There have been other problems encountered with trying to assign a σ_I value to $-\text{NH}_3^+$. ^{19}F NMR has been used to assign σ values based on the changes in chemical shifts of substituted fluorobenzenes¹¹ and fluoronaphthalenes,¹² but little consensus has been reached for a σ_I value of NH_3^+ using this technique. Values range from 0.40¹² to 0.79.¹¹ One reason for this discrepancy is that the studies were done in different solvent systems. The inductive (through-bond) effect is relatively independent of the solvent whereas the field effect is quite sensitive to solvent. Dewar and Marchand¹³ found that the substituent effect from the $-\text{N}(\text{CH}_3)_3^+$ group derives more from a field effect than an inductive effect. For this reason its polar effect is very sensitive to solvent and displays smaller effects in polar solvents such as D_2O than in non-polar solvents such as CH_3NO_2 .

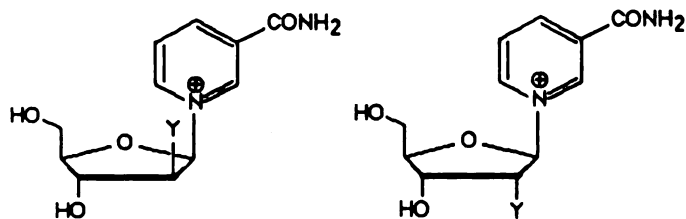
All substituents are thought to exert an influence from a combination of field and inductive effects. Uncharged substituents have field and inductive effects that work in the same direction and contribute in the same relative proportion.¹⁴ Charged substituents, however, are less predictable. Some systems may be influenced more by inductive effects and others more by field effects. The relative influence of each of these factors is dependent on the reaction mechanism, the configuration and conformation of the molecule, and the number of intervening bonds between the substituent and reaction center.^{14,15} The unreliability of sigma values of charged substituents that Taft reported¹ may originate from varying contributions from these factors. What is needed in the case of the nicotinamide nucleosides is an independent measure of the actual polar effect of the ammonium substituent without regard to the origin of the effect.

Reevaluating the sigma constant for $-\text{NH}_3^+$

In the course of synthesizing the 2'-substituted nicotinamide nucleosides it was observed that the 2'-substituent had a large effect on the chemical shifts of the sugar protons. For example, upon dithiothreitol reduction of the 2'-azido arabinoside to the 2'-amine, the chemical shift of the 2'-proton migrated upfield by about 1 ppm. This observation is reasonable because chemical shifts can be viewed as a measure of the electron density around the nucleus and are sensitive to

the shielding or deshielding effects of neighboring substituents. Table 5.4 summarizes the chemical shifts of the 2' proton and the rate constants for hydrolysis. When these data are plotted in Figure 5.8, a linear relationship between chemical shift and the log of the rate constant is revealed. Most interesting is that the points for the 2'-NH₃⁺ substituted nucleosides also fall on the line. Figure 5.9 shows that the chemical shifts correlate well with the Taft sigma constants. Knowing the ¹H NMR chemical shifts of the 2'-NH₃⁺ β-ribo- and arabinofuranosides (4.48 and 4.58 ppm), a new value of sigma can be calculated using the equations of the lines from Figure 5.9. This gives σ_I = 0.26 for both isomers. Figure 5.10 demonstrates that the new sigma value for -NH₃⁺ correlates well with the rates of hydrolysis.

Table 5.4. ¹H NMR chemical shift of the 2'-proton (ppm) and hydrolysis rate constants at 37 °C for the 2'-substituted nicotinamide nucleosides.



2'-substituent	σ _I	<u>Arabinosides</u>		<u>Ribosides</u>	
		2'-H (ppm)	k (s ⁻¹) x 10 ⁸	2'-H (ppm)	k (s ⁻¹) x 10 ⁸
H	0	3.05	14,454	2.85	14,454
NH ₂	0.12	4.05	1,071	3.76	1,778
NH ₃ ⁺	0.60	4.58	135	4.48	77.0
NHAc	0.26	4.96	99.3	4.70	54,998
OH	0.25	4.83	97.1	4.52	169
N ₃	0.41	5.05	20.0	4.92	28.2
F	0.50	5.55	4.17	5.40	3.00

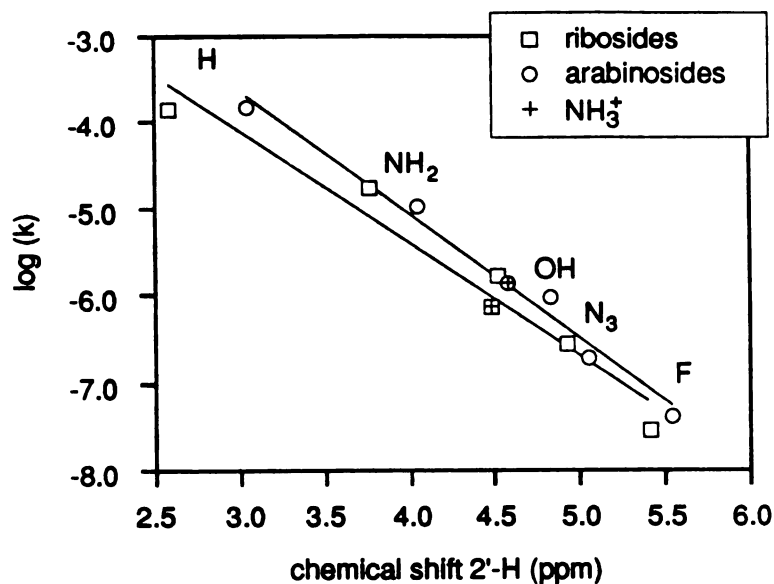


Figure 5.8. The log of the hydrolysis rate constants versus the ^1H NMR chemical shift of the 2'-proton for the 2'-substituted- β -D-ribo- and arabinofuranosides.

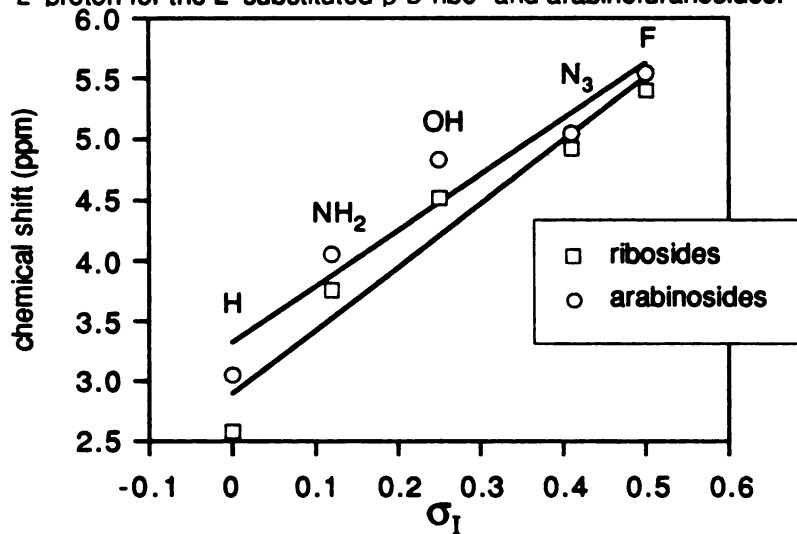


Figure 5.9. The chemical shift of the 2'-proton versus the Taft inductive sigma constant for the 2'-substituted- β -D-ribo- and arabinofuranosides.

The NMR chemical shifts provide a probe to directly measure the polar effect of the 2'-substituent. This approach ignores the question of whether the substituent effect originates from an inductive or a field effect. Rather it is intended as an independent calibration of the sigma value of a charged substituent. The new values for sigma are not purported to be more useful in all situations than the previously published values. As has been discussed previously, establishing

sigma values for charged substituents poses difficulties from the complicated interplay between inductive and field effects. This may require that new sigma values be determined for every new class of substrate under investigation. The new sigma values reported here should work well for riboside hydrolysis reactions that proceed via a one-step S_N1 mechanism. The new sigma value would be expected to fail for reactions involving a pre-protonation equilibrium step, such as acid-catalyzed acetal or glycoside hydrolysis. Nevertheless, this investigation has shown the usefulness of NMR as a calibration of sigma values.

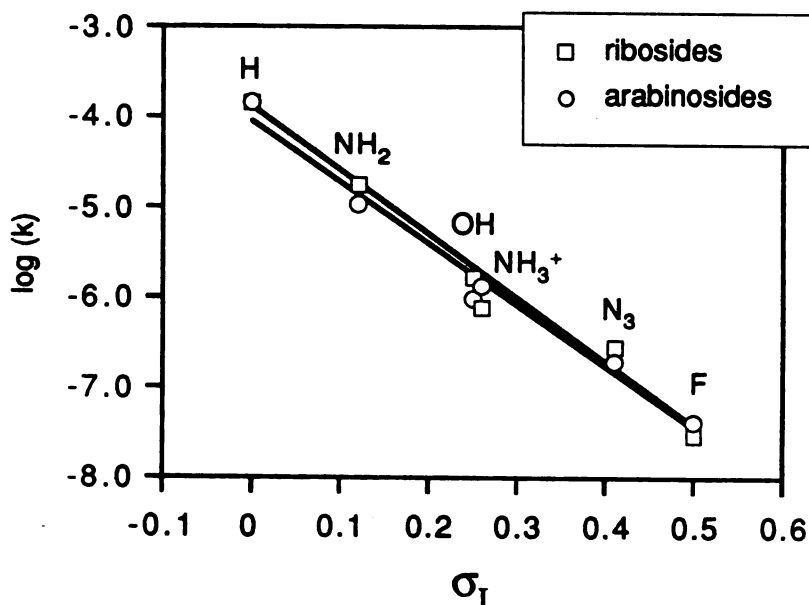


Figure 5.10. Log (k) versus sigma for the hydrolysis of the nicotinamide 2'-substituted- β -D-ribo- and arabinofuranosides incorporating the new sigma value for $-NH_3^+$.

Experimental

NMR

Samples were prepared in D₂O and were 2-5 mM in nucleoside. The samples were maintained at 20 °C. The spectral width was \pm 3000 Hz and quadrature phase detection was employed. The free induction decays were acquired using a 16 bit digitizer and stored in 16K data points. The FID was apodized with a single exponential before Fourier transformation resulting in a line broadening of 0.2 Hz. Chemical shifts were referenced to internal 3-(trimethylsilyl)propionic-[2,2,3,3-²H₄] acid (TSP).

NMR Titrations

The conditions described above were employed with the following exceptions. The samples were prepared in H₂O with 5% D₂O added to provide a lock signal. The sample temperature was maintained at 37.0 °C in the spectrometer. A 1:3:3:1 pulse sequence¹⁶ was used to suppress the water peak.

Hydrolysis

The nicotinamide nucleosides (initial concentration ~0.8 mM) were incubated in 1 mL septum sealed vials containing 0.2 M buffer and 1.0 M potassium chloride and maintained at constant temperature (\pm 0.5 °C) in a heat block. The hydrolysis of the glycosyl-pyridinium bond was monitored by a discontinuous spectrophotometric assay based on the cyanide addition reaction.¹⁷ All buffers were purchased from Sigma Chemical Company and were used in the following pH ranges: <pH 1.5, HCl; pH ranges 1.6-3.0, 6.5-8.0 and 11.5 - 13.0, phosphate; 3.7-5.5, acetate; 5.6 - 6.4, MES; 8.1-9.1, TAPS; 9.6-11.4, CAPS; >pH 12 KOH. The temperature dependence was analyzed by conducting the hydrolysis at four temperatures between 27 °C and 73 °C.

HPLC

The reaction mixtures were analyzed by HPLC on a Hewlett Packard HP-1090 instrument equipped with a diode array detector. Mobile Phase: 10 mM ammonium phosphate buffer (pH 5.5) with 2.5% acetonitrile. Stationary phase: Rainin Dynamax-300A 5 μ m C18 reverse-phase column (25 cm x 4.6mm). Flow rate: 1ml/min. Retention times: nicotinamide (λ_{\max} 260 nm) 7.2 min; nicotinic acid (λ_{\max} 260 nm) 3.5 min; 2-hydroxypyridinealdehyde (λ_{\max} 350 nm) 6.1 min. In all cases the product from the pH-independent reaction was nicotinamide.

References

- (1) Taft, R.W. and Lewis, I.C. *J. Am. Chem. Soc.* **1958**, *80*, 2434-2443.
- (2) Hine, J. *Structural Effects on Equilibria in Organic Chemistry*; Wiley-Interscience: New York, 1975; pp.97-99.
- (3) Johnson, R.W.; Marschner, T.M. and Oppenheimer, N.J. *J. Am. Chem. Soc.* **1988**, *110*, 2257-22263.
- (4) Cleland, W.W. *Adv. Enzymol.* **1967**, *29*, 1-32.
- (5) Silverstein, R.M.; Bassler, G.C. and Morrill, T.C. *Spectrometric Identification of Organic Compounds*; John Wiley and Sons: New York, 1981; p.210.
- (6) Carpenter, B.K. *Determination of Organic Reaction Mechanisms*; Wiley-Interscience: New York, 1984; pp.124-135.
- (7) Charton, M. *J. Org. Chem.* **1964**, *29*, 1222-1227.
- (8) Lowry, T.H. and Richardson, K.S. *Mechanism and Theory in Organic Chemistry*; Harper and Row: New York, 1981; p.139.
- (9) Grob, C.A.; Schaub, B. and Schlageter, M.G. *Helv. Chim. Acta* **1980**, *63*, 57-62.
- (10) Marshall, R.D. *Nature* **1963**, *199*, 998-999.
- (11) Weigert, F.J. and Sheppard, W.A. *J. Org. Chem.* **1976**, *41*, 4006-4012.
- (12) Adcock, W.; Alste, J.; Rivzi, S.Q.A. and Aurangzeb, M. *J. Am. Chem. Soc.* **1976**, *98*, 1701-1711.

- (13) Dewar, M.J.S. and Marchand, A.P. *J. Am. Chem. Soc.* **1966**, *88*, 354-358.
- (14) Wilcox, C.F. and Leung, C. *J. Am. Chem. Soc.* **1968**, *90*, 336-341.
- (15) Stock, L.M. *J. Chem. Ed.* **1972**, *49*, 400-404.
- (16) Horre, P.J. *J. Magn. Reson.* **1983**, *55*, 283-300.
- (17) Colowick, S.P.; Kaplan, N.O. and Ciotti, M.M. *J. Biol. Chem.* **1951**, *191*, 447-59.

Chapter 6

Cyanide Addition to the 2'-Substituted Nicotinamide Nucleosides: Modelling the Influence of the Carbohydrate Moiety on the NAD⁺/NADH Couple

Introduction

In 1938, Meyerhof et al. observed that NAD^+ reacts reversibly with cyanide and recognized that the resulting UV absorption spectrum resembled the spectra obtained from the alcohol dehydrogenase reduction of NAD^+ .¹ The 260 nm absorption band diminishes and a new band with λ_{max} 327 nm appears which is characteristic for dihydropyridine derivatives of NAD^+ . In 1951, Kaplan and coworkers showed that this reaction could be used as a sensitive assay for NAD^+ in solution.² Since that time, it has been shown that cyanide forms adducts with many N-alkyl nicotinamide cations³ and that the initial attack of cyanide is at the 4-position of the nicotinamide ring giving the electron-rich 1,4-dihydropyridine derivative (Figure 6.1).⁴

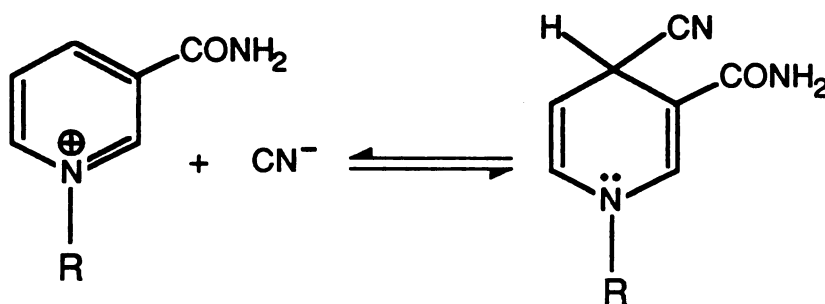


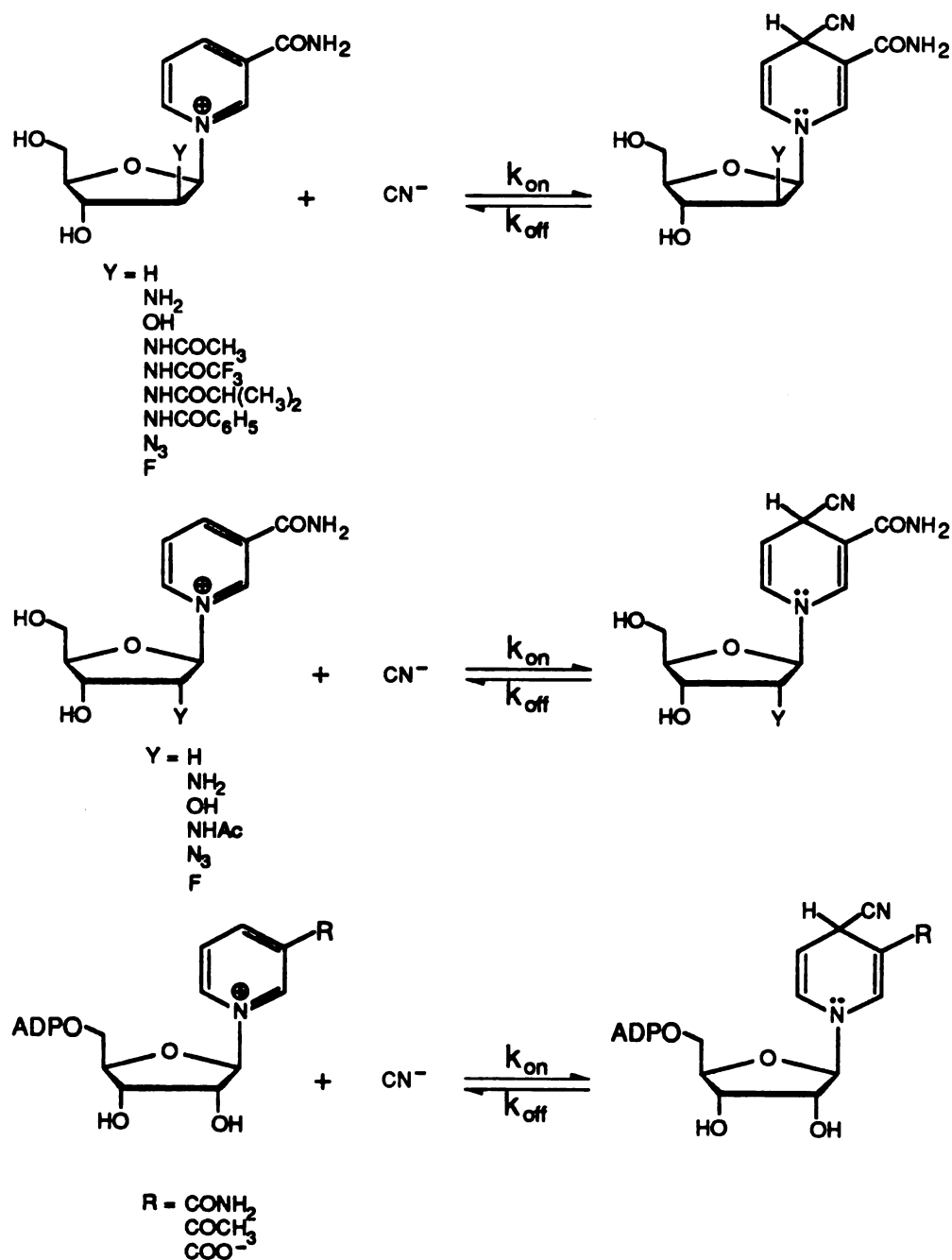
Figure 6.1. N-substituted nicotinamide cations (including NAD^+) react with cyanide to form 1,4-dihydro derivatives analogous to NADH.

The reversible formation of cyanide addition complexes with NAD^+ has received considerable attention because of its analogy with the NAD^+/NADH couple. It is considered a convenient model system for studying the oxidation/reduction equilibrium because both the forward and reverse reactions occur readily in the absence of enzyme. Although several studies have investigated the influence of the pyridine ring on the cyanide addition and on the redox properties of NAD^+ ,⁵ none have systematically analyzed the influence of the carbohydrate moiety. This is a significant omission because it has been proposed that the steric influence of

the 2'-OH cis to the nicotinamide ring is responsible for the 20 mV difference in redox potential between the α and β anomers of NADH and between NADH and ara-NADH.⁶

This chapter will investigate the cyanide addition reaction of a series of 2'-substituted nicotinamide β -D-ribo- and arabinofuranosides and β -NAD⁺ analogs (Scheme 6.1). These

Scheme 6.1



nucleosides represent an excellent system for investigating the influence of the steric, polar and stereochemical influence of the 2'-substituent. This represents the first investigation into substituent effects on the cyanide addition reaction of carbohydrate substituted analogs. The results have important implications for the mechanism of NAD⁺ dependent dehydrogenases. Finally, this study could provide an important base from which to design NAD⁺ analogs with altered redox properties.

Results

Figure 6.2 shows the UV absorption spectrum of nicotinamide ribofuranoside before and after the addition of cyanide. The cyanide adduct gives a new band at 324 nm which can be used to follow the course of the reaction. The cyanide addition experiments were conducted in thermostatted cuvettes at 25 °C and pH 8.0. By following the A_{324} versus time, the initial rate of cyanide addition was determined. The cyanide addition was followed until the system reached equilibrium at which point the free nucleoside to cyanide adduct ratio was calculated. The cyanide addition experiments were repeated using different concentration of cyanide (5-10mM). As expected, increasing the concentration of cyanide results in faster adduct formation and higher concentration of adduct at equilibrium as shown in Figure 6.3. The 2'-substituent also influenced the rate and equilibrium constant as shown in Figure 6.4. The hydrolytically labile nucleosides (2'-deoxy and 2'-N-acetyl riboside) were studied using high concentrations of cyanide (50-100mM) to minimize the amount of hydrolysis over the course of the experiment. Under these conditions, the A_{324} reaches a maximum in about 15 minutes. Nevertheless, a decrease in the A_{324} is seen over time (Figure 6.5) as the free pyridinium nucleoside undergoes hydrolysis and pulls the cyanide equilibrium toward the right (equation 6.1, N⁺ is nucleoside and N-CN is the cyanide-nucleoside adduct). The cyanide adduct concentration at equilibrium was calculated by extrapolating to 0% hydrolysis.

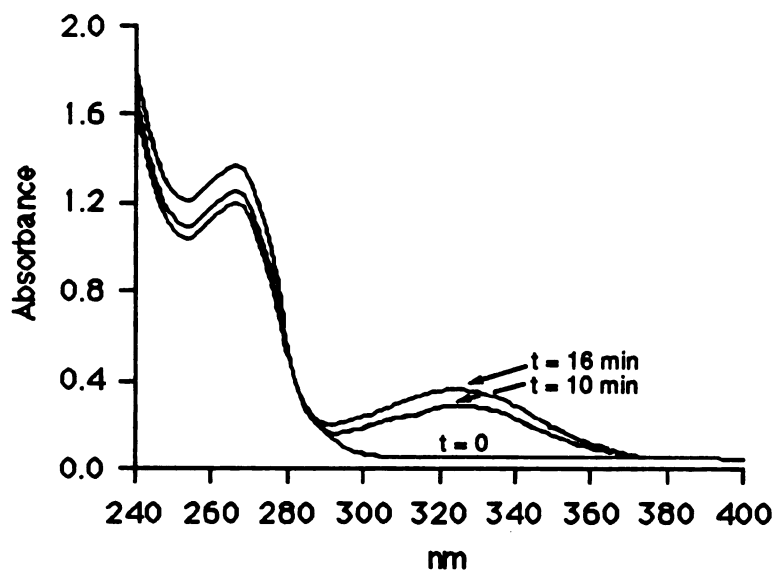
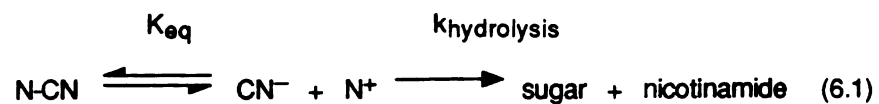


Figure 6.2. The UV spectra of nicotinamide riboside before cyanide addition and at 10 and 16 minutes after the addition of cyanide (to 10 mM KCN).

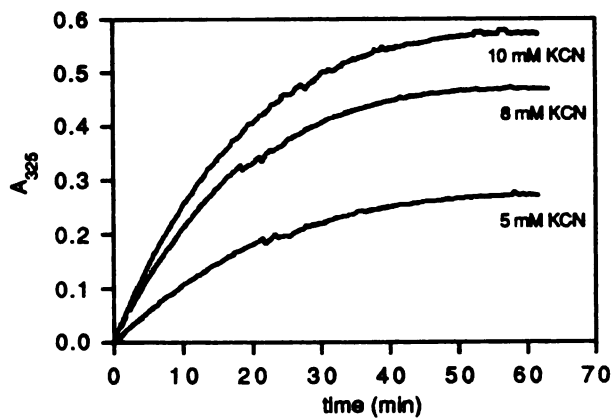


Figure 6.3. Plot of the absorbance at 324 nanometers versus time for the addition of cyanide to nicotinamide 2'-azido- β -D-ribofuranoside in 5, 8, and 10 mM KCN.

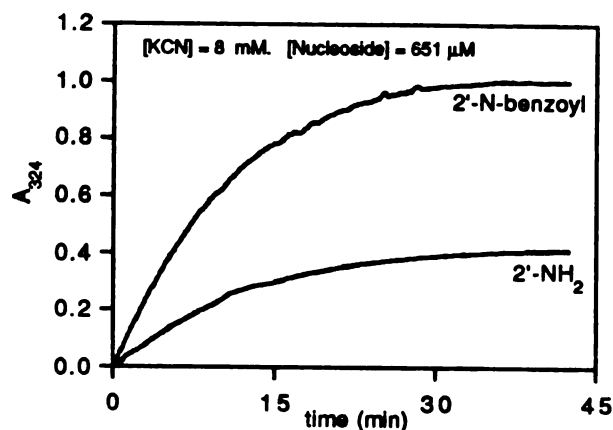


Figure 6.4. Plot of the absorbance at 324 nanometers versus time for the addition of cyanide to nicotinamide 2'-N-benzoyl and 2'-amino-β-D-arabinofuranoside.

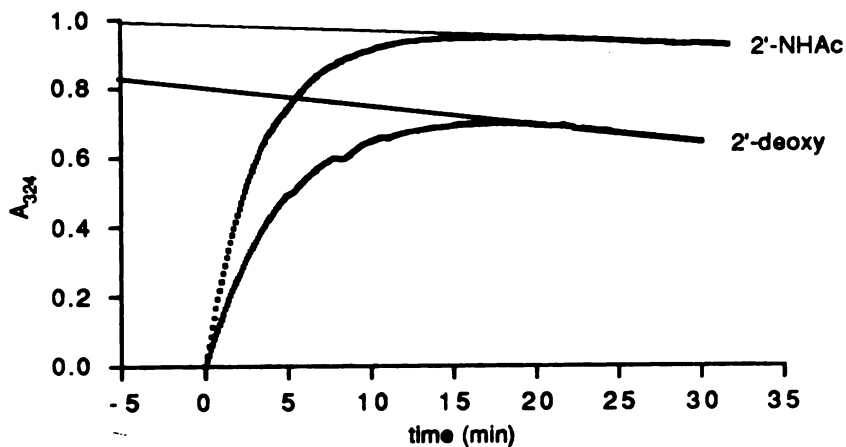


Figure 6.5. Plot of the absorbance at 324 nanometers versus time for the addition of cyanide to nicotinamide 2'-N-Acetyl and 2'-deoxy-β-D-ribofuranoside.

The cyanide addition kinetics experiments were performed in duplicate or triplicate. The K_{eq} values were calculated according to Kaplan and Ciotti⁷ (equation 6.2).

$$K_{eq} = \frac{[N-CN][H^+]}{[N][CN]} \quad (6.2)$$

The equilibrium constants and second order rate constants of addition to the arabino- and ribofuranosides are summarized in Tables 6.1 and 6.2. Figure 6.6 illustrates that the log K_{eq} values do not correlate with the Van Der Waals volume of the substituent.⁸ Thus, the steric bulk of the 2'-substituent alone does not determine cyanide affinity. There is, however, evidence for a stereochemical component to cyanide affinity with the ribofuranosides showing larger K_{eq} values and k_{on} values than the corresponding arabinofuranosides. The influence of the polarity of the substituent was analyzed by plotting the log K_{eq} values versus the inductive sigma⁹ constants in Figures 6.7 and 6.8. The correlation between cyanide affinity and polarity of the 2'-substituent is good; a linear least-squares analysis yielded a correlation coefficient (R) of 0.99 for the arabinosides and 0.96 for the ribofuranosides.

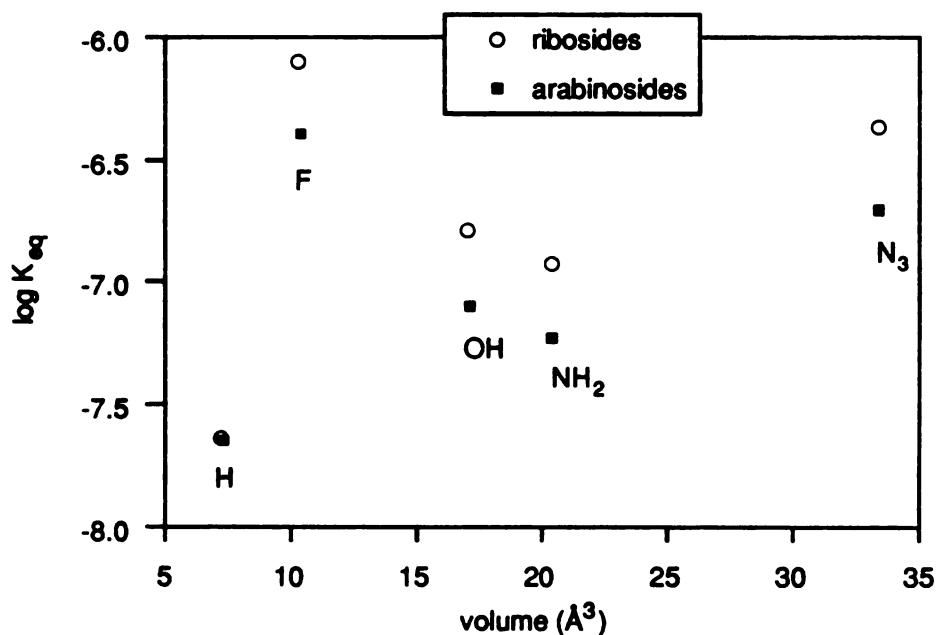
Table 6.1

Cyanide addition results for the nicotinamide 2'-substituted β -D-arabinofuranosides at 25 °C.

2'-substituent	$K_{eq} \times 10^8$	$k_{on} \times 10^3 (M^{-1}s^{-1})$	$k_{on}/K_{eq} \times 10^{-4}$
H	2.3 ± 0.5	7.4 ± 0.4	32.0 ± 6.5
NH ₂	6.1 ± 0.1	11.2 ± 0.1	18.5 ± 0.4
OH	8.1 ± 0.1	11.0 ± 1.4	13.7 ± 1.7
N ₃	19.9 ± 0.1	19.4 ± 0.2	12.4 ± 0.1
F	41.2 ± 1.0	38.2 ± 0.6	9.3 ± 0.3
NHCOCH ₃	45.0 ± 0.5	51.1 ± 0.1	11.5 ± 0.1

Table 6.2Cyanide addition results for the nicotinamide 2'-substituted β -ribofuranosides and β -NAD⁺ at 25 °C.

2'-substituent	$K_{eq} \times 10^8$	$k_{on} \times 10^3 \text{ (M}^{-1}\text{s}^{-1}\text{)}$	$k_{on}/K_{eq} \times 10^{-4}$
H	2.3 ± 0.5	7.4 ± 0.4	32.0 ± 6.5
NH ₂	11.9 ± 0.1	14.0 ± 2.1	11.8 ± 1.8
OH	16.3 ± 0.6	18.1 ± 0.7	11.1 ± 0.6
NHCOCH ₃	16.5 ± 0.8	27.9 ± 2.1	16.9 ± 1.5
N ₃	43.5 ± 1.9	27.3 ± 2.0	6.9 ± 0.6
F	78.8 ± 2.2	39.3 ± 3.8	5.0 ± 0.5
NAD ⁺	11.9 ± 0.7	9.4 ± 0.1	7.9 ± 0.5

**Figure 6.6.** Log(K_{eq}) for the addition of cyanide to the nicotinamide 2'-substituted- β -D-ribo- and arabinofuranosides versus volume of the substituent.

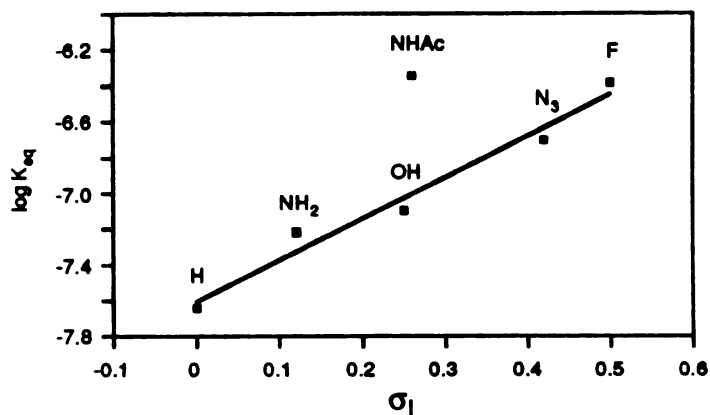


Figure 6.7. The log of the equilibrium constant for cyanide addition versus sigma for the 2'-substituted nicotinamide arabinosides.

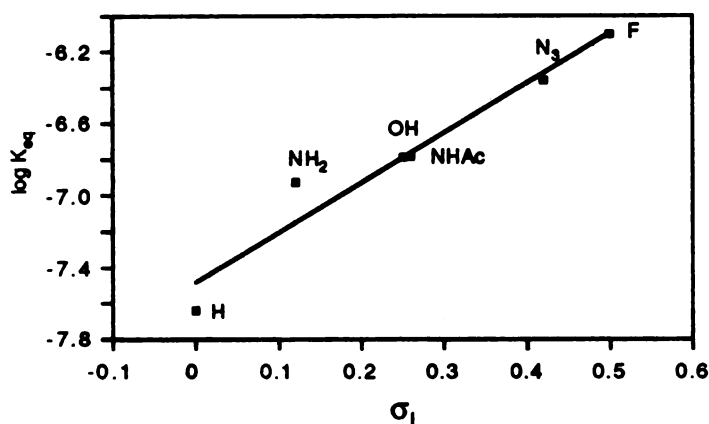


Figure 6.8. The log of the equilibrium constant for cyanide addition versus sigma for the 2'-substituted nicotinamide ribofuranosides.

The log of the second order rate constants for cyanide addition are plotted versus inductive sigma in Figure 6.9. The k_{off} values can be calculated from k_{on}/K_{eq} and are plotted against sigma in Figure 6.10. Note that both the on rates and off rates contribute to the substituent effects observed. The rate of formation of the 2'-N-acetyl arabinoside cyanide adduct is anomalously high and the off rate is slow with respect to its sigma constant.

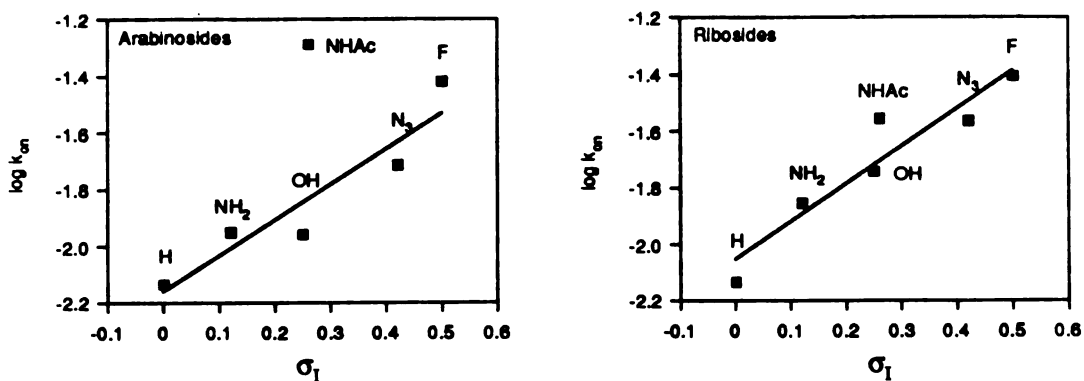


Figure 6.9. Second order rate constants for the addition of cyanide versus sigma for the nicotinamide 2'-substituted-β-D arabino- and ribofuranosides

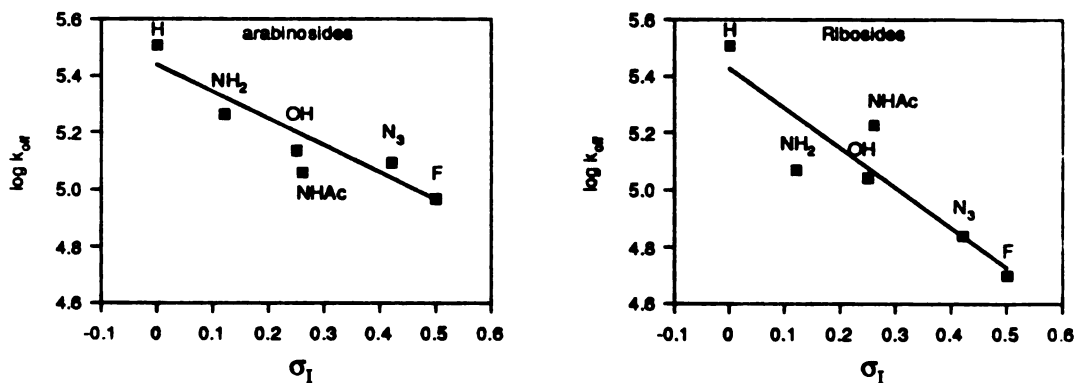


Figure 6.10. Rate constants for the dissociation of cyanide versus sigma for the nicotinamide 2'-substituted-β-D arabino- and ribofuranosides

Figures 6.7 and 6.8 demonstrate that the equilibrium constant for the 2'-N-acetyl arabinoside is much greater than would be expected on the basis of its sigma constant, whereas the corresponding riboside equilibrium constant correlates well with sigma. Initially this was thought to result from the steric bulk of the N-acetyl group. Brewster et al.¹⁰ reported that large hydrophobic groups on N-substituted nicotinamides alter the solvation of the cationic pyridinium

and increase the reactivity to the dihydro form. In the same way, the N-acetyl group cis to the nicotinamide ring could potentially cause a change in conformation or solvation of the pyridinium and create a more stable cyanide adduct. Three other 2'-N-acyl arabinosides were synthesized including the bulky N-isobutyryl and N-benzoyl derivatives to investigate this effect further. The cyanide addition equilibrium constants and rate constants for these nucleosides are summarized in Table 6.3. The log K_{eq} versus sigma plot in Figure 6.11 shows that the K_{eq} values do not correlate with the polar effect of the substituents and are also independent of the size of the N-acyl substituent. The k_{on} and k_{off} values are plotted versus sigma in Figures 6.12 and 6.13. The slope (ρ_I) of -0.81 (Figure 6.13), is close to the ρ_I observed for the other 2'-substituted arabinofuranosides, but the ρ_I for the on rate, k_{on} , in Figure 6.12 is of the opposite sign than what was observed for the other 2'-substituted arabinofuranosides. The amide bond of the 2'-NHCOCF₃ arabinoside hydrolyzes with a half-life of ca. 24 h at 37 °C. To insure that no amide hydrolysis occurred during CN addition, the reaction of 5 mM 2'-NHCOCF₃ arabinoside with 200 mM KCN was monitored for 30 min by ¹H NMR. The reaction proceeded to 90% adduct formation with only 1 set of adduct resonances appearing; no hydrolysis of the amide was seen.

Table 6.3

Cyanide addition results for the nicotinamide β -D-2'-N-acyl arabinofuranosides at 25°C.

2'-substituent	$K_{eq} \times 10^8$	$k_{on} \times 10^3 \text{ (M}^{-1}\text{s}^{-1}\text{)}$	$k_{on}/K_{eq} \times 10^{-4}$
NHCOCH ₃	45.0 ± 0.5	51.2 ± 0.2	11.5 ± 0.3
NHCOCF ₃	51.0 ± 3.3	39.2 ± 2.7	7.7 ± 0.7
NHCOCH(CH ₃) ₂	45.8 ± 0.2	52.8 ± 1.9	11.5 ± 0.4
NHCOCH ₂ Ph	45.4 ± 0.2	41.5 ± 2.9	9.1 ± 0.6

To explore the possible influence of intramolecular hydrogen bonding between the nicotinamide carboxamide and the 2'-N-acyl substituent, the cyanide addition experiments were repeated in the presence of 3 M guanidine hydrochloride. This was expected to disrupt any intramolecular hydrogen bonds present. The guanidine did not affect the cyanide addition equilibria.

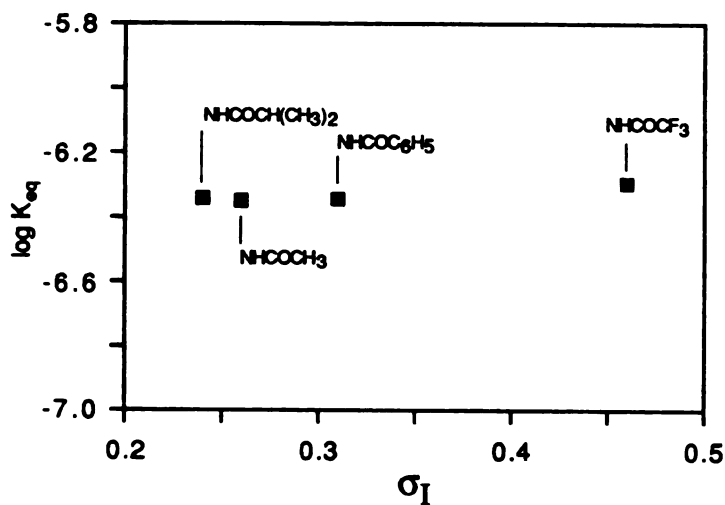


Figure 6.11. The log of the equilibrium constant for cyanide addition versus sigma for the nicotinamide 2'-N-acyl - β -D-arabinosides.

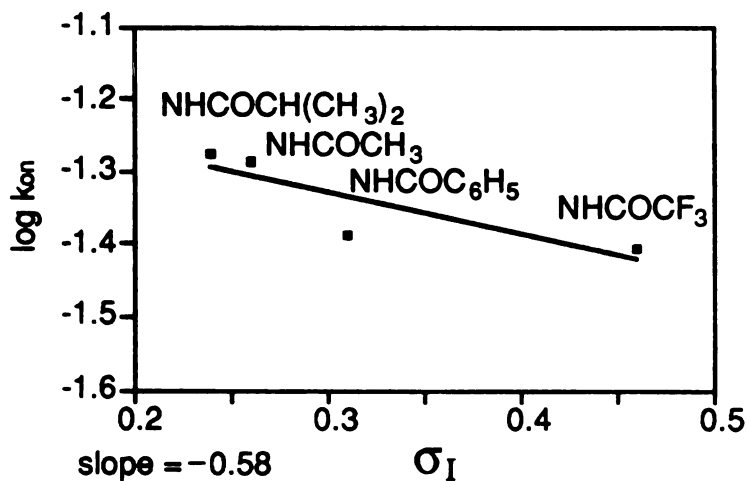


Figure 6.12. The log of the second order rate constant for cyanide addition versus sigma for the nicotinamide 2'-N-acyl - β -D-arabinosides.

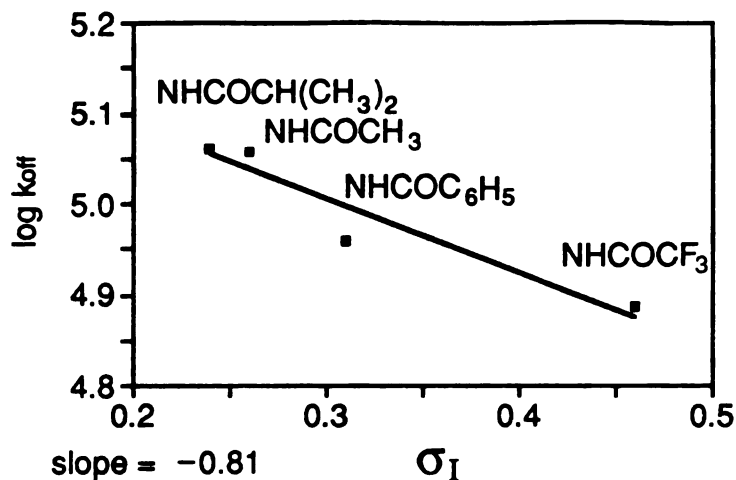


Figure 6.13. The log of the rate constant for cyanide dissociation versus sigma for the nicotinamide 2'-N-acyl-arabinosides.

The cyanide addition reaction of several 2'-substituted arabino-NAD⁺ analogs was investigated and demonstrated the same substituent effects as the 2'-substituted nicotinamide nucleosides.* The equilibrium constants are summarized in Table 6.4 and plotted against sigma in Figure 6.14. The rates of addition were not measured in this series of experiments. The higher cyanide affinity of β -NAD⁺ as compared to ara-NAD⁺ is also consistent with the nucleoside results.

Table 6.4.

Equilibrium constants for cyanide addition to the 2'-substituted β -ara-NAD⁺ analogs and β -NAD⁺

2'-substituent	$K_{eq} \times 10^8$
NH_2	4.7 ± 0.2
OH ("ara- NAD ⁺ ")	7.4 ± 0.3
β -NAD ⁺	11.9 ± 0.7
N_3	20.5 ± 1.1
F	28.5 ± 0.6

*The 2'-deoxy derivative is not available because the instability of this nucleoside has precluded the further manipulations necessary to synthesize the NAD⁺ analog.

The electronic influence of the nicotinamide carboxamide moiety was also investigated. The 3-acetyl pyridine adenine dinucleotide and the nicotinic acid adenine dinucleotide were subject to cyanide addition and the K_{eq} and k_{on} results are summarized in Table 6.5. Because the substituents at position 3 were thought to interact directly with the lone pair of electrons on the nitrogen atom through a resonance interaction (Figure.6.15), the K_{eq} and k_{on} values are plotted against the sigma (-) constant in Figures 6.16 and 6.17. The sigma (-) parameter is related to the ability of a particular substituent to delocalize a pair of electrons.¹¹

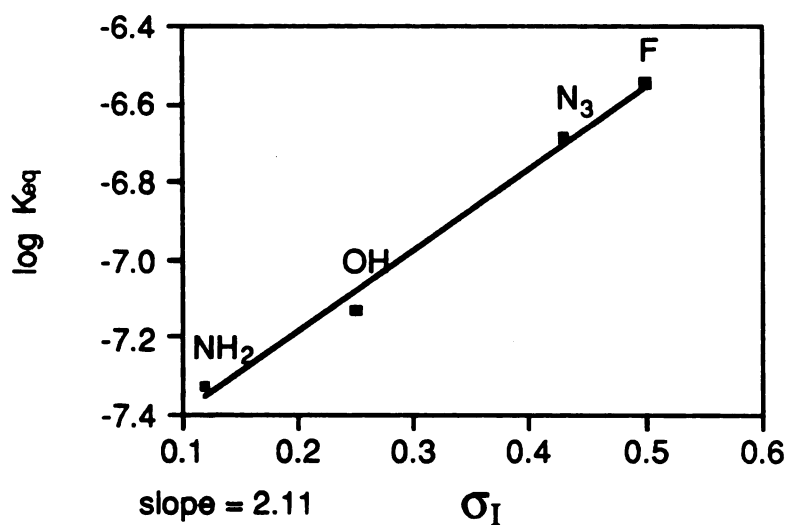


Figure 6.14. The log of the equilibrium constant for cyanide addition versus sigma for the 2'-substituted NAD⁺ analogs.

Table 6.5. 3-substituted pyridine adenine dinucleotide analogs

N-3 substituent	$K_{eq} \times 10^9$	$k_{on} \times 10^3 \text{ (M}^{-1}\text{s}^{-1}\text{)}$	$k_{on}/K_{eq} \times 10^{-3}$
COCH ₃	11,200. ± 890	63.6 ± 4.8	5.68 ± 0.62
CONH ₂ (NAD ⁺)	119. ± 7.1	9.43 ± 0.58	79.2 ± 6.79
COO ⁻	8.53 ± 0.42	1.84 ± 0.16	216. ± 21.5

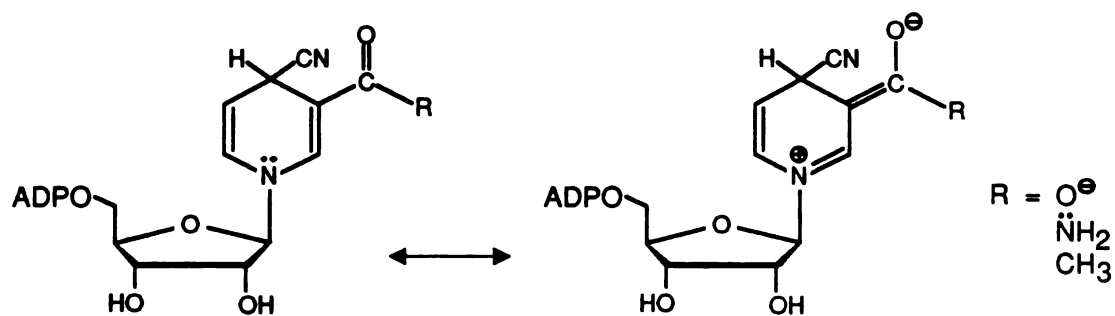


Figure 6.15. Resonance interaction of the 3-substituent with the lone pair on the dihydropyridine nitrogen

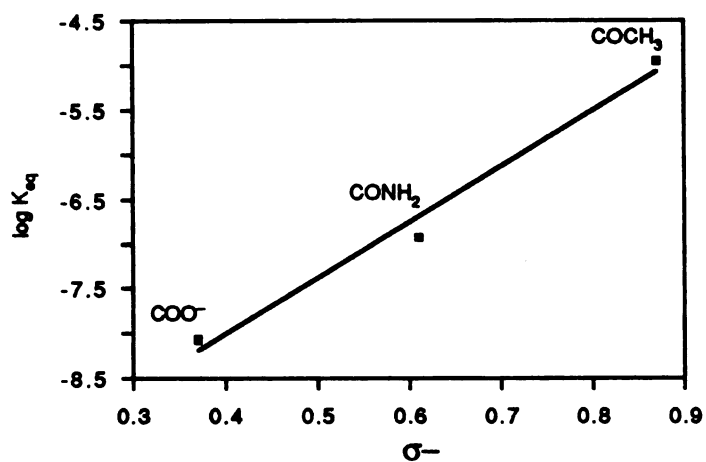


Figure 6.16. Log K_{eq} versus σ^- for the addition of cyanide to the 3-substituted

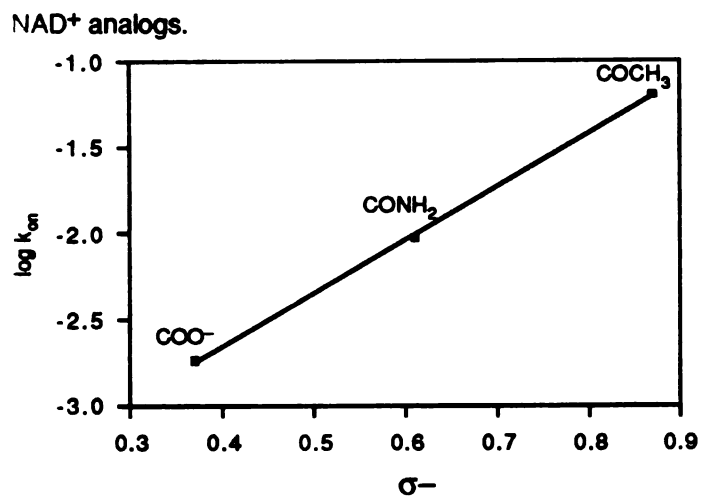


Figure 6.17. Log k_{on} versus σ^- for the addition of cyanide to the 3-substituted NAD⁺ analogs

Discussion

Studies on cyanide addition to N-substituted nicotinamide derivatives

The substituent effects on the cyanide addition reaction of N-substituted nicotinamide derivatives have received considerable attention.^{4,12-15} Wallenfels and Diekmann¹² determined the equilibrium constants for a series of 10 N-alkyl substituted nicotinamides; however, these values were not related to the polar effect of the substituent in a systematic way. They also studied 7 N-benzyl pyridinium analogs with various substituents at the 3-position of the pyridine ring including -COCH₃, -COO⁻, and -CONH₂ and demonstrated that the equilibrium constants for cyanide addition parallel the reduction potentials of the corresponding NAD⁺ analogs. Bunting and Sindhuatmadja¹⁴ determined the equilibrium constants for cyanide dissociation from a series of 1-benzyl-4-cyano-nicotinamide analogs with various substituents on the benzyl ring. A Hammett correlation gave ρ_1 values of -0.88 which is consistent with the development of a positive charge on the nitrogen atom in the transition state. Lindquist and Cordes⁴ synthesized several N-alkyl nicotinamide derivatives and determined the equilibrium constants for the dissociation of cyanide as well as the k_{on} for the addition of cyanide. They related these constants to the polar effect of the N-substituent in a Hammett-Taft correlation and found $\rho_1 = -3.7$ and 2.2 for the equilibrium and rate constants, respectively. They also found that β -NAD⁺ and nicotinamide mononucleotide show abnormally large affinities for cyanide. β -NAD⁺ has an affinity for cyanide five times greater than the N-(2-chloro-4-nitrobenzyl) derivative, the most electronegative N-substituent studied. Cordes and Lindquist did not explain the anomalous behavior for β -NAD⁺ but suggested that it may reflect the polar environment at the anomeric position of the ribose moiety.

The polar substituent effects observed for the 2'-substituted nicotinamide nucleosides are in accord with those reported by other researchers. The ρ_1 values from the Taft σ_1 correlations are summarized in Table 6.6. The equilibrium ρ_1 values correspond to *dissociative* ρ_1 values of -2.3 and -2.8 for the arabino and ribo series, respectively. Thus, there is less sensitivity of the

equilibrium constant to the carbohydrate substituents as compared to the Lindquist and Cordes study in which the substituents are placed directly on the nicotinamide nitrogen atom. The same attenuation of substituent effects is seen in the ρ_I values for the second order rate constants. Despite the lesser influence of substituents in the 2'-substituted nucleosides, the results should be more biologically relevant. The nucleosides are clearly better models of NAD⁺ and the altered cyanide affinities should directly parallel hydride affinities for the corresponding NAD⁺ analogs. The cyanide addition results for the 2'-substituted ara-NAD⁺ analogs ($K_{eq} \rho_I = 2.1$) confirm that the substituent effects observed for the nucleosides are maintained at the dinucleotide level. These results could guide the rational design of 2'-substituted NAD⁺ analogs with altered redox properties.

Table 6.6
Summary of the ρ_I values.

analog series	$\rho_I (K_{eq})$	$\rho_I (k_{on})$	$\rho_I (k_{off})$
2'-substituted arabinosides	2.3	1.3	-0.95
2'-substituted ribosides	2.8	1.4	-1.3
2'-N-acyl arabinosides	0.23	-0.58	-0.81
3-substituted pyridine adenine dinucleotides	6.3	3.1	-3.2

Substituent effects on the kinetics of cyanide addition.

The ρ_I values for the kinetics of cyanide addition to the 2'-substituted ara- and ribofuranosides (Table 6.6) show that both the on and off rates are sensitive to the 2'-substituent. Furthermore, the substituent effects on k_{on} and k_{off} contribute in roughly the same magnitude to the cyanide addition equilibria implying that the transition state structure is approximately midway between pyridinium and dihydro structures. The electron-withdrawing 2'-substituents stabilize

the transition state for cyanide attack by inductively stabilizing the pair of electrons on the nicotinamide nitrogen atom. The same substituents will tend to destabilize the quaternary nitrogen atom of the pyridinium form. In this way, the 2'-substituent regulates the electronic environment of the N-1 atom. The polar effect is then transmitted to the relatively remote 4-position of the nicotinamide ring by resonance interactions through the ring.

Effect of configuration

Due to the locked geometry around the anomeric carbon, the nicotinamide nucleosides represent an excellent system to investigate the effect of configuration. The plot in Figure 6.6 and the data in Table 6.7 suggest a stereoelectronic effect with the ribofuranosides showing a larger K_{eq} than the corresponding arabinofuranosides. The Gibb's free energy difference in Kcal/mol between the arabinofuranosides and the ribofuranosides is roughly comparable for each of the 2'-substituents. The electron-withdrawing effect of the 2'-substituent is probably transmitted to the reaction center more strongly when the substituent is aligned antiperiplanar to the lone pair of electrons on the nitrogen atom.

Table 6.7 Cyanide addition equilibria: Gibb's free energy differences between the ara- and ribosides.

2'-substituent	$\log K_{ribo} - \log K_{ara}$	$\Delta\Delta G$ (Kcal/mol)	$\Delta\Delta G$ (mV/mol)
NH ₂	0.29	0.40	8.7
OH	0.30	0.41	8.9
N ₃	0.34	0.46	10.0
F	0.28	0.38	8.3

The stereoelectronic effects seen with the 2'-substituted nicotinamide nucleosides are consistent with earlier observations of the hydride and cyanide affinities of pyridine nucleotide coenzymes. Lindquist and Cordes observed that β -NAD⁺ has more affinity for cyanide than α -NAD⁺, and β -NAD⁺ is also a more powerful oxidizing agent.⁴ They proposed that the different affinities of the two anomers originate from an interaction between the adenine and nicotinamide rings. However, a similar difference in cyanide affinities is seen between the ara and ribo nucleosides where there can be no adenine interaction. Thus, it seems more likely that it is the *configuration* of the 2'-substituent with respect to the nicotinamide ring that affects cyanide affinity. Glasfeld et al.⁶ have considered the effect of configuration on the reduction of NAD⁺. They propose that the 20 mV difference in reduction potential between α - and β -NAD⁺ and between the ara and ribo configurations originates from a steric interaction of the 2'-hydroxyl which alters the torsional geometry around the glycosyl bond and, in turn, lowers the reduction potential of the coenzyme. However, the 2'-substituted nicotinamide arabinoside results (Figure 6.6) show that the steric bulk of the 2'-substituents does not correlate with cyanide affinity. The two smallest substituents in the arabino series (2'-H and 2'-F) are at the extremes of cyanide affinity. Bulkier substituents such as hydroxyl and azido are located midway in the cyanide affinity continuum. Even if the 2'-F point is considered anomalous and discarded, the observed trend is opposite to what Glasfeld et al. would predict; i.e. the larger substituents give larger cyanide K_{eq} values implying that steric bulk leads to larger reduction potentials. The data in Table 6.7 show that the ΔK_{eq} between the ara- and ribofuranosides gives a reduction potential difference of similar magnitude to what Glasfeld et al. reported *regardless of the steric bulk* of the 2'-substituent. Thus, these results suggest that the stereochemical influence of the 2'-substituent derives from an electronic rather than a steric effect.

Substituent effects in cyanide addition versus glycosyl hydrolysis

The cyanide addition results provide an interesting contrast to the glycosyl hydrolysis results. Placing electron withdrawing substituents at the 2'-position does nothing to increase the

rate of nucleophilic attack at the anomeric position (leading to glycosyl bond cleavage) yet it increases the rate of nucleophilic attack of cyanide at the relatively remote 4-position of the nicotinamide ring. This comparison points up the difference in mechanism between cyanide addition and glycosyl bond cleavage. The first is an associative reaction and the second is dissociative bond cleavage which is not promoted at all by the presence of strong nucleophiles.¹⁶

The explanation for the effect of configuration between the two reactions is less obvious. As demonstrated in Table 6.7, the ribosides have larger cyanide affinities. Thus, the ribo substituents behave as if they are more electron withdrawing vis-a-vis the arabino substituents. In contrast, the ribo substituents behave as if they are more electron *donating* in the hydrolysis reaction. This is shown most clearly in Table 5.4: the ribosides hydrolyze more quickly, and the chemical shifts of the riboside 2'-protons are upfield of the corresponding arabinoside protons. The stereochemical effect differences between the two reactions must involve different stereoelectronic interactions of the 2'-substituent with their respective transition states, but the exact mechanism for the transmission of the effects is not clear at this time.

Cyanide addition to the 2'-N-acyl arabinofuranosides

The 2'-N-acyl-substituted nicotinamide arabinoside results pose other interesting questions. These derivatives were made initially to investigate the effect of steric bulk of substituents cis to the nicotinamide ring. Figure 6.11 demonstrates that the affinities for cyanide are independent of the size of the acyl group. Furthermore, the K_{eq} values are independent of the polar effect of the substituent. The N-acyl substituents do have a powerful effect on the cyanide affinity, however, as shown in Figure 6.7. The affinity of the N-acetyl is about 6 times what is expected on the basis of its sigma value. Table 6.6 shows that the ρ_1 for dissociation of cyanide from the dihydropyridine ring is close to that seen for the other arabinosides (-0.81 versus -0.95). On the other hand, the ρ_1 for the rate of cyanide addition on the 2'-N-acyls is opposite in sign to what is seen for the other arabinosides. That is, as more electron withdrawing groups are placed on the acyl function, the rate of cyanide addition *decreases*.

Because the anomalous 2'-N-acyl substituent effects are only seen in the arabinosides and do not derive from inductive effects, it seems that their effects originate from a direct interaction with the nicotinamide ring. Model building showed that the N-acyl carbonyl could be hydrogen-bonding with the carboxamide of the nicotinamide ring as illustrated in Figure 6.18 or it could be pointed at the center of the pyridinium ring. However, both of these interactions would be expected to cause an electrostatic *stabilization* of pyridinium rather than increased reactivity. The anomalous 2'-N-acyl substituent effects have important implications for how the redox properties of NAD⁺ can be influenced by through-space interactions with other functional groups in close proximity. The origin of these effect is worth further investigation.

Enzymatic oxidation and reduction of NAD⁺

The cyanide addition results have important implications for the mechanism of dehydrogenases. The results demonstrate that the equilibrium between the oxidized and dihydro species is altered by changing the electronic environment on the sugar ring. The dehydrogenases may be able to effect the analogous changes. For example, a residue in the enzyme active site may interact with the ribose diol to increase the electron density at the anomeric carbon and perturb the reduction potential of the coenzyme. In addition, it has been shown that placing N-acyl groups adjacent to the nicotinamide ring has a potent effect on reactivity *not* related to a polar effect. Such through-space effects are certainly important in the enzyme active site. These results suggest that by subtly altering the chemical environment around the nicotinamide ring, an enzyme can fine-tune the reduction potential of the coenzyme.

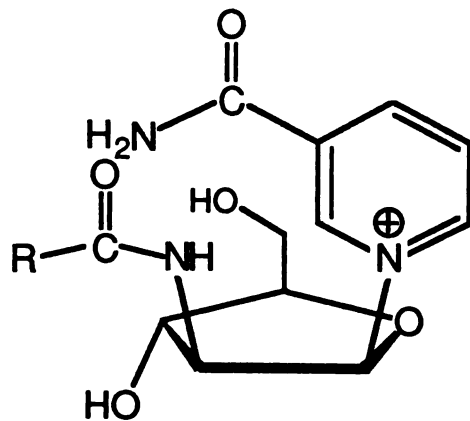


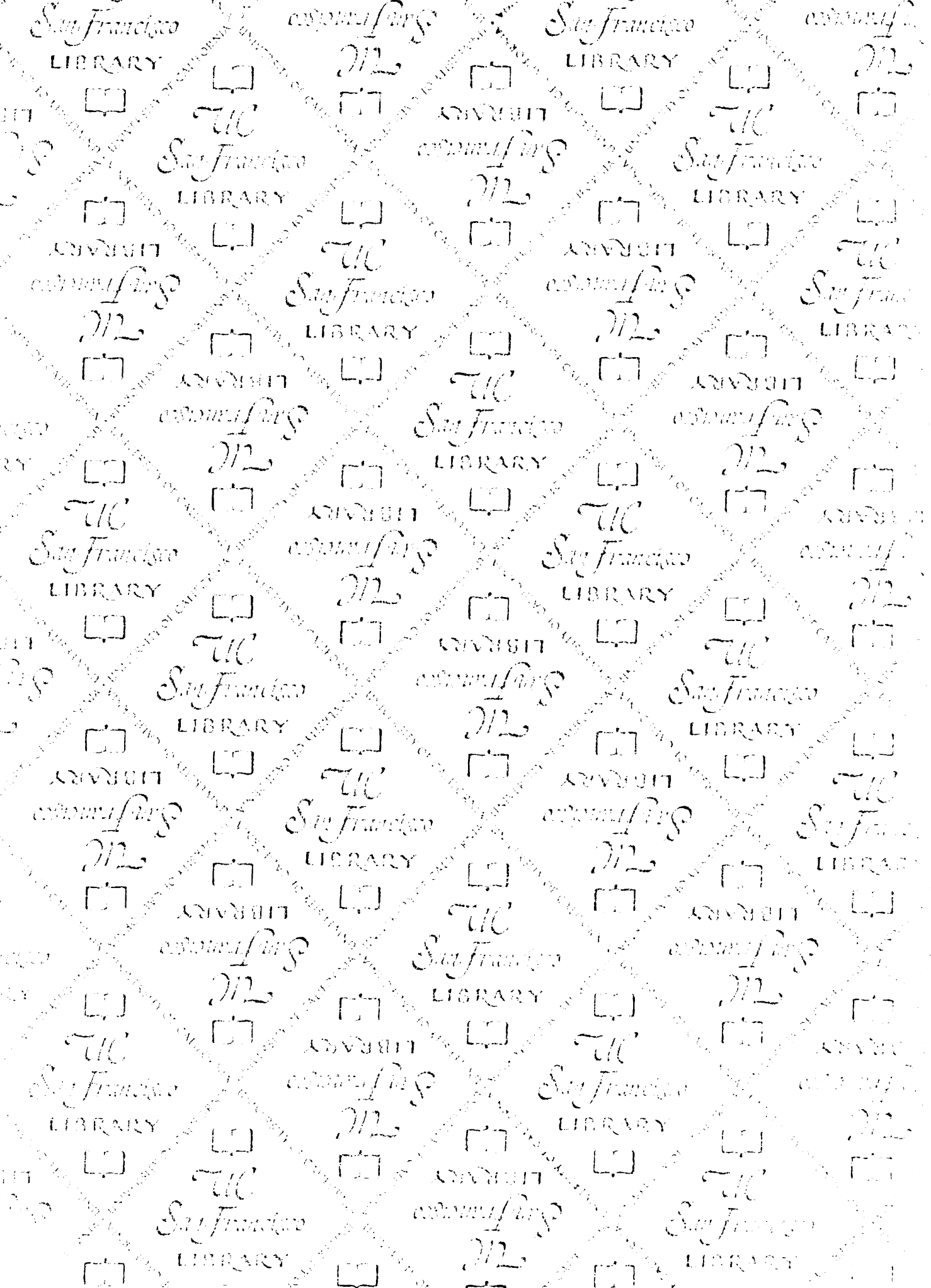
Figure 6.18. Potential hydrogen bonding interaction between the 2'-N-acyl substituent and the carboxamide of the nicotinamide ring.

Experimental

The 3-acetyl pyridine adenine dinucleotide and the nicotinic acid adenine dinucleotide were purchased from Sigma Chemical Company. The synthesis, purification and characterization of the 2'-substituted nicotinamide nucleosides are described in chapter 3. Kinetic measurements were carried out spectrophotometrically using a Hewlett-Packard 8452A diode array spectrophotometer equipped with a cell holder thermostatted at 25 °C. All reactions of cyanide with 2'-substituted nicotinamide nucleoside were conducted in aqueous solution maintained at pH 8.0 with 400 mM TAPS buffer. The nucleosides were present in 300-700 μ M concentration. The reactions were initiated by adding 50-100 μ l of 100 mM KCN and monitored by following the change in absorbance at the λ_{max} for the cyanide adduct (324 nm) until the system returned to equilibrium (20-50 minutes). The initial rate of addition was determined from the first 90 seconds of reaction in which the absorbance versus time plot is linear. The absorbance at equilibrium was used to calculate the concentration of cyanide adduct and, by subtracting from the known initial amount of nucleoside, the concentration of unreacted nucleoside.

References

- (1) Meyerhof, O.; Ohlmeyer, P. and Mohle, W. *Biochem. Z.* **1938**, *297*, 113-118.
- (2) Colowick, S.P.; Kaplan, N.O. and Ciotti, M.M. *J. Biol. Chem.* **1951**, *191*, 447-459.
- (3) Lamborg, M.R.; Burton, R.M. and Kaplan, N.O. *J. Am. Chem. Soc.* **1957**, *79*, 6173-6177.
- (4) Lindquist, R.N. and Cordes, E.H. *J. Am. Chem. Soc.* **1968**, *90*, 1269-1274.
- (5) Anderson, B.M., in "The Pyridine Nucleotide Coenzymes"; J. Everse, B. M. Anderson and K.-S. You, Eds. Academic Press: New York, 1982; pp. 109-110.
- (6) Glasfeld, A.; Zbinden, P.; Dobler, M.; Benner, S.A. and Dunitz, J.D. *J. Am. Chem. Soc.* **1988**, *110*, 5152-5157.
- (7) Kaplan, N.O. and Ciotti, M.M. *J. Biol. Chem.* **1956**, *221*, 823-832.
- (8) Volumes calculated using the grid matrix method by Lydia Gregoret and Fred Cohen at the Department of Pharmaceutical Chemistry; University of California, San Francisco.
- (9) Charton, M. *J. Org. Chem.* **1964**, *29*, 1222-1227.
- (10) Brewster, M.E.; Simay, A.; Czako, K.; Winwood, D.; Farag, H. and Bodor, N. *J. Org. Chem.* **1989**, *54*, 3721-3726.
- (11) Hansch, C. and Leo, A. *Substituent Constants for Correlation Analysis in Chemistry and Biology*; Wiley and Sons: New York, 1979;
- (12) Wallenfels, K. and Diekmann, H. *Justus Liebigs Ann. der Chemie* **1959**, *621*, 166-177.
- (13) Okubo, T. and Ise, N. *J. Am. Chem. Soc.* **1973**, *95*, 4031-4036.
- (14) Bunting, J.W. and Sindhuatmadja, S. *J. Org. Chem.* **1980**, *45*, 5411-5413.
- (15) Lovesey, A.C. *J. Med. Chem.* **1969**, *12*, 1018-1023.
- (16) Johnson, R.W.; Marschner, T.M. and Oppenheimer, N.J. *J. Am. Chem. Soc.* **1988**, *110*, 2257-2263.



FOR REFERENCE

NOT TO BE TAKEN FROM THE ROOM



CAT. NO. 23 012

PRINTED
U.S.A.

